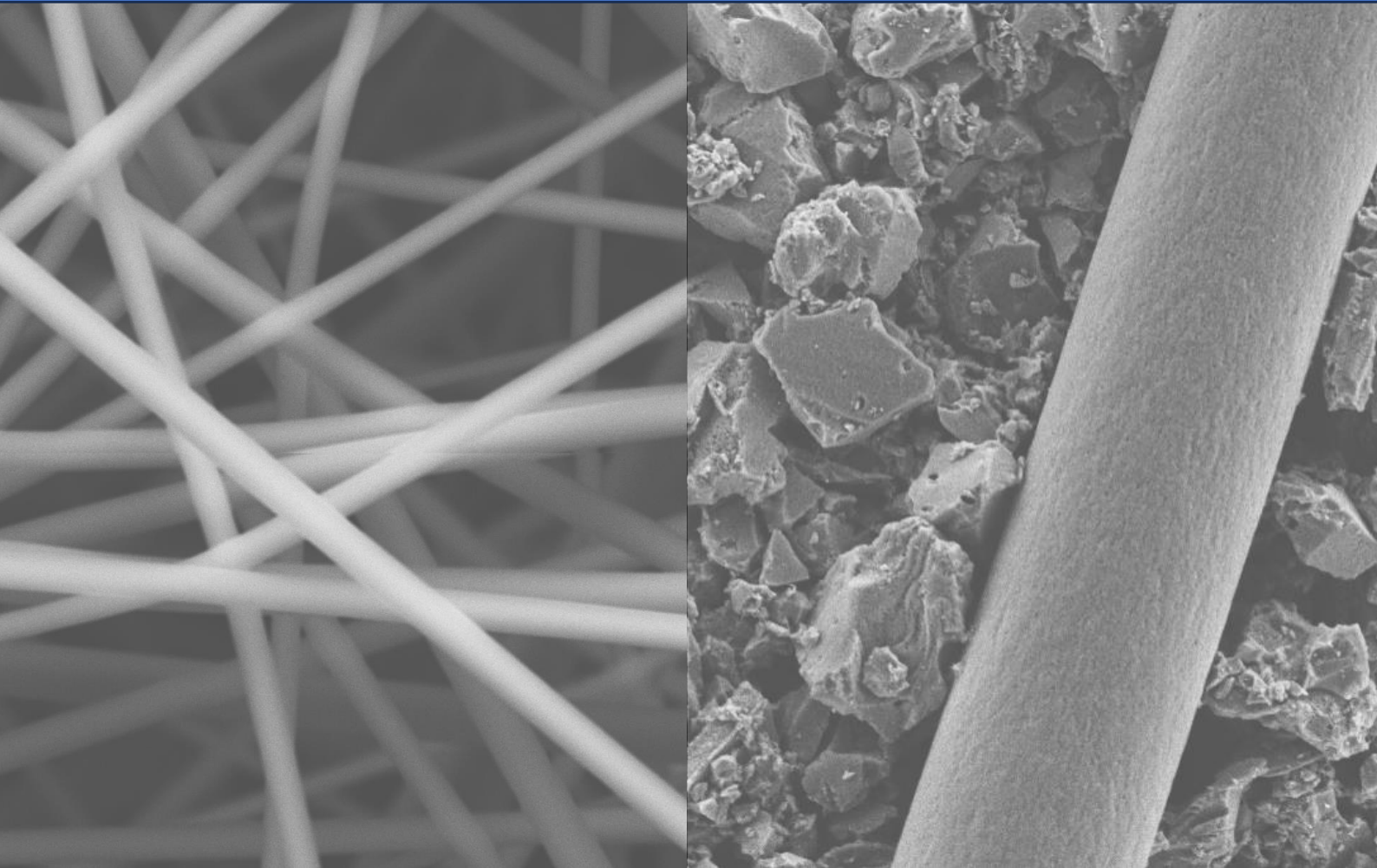


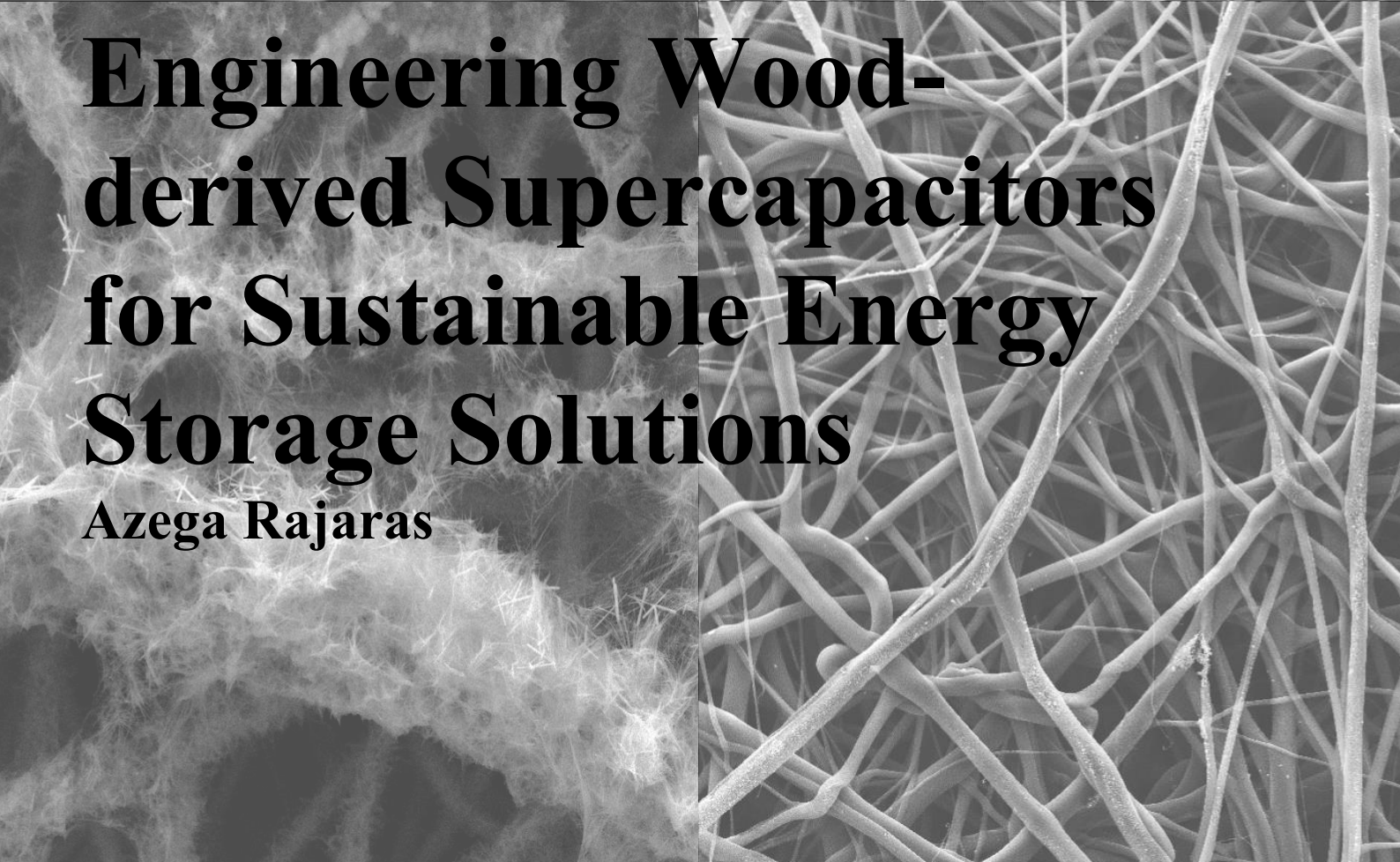


CHALMERS
UNIVERSITY OF TECHNOLOGY



Engineering Wood- derived Supercapacitors for Sustainable Energy Storage Solutions

Azega Rajaras



THESIS FOR THE DEGREE OF DOCTOR OF PHILOSOPHY

Engineering Wood-derived Supercapacitors for Sustainable Energy Storage Solutions

R.K. Azega



Department of Microtechnology and Nanoscience

CHALMERS UNIVERSITY OF TECHNOLOGY

Gothenburg, Sweden 2024

Engineering Wood-derived Supercapacitors for Sustainable Energy Storage Solutions

Doctoral thesis at Chalmers University of Technology

© R.K. AZEGA, 2024.

ISBN 978-91-8103-157-7

Series number: 5615

ISSN 0346-718X

Cover illustration: Microstructural designs of different lignin-derived carbon fiber materials for energy storage application.

Department of Microtechnology and Nanoscience - MC2

Chalmers University of Technology

SE-412 96 Gothenburg, Sweden

Telephone + 46 (0)31-772 1000

Printed by Chalmers Reproservice

Gothenburg, Sweden 2024

We are like butterflies who flutter for a day and think it is forever. Yet, in that brief time, we have the ability to understand the universe that made us.

- **Carl Sagan**

Abstract

This thesis addresses the growing need for sustainable energy storage systems by exploring wood-derived lignin as a renewable precursor for supercapacitor materials. With a focus on improving the environmental footprint of energy storage technologies, the research investigates several innovative approaches to utilizing lignin for high-performance supercapacitor devices.

The work presents a comprehensive study of plasma-treated electrospun lignin carbon fibers (ELCFs) to enhance electrode-electrolyte interactions. By modifying the fiber surface, both wettability and active site accessibility were improved, leading to significant gains in electrochemical performance. Additionally, the inclusion of lignin carbon fibers (LCFs) in activated carbon (AC) matrices was explored, demonstrating improved conductivity and performance in thicker electrodes, which are essential for increasing energy density.

The thesis also examines macro lignin-cellulose carbon fibers, characterizing their mechanical and electrical properties. These fibers show promise as potential candidates for wearable and flexible electronics. Furthermore, electrospun lignin fibers were studied for their application as separator materials, emphasizing their multifunctional potential in supercapacitor devices.

To provide context and insight, the thesis includes an extensive review of lignin-based supercapacitor materials, categorizing them by energy storage mechanisms and device configurations. This analysis serves as a comparative framework for evaluating the performance of the developed materials against other lignin-based systems in the energy storage landscape.

Through these contributions, this work highlights the versatility and potential of lignin as a green material for advancing supercapacitor technology, paving the way for sustainable energy storage solutions.

Keywords: Lignin-based supercapacitors, lignin carbon fibers, lignin-cellulose carbon fibers, wood-based carbon, sustainable energy storage systems

Acknowledgments

Well, here we are – five years, one thesis, countless energy drinks (to which I'm now happily sober), and way too many wrong winter clothing choices later. Moving to Sweden for my Ph.D. was nothing short of a bold move, and if I had known the cold would turn my tropical soul into a human popsicle, I might have reconsidered – haha, in hindsight, the beautiful warm summers are absolutely made for me. Here I am, a little less frozen, a lot wiser, and with a thesis in hand!

First, my heartfelt thanks go to my supervisor Per Lundgren. Your endless support, your inspiring passion for both your work and family, and those insightful weekly meetings, where we explored various hypotheses to make sense of puzzling research results, often uncovering interesting ideas to untangle complex problems, it all kept me going. Your understanding, patience, and occasional reality checks have kept me grounded and motivated throughout this journey, and for that, I am deeply grateful.

To my co-supervisor Hans Theliander – thank you for not only sharing your guidance and knowledge but also infusing me with an enthusiasm for researching lignin that I didn't even know I had. And to Professor Peter Enoksson – none of this would've been possible without your unwavering support, from helping me start my research at Chalmers to your ongoing encouragement, and for sharing your wisdom during your visits. You all made me feel like part of a brilliant, slightly nerdy family.

My gratitude also extends to the organizations that supported my research. The Wallenberg Wood Science Center, financed by the Knut and Alice Wallenberg Foundation, and Chalmers University of Technology - thank you for providing the financial support, amazing research schools, and the wealth of knowledge I was able to draw from. I am also deeply grateful to the GreEnergy Project for supporting our group's efforts and contributing to this journey.

A huge shoutout to my colleagues, who turned this PhD journey into something far more bearable. Your camaraderie, laughs, and willingness to endure my occasional (read: frequent) existential crises made even the longest lab days manageable.

To all my friends here in Sweden you turned my weekends (and sometimes my weekdays, let's be honest) into moments of joy. From hanging out, cooking warm meals together, and indulging in cozy evenings to simply being there for a good laugh or venting session, you made cold, dark times feel like home. And to my LDR (long-distance relationship) survival squad - thank you for the endless VCs, for checking on me, and for reminding me to stay alive even during my "living in the lab" phases. Your care has been nothing short of lifesaving.

To Sweden, with its freezing winters, unfamiliar food, and my awkward attempts at mastering fika - I've loved the journey of discovering a new culture, a new city, and even a new version of myself. My gym hours helped me flex my perseverance muscles, while every failure taught me to bounce back stronger (albeit with sore quads).

Finally, to my parents - thank you for calling to remind me not to travel during my weekend breaks (which I may or may not have ignored). Your love and concern, even from afar, have been the warmest thing in my life these past five years.

So, here's to bold decisions, research challenges, incredible support systems, and the occasional complaint about the cold. This journey has been nothing short of life-changing, and I wouldn't trade it for anything - except maybe a vacation right about now.

Gothenburg, December 2024
Azega

List of Publications

Appended publications related to this thesis

Paper I R.K. Azega, Mazharul Haque, Qi Li, Omid Hosseinaei, Hans Theliander, Peter Enoksson, and Per Lundgren, “Effect of plasma treatment on the electrochemical performance of lignin carbon fibers for supercapacitor application,” *Journal of Electroanalytical Chemistry*, Volume 946, October 2023. DOI: <https://doi.org/10.1016/j.jelechem.2023.117723>

Paper II R.K. Azega, Mazharul Haque, Agin Vyas, P.L. Tam, Anderson David Smith, Per Lundgren, Peter Enoksson, “Durable activated carbon electrodes with a green binder,” *Physica Status Solid B*, Volume 259, Issue 2, January 2022, DOI: <https://doi.org/10.1002/pssb.202100311>

Paper III R.K. Azega, Jenny Bengtsson, Mazharul Haque, Hans Theliander, Peter Enoksson, Per Lundgren, “The Influence of Hardwood Lignin Blending on the Electrical and Mechanical Properties of Cellulose Based Carbon Fibers,” *ACS Sustainable Chemistry & Engineering*”, *ACS Sustainable Chem. Eng.* 2024, Volume 12, Issue 30, 11206–11217, DOI: <https://doi.org/10.1021/acssuschemeng.4c02052>

Paper IV R.K. Azega, Anderson David Smith, Niladri Roy Chowdhury, Agin Vyas, Qi Li, Mazharul Haque, Qian Xun, Xiaoyan Zhang, Shameel Thurakkal, Torbjörn Thiringer, Peter Enoksson, Per Lundgren, “Supercapacitors and Rechargeable Batteries, a Tale of Two Technologies: Past, Present and Beyond,” *Sustainable Materials and Technologies*, Volume 41, 2024, e01111, DOI: <https://doi.org/10.1016/j.susmat.2024.e01111>

Other publications related to the author that is not included in the thesis

[1] “Spin-Coated Heterogenous Stacked Electrodes for Performance Enhancement in CMOS-Compatible On-Chip Microsupercapacitors,” Agin Vyas, Simin Zare Hajibagher, Ulises Méndez-Romero, Shameel Thurakkal, Qi Li, Mazharul Haque, **R.K. Azega**, Ergang Wang, Xiaoyan Zhang, Per Lundgren, Peter Enoksson, Anderson Smith, *ACS Applied Energy Materials*, March 2022, DOI: <https://doi.org/10.1021/acsaem.1c03745>

[2] “Alkyl-Amino Functionalized Reduced-Graphene-Oxide–heptadecan-9-amine-Based Spin-Coated Microsupercapacitors for On-Chip Low Power Electronics,”

Agin Vyas, Simin Zare Hajibagher, Ulises Mendez Romero, **R.K. Azega**, Ergang Wang, Per Lundgren, Peter Enoksson, Anderson D. Smith, *Physica Status Solid B*, Volume 259, Issue 2, February 2022, DOI: <https://doi.org/10.1002/pssb.202100304>

[3] “Exploiting low-grade waste heat to produce electricity through supercapacitor containing carbon electrodes and ionic liquid electrolytes,” Mazharul Haque, Iqbaal Abdurrokhman, Alexander Idström, Qi Li, **R.K. Azega**, Anna Martinelli, Lars Evenäs, Per Lundgren, Peter Enoksson, *Electrochimica Acta*, Volume 403, 139640, January 2022, DOI: <https://doi.org/10.1016/j.electacta.2021.139640>

[4] “Identification of self-discharge mechanisms of ionic liquid electrolyte based supercapacitor under high-temperature operation,” Mazharul Haque, Qi Li, Cristina Rigato, **R.K. Azega**, Anderson D. Smith, Per Lundgren, Peter Enoksson, *Journal of Power Sources*, Volume 485, 229328, February 2021, DOI: <https://doi.org/10.1016/j.jpowsour.2020.229328>

Conference and workshop contributions

[1] “Investigations on the capacitance increase during repetitive charging/discharging of lignin carbon nanofiber-based supercapacitors”, **R.K. Azega**, Qi Li, Mazharul Haque, Per Lundgren, and Peter Enoksson, 2021 Virtual MRS Spring Meeting & Exhibit, April 2021.

[2] “Durable activated carbon electrodes with a green binder”, **R.K. Azega**, Mazharul Haque, Agin Vyas, Anderson David Smith, Per Lundgren, Peter Enoksson, Compound Semiconductor Week, May 2021.

[3] “Enhancing Carbon Fiber Properties Through Lignin-Cellulose Composites: A Comparative Study of Hardwood vs. Softwood Lignin Sources” **R.K. Azega**, Mazharul Haque, Peter Enoksson, Per Lundgren, ECS Conference, October 2023.

[4] “Investigation of Electrospun Lignin Carbon Fiber Separators for Supercapacitor Applications”, **R.K. Azega**, Mazharul Haque, Peter Enoksson, Per Lundgren, PRiME Conference, October 2024.

Contents

Chapter 1: Introduction	1
1.1. Motivation.....	1
1.2. Scope of This Thesis.....	2
Chapter 2: Background	5
2.1. Evolution of Supercapacitors into the Energy Landscape	5
2.2. Supercapacitors vs. Batteries: What is the Advantage?.....	6
2.3. Energy Storage Mechanisms in Wood-based-lignin, -cellulose Supercapacitors	8
2.3.1. Electrochemical Double Layer Capacitors	10
2.3.2. Pseudocapacitors	15
2.3.3. EDLC/pseudocapacitor Composites	17
2.4. Classification of Supercapacitors Based on Device Configuration	20
2.4.1. Asymmetric Supercapacitors	20
2.4.2. Hybrid Supercapacitors	22
2.5. Performance of Wood-based Supercapacitors in the Energy Landscape.....	24
2.6. Deconvolution of Different Capacitive Behaviors	25
2.7. Classification of Supercapacitor Configuration Based on Application	28
2.7.1. Micro-supercapacitors	28
2.7.2. Flexible and Wearable Supercapacitors.....	30
2.2. Major Wood Components.....	32
2.2.1. Lignin	32
2.2.2. Cellulose.....	36
2.2.3. Hemicellulose	37
2.3. State-of-the-Art in Wood-Derived Components: Lignin and Cellulose for Supercapacitors	37
2.3.1. Electrode.....	37
2.3.2. Separator.....	38
2.3.3. Electrolyte.....	42
2.3.4. Binders and Additives	44
Chapter 3: Methodology	47
3.1. Extraction and Purification Techniques	47
3.1.1. Kraft Pulping Process	47
3.1.2. Extraction of Lignin from Black Liquor.....	47
3.2. Synthesis Methods for Lignin Fibers.....	48
3.2.1. Lignin Fractionation	48

3.2.2. Spinning Methods	49
3.3. Synthesis of Lignin-based Carbon Electrode Materials.....	50
3.3.1. Thermostabilization	51
3.3.2. Carbonization.....	51
3.3.3. Activation	53
3.3.4. Graphitization	53
3.4. Characterization Techniques.....	54
3.4.1. Scanning Electron Microscopy	54
3.4.2. Raman Spectroscopy	55
3.4.3. X-ray Photoelectron Spectroscopy	56
3.4.4. X-Ray Diffraction.....	56
3.4.5. Thermogravimetric Analysis	57
3.4.6. Carbon Hydrogen Nitrogen Sulfur (CHNS) Analysis	57
3.4.7. Mechanical Testing.....	58
3.4.8. Electrical Conductivity	58
3.5. Electrochemical Testing Procedures	59
3.5.1. Fabrication of Test Cells and Experimental Configurations.....	60
3.5.1. Experimental Conditions	61
3.5.1. Voltammetric and Galvanostatic Charge-discharge Methods	62
3.5.2. Electrochemical Impedance Spectroscopy Method	63
Chapter 4: Enhancement of Electrode Materials.....	65
4.2. Performance Enhancement of Electrode Materials.....	65
4.2.1. Surface Modification	65
4.2.2. Metal Oxide Decoration to Enhance Performance in Lignin-Based Carbon Fiber Electrodes.....	66
4.2.3. Blending Lignin with Cellulose for Composite Electrode Materials.....	68
Chapter 5: Electrochemical Performance Evaluation	71
5.1. Electrochemical Performance of Electrospun Lignin Carbon Fibers as Electrodes	71
5.1.1. Effect of O-functional Groups on Electrochemical Behavior.....	71
5.3. Electrochemical Performance of Lignin-Cellulose-based Carbon Fibers as Electrodes.....	72
5.4. Towards Thicker Electrodes	74
5.4.1. Electrochemical performance of AC/LCF Composite and Cellulose Binder Electrodes	75
Chapter 6: Analysis and Future Perspectives	77
6.1. Comparison with State-of-the-Art Electrode Materials	77
Chapter 7: Conclusion.....	81

Whispers of time

*From ancient trees to modern wood,
A masterpiece in fibers stood.
Cell walls woven, tight and strong,
Adapting, growing, all along.*

*Through time's embrace, it found its form,
A structure built to weather storm.
With veins that carry life's own blood,
Wood evolves, both strong and good.*

*Its fibers twist in patterns grand,
A work of nature, finely planned.
In every ring, a story told,
Of centuries, both young and old.*

Azega

The silent strength

*In nature's fabric, woven deep,
Where trees and forests softly sleep,
Lies lignin's strength, a binder true,
A polymer with power to renew.*

*Cellulose, the fiber's thread,
A sturdy web in trees widespread,
Carries the essence of life's green flow,
A gift from earth in sun's warm glow.*

*With climate's toll and fuels deplete,
We turn to wood, its promise sweet.
Lignin, with its rigid might,
Holds energy, a beacon bright.*

*Cellulose, the flexible form,
Stores power, and keeps it warm.
Together, they build a bridge anew,
For energy storage, clean and true.*

*No longer bound to fossil's grip,
We seek the future, let it slip,
Through trees that breathe, the world's embrace,
For in their fibers, hope finds place.*

Azega

Chapter 1

Introduction

1.1. Motivation

The pursuit of sustainable and efficient energy storage solutions is critical in addressing the global challenges posed by climate change and the depletion of fossil fuels. Traditional energy storage devices, such as batteries and capacitors, rely heavily on non-renewable and often toxic materials, raising concerns about their long-term viability and environmental impact. In this context, the exploration of renewable and biodegradable resources for advanced energy storage technologies is both a timely and necessary endeavor.

Wood, an abundant and renewable natural resource, offers potential for sustainable energy storage solutions. Its key biopolymers, lignin and cellulose, possess unique properties that make them promising materials for this application. Lignin's aromatic structure provides excellent electrochemical stability, while cellulose's high surface area and mechanical strength create an ideal scaffold for robust and efficient components for energy storage devices.

Annually, the paper and pulp industry produces about 260 million tons of black liquor as a by-product (Di Francesco et al., 2021). It is an organic-inorganic mixture of lignin, hemicellulose, and processing chemical residues from the pulpwood digestion unit. This renewable fuel has been utilized in a power boiler to generate steam for various heating applications within the mill, as well as for the production of electricity. The full potential of this material is yet to be exploited and should be put to better use than as a mere boiler fuel. Furthermore, modern kraft pulp mills are very energy efficient and as a consequence, all lignin is not necessary to use as fuel in these pulp mills. Extracting the excess lignin from the black liquor has the potential to provide a functional resource to make various value-adding products. Lignin as a carbon-rich bio-component is attributed to be a suitable candidate to manifest various carbon materials. With that interest, research on lignin-based carbon fibers in energy storage devices, particularly supercapacitors, has been conducted in the making of this thesis. Also utilizing wood's other constituent, cellulose, as non-electrode component (Kasprzak et al., 2018) in supercapacitors would be interesting for exploration replacing toxic materials that are currently functional in standard electrodes (Rashid Khan & Latif Ahmad, 2024). Understanding the performance of these materials can lay the path to explore more sustainable supercapacitors. With a better understanding of the charge storage mechanisms, supercapacitors are likely to suit applications either as a standalone power source or a battery-supported system. Beyond their scope as supercapacitor electrodes, wood and wood-derived components can also be attempted to replace the graphite electrodes in lithium batteries (Fu et al., 2025; Lu Huiran, 2017; Sagues et al., 2020). This is one of the visions of the Finland-based company Stora Enso joining hands with NorthVolt (Mäntyranta, 2023; "Stora Enso and Northvolt Partner to Develop Wood-Based Batteries," 2022).

Advancing forest resources like wood-derived components for future energy storage materials can be a big step toward creating a more sustainable world. The research discussed and the papers attached to this thesis aim to harness and motivate the potential of wood-derived lignin and cellulose to develop future-generation supercapacitors. Supercapacitors are highly valued for their exceptional power density, fast charge and discharge capabilities, and extended lifespan, making them suitable for applications ranging from portable electronic devices to large-scale renewable energy systems. By leveraging the intrinsic properties of lignin and cellulose, this work seeks to create supercapacitors that are both environmentally sustainable and high performing.

1.2. Scope of This Thesis

One scope of the thesis concerns novel lignin and cellulose composite carbon fibers and explores their potential as environmentally friendly alternatives to current commercially available fossil-based carbon fiber materials. Funded by the Wallenberg Wood Science Center and the Horizon 2020 project GreEnergy, my PhD work includes the synthesis and characterization of lignin-cellulose composite carbon fibers, focusing on their mechanical and electrical properties, but with the application as supercapacitors electrodes in wearable devices in mind. By addressing the balance between electrochemical performance and mechanical stability, this research provides valuable insights into the potential of wood-derived carbon fibers in advancing supercapacitor technology with a sustainable approach. Attention is also given to enhancing the surface area and optimizing the electrode-electrolyte interface in electrospun lignin carbon fibers, as well as in activated carbon electrodes with lignin carbon fiber inclusions serving as conductive agents. Further we investigate the impact of various strategic solutions on the structural and electrochemical properties of these materials, aiming to maximize active site accessibility and improve overall supercapacitor performance. Additionally, the thesis explores the use of lignin as a separator material for supercapacitors (Section 2.3.2) and touches briefly upon the effects of incorporating nanocellulose, alkali lignin and carbon black as additives to make efficient gel electrolytes (Section 2.3.3). These efforts aspire to contribute to the development of fully wood-based supercapacitors in the future, utilizing components sourced entirely from green materials to create completely sustainable devices without significant compromises on performance.

Chapter 2 presents a comprehensive overview of energy storage technologies, with a specific focus on supercapacitors and the chemistry of lignin and cellulose. It offers a systematic categorization of supercapacitors based on their storage mechanisms and device configurations, providing insights into the fundamental principles governing their operation. The chapter also delves into the various methodologies employed for analyzing charge storage behaviors.

Chapter 3 details the methodologies for selecting, extracting, and purifying lignin and cellulose from wood sources. It focuses particularly on the process of obtaining lignin from black liquor and its subsequent transformation into carbon fiber materials. The chapter elucidates the various characterization techniques employed to evaluate the morphological, chemical, structural, and electrochemical properties of these materials. Additionally, it provides a comprehensive overview of the synthesis and processing procedures involved in converting lignin-based precursors into high-performance carbon fibers, highlighting the key steps and parameters that influence the final product's characteristics.

Chapter 4 provides a concise overview of the techniques employed to enhance electrode in the appended papers and from unpublished preliminary research. with a primary focus on surface modification and compositing methods. It examines both successful enhancements and unsuccessful attempts, particularly focusing on the challenges encountered during fabricating, analyzing and testing of electrode materials.

Chapter 5 provides a comprehensive analysis of the electrochemical performance of various materials developed in the appended papers. These approaches, which are detailed in the appended papers of this thesis, aim to improve the electrochemical properties and overall efficiency of the electrodes.

Finally, Chapter 6 and 7 present a comprehensive synthesis of the major research contributions made to the field of supercapacitors, with a particular focus on lignin-based carbon electrodes developed in this thesis. The first chapter offers a comparative analysis of these electrodes against

other state-of-the-art lignin-based carbon materials, contextualizing the advancements achieved. Additionally, an attempt to identify key challenges encountered during the research and proposes future research directions aimed at enhancing the sustainability and efficiency of lignin and cellulose-based supercapacitor energy storage devices in examined. The concluding chapter summarizes the thesis findings by providing motivation for future investigations in this promising area of sustainable energy storage.

Chapter 2

Background

2.1. Evolution of Supercapacitors into the Energy Landscape

About 390 million years ago, during the mid-Devonian period, *plants developed wood* - a vital transformative adaptation that marked a pivotal stage in their evolution (Driese et al., 1997). This new tissue, capable of conducting water and minerals upward from roots to leaves, allowed plants to grow taller and sturdier, supporting broader access to sunlight and enhancing photosynthesis. Over generations, these woody structures became more complex and efficient, creating an evolutionary advantage that fueled a competitive race for survival. This drive to reach higher to thrive in dense ecosystems shaped the sophisticated wood anatomy we recognize in today's trees. Only 1 million years ago, early humans, specifically *Homo erectus*, began harnessing *wood as a source of thermal energy* - a fundamental leap that set the stage for wood's role in sustaining human society. This practice has endured, and today, around 6% of the global population still relies on wood as a primary energy source (Sreevani, 2018). However, it was not until the mid-20th century that carbon/wood was considered for advanced applications as a direct component in energy storage devices. Since then, our understanding of wood's cellular and chemical structure has deepened, allowing us to recognize its potential as a renewable, carbon-rich material capable of supporting electrochemical processes.

The basic concept of storing electrical energy on material surfaces due to electrostatic charge buildup dates to the simple discovery of rubbing amber with fur. In 1957, H. I. Becker proposed an *electrolytic capacitor using porous carbon electrodes*, demonstrating capacitance from the electrostatic double layer at the electrode/electrolyte interface, a phenomenon understood by Hermann von Helmholtz as early as 1879 (I. Becker, 1957). However, significant research in this field only gained momentum in the early 1990s when NEC in Japan developed their energy storage technology, coining the term "*super-capacitor*" for these devices. Technically known as **electric double layer capacitors (EDLCs)**, the term "supercapacitor" stuck, although some companies like Maxwell Technology commercially branded their EDLC devices as "ultracapacitors".

The technology advanced with the discovery of high-capacity metal oxide electrodes, when Trasatti and Buzzanca identified the electrochemical behavior of hydrous RuO₂ thin films as capacitor-like in 1971 (Trasatti & Buzzanca, 1971). Since then, numerous electrochemical-capacitive materials have been discovered (Hsieh et al., 2008; H. Y. Lee & Goodenough, 1999). While RuO₂ stores energy in a manner similar to capacitors, it does so through a distinct energy storage mechanism involving *Faradaic (charge-transfer) reactions using redox-active materials*. This recognition of *pseudo-capacitance* led to the emergence of a new class of energy storage devices known as **pseudocapacitors** around the 1980s. The term "pseudo-" reflects their mimicked capacitive behavior, despite the different energy storage mechanism. Although pseudocapacitors are considered a type of supercapacitor, they are not synonymous with supercapacitors, as they involve additional electrochemical processes.

As the story of energy storage devices evolved, the quest for more efficient and higher-capacity systems led to the development of **batteries**. Unlike capacitors, batteries store energy through *chemical reactions that involve the transfer of electrons between materials*. The idea of batteries originated in the late 18th century when Alessandro Volta, an Italian scientist, developed the first functional battery called the Voltaic pile (Volta, 1800). This invention consisted of alternating zinc

and copper discs that produced a continuous electric current, forming the basis of modern battery technology. Over the years, innovations such as the lead-acid battery in the 19th century, and later the lithium-ion battery (LIB), revolutionized portable energy storage, pushing forward applications in everything from electronics to electric vehicles.

2.2. Supercapacitors vs. Batteries: What is the Advantage?

When comparing supercapacitors, pseudocapacitors, and LIB, the key differences lie in their charge storage mechanisms, energy and power densities, operating conditions, and lifecycle (**Table 1**).

Table 1: Supercapacitor performance metrics compared to standard lithium-ion batteries.

	Supercapacitor	Lithium-ion battery ^a (Nitta et al., 2015; Zubi et al., 2018)
Charge storage	Double-layer capacitance (electrostatic)	Intercalation
Electrodes	Carbon materials	LiCoO ₂ cathode and graphite anode
Electrolyte	Organic	Lithium salt in an organic solvent
Operating voltage	Up to 3 V	3 - 4.4 V
Energy density	~3 - 5 Wh/kg	120 - 190 Wh/kg
Power density	9000 W/kg	1000 - 3000 W/kg
Thermal runaway risk	No danger	Yes
Operating temperature	-40 °C to +65 °C	0 - 45 °C
Self-discharge	High (weeks)	Less (years)
Operation lifetime at RT	10 - 20 years	2 - 3 years
High temperature operation ^b	2000 hours	Deteriorates device life
High voltage operation ^b	1500 hours	Becomes unstable
Cycle life	1000000 cycles	>500 cycles
Shelf life	10 - 18 years	7 - 15 years
Availability	Commercially available	Commercially available
Cost/kWh	\$100 - 500	\$100 - 170
Current applications	Energy backup for memory and data protection, voltage stabilization in power systems, regenerative braking in electric and hybrid vehicles, power assist for acceleration in EVs, short-term storage in solar energy systems	Portable electronics (smartphones, laptops, tablets), electric and hybrid vehicles, renewable energy storage (solar, wind), grid energy storage and stabilization, medical devices (pacemakers, hearing aids), military and aerospace applications, Internet of Things (IoT) devices and sensors
Toxic level	Low	High

^a The LiCoO₂ cathode-based LIB, which is typically used to power portable consumer gadgets, serves as a representative of the LIB family. ^b Typically beyond prescribed operating temperatures or voltages.

Supercapacitors, including pseudocapacitors, rely on electrostatic (double-layer capacitance) charge storage and Faradaic reactions, respectively. EDLCs typically use carbon-based materials for electrodes and organic electrolytes, offering a *high operating voltage* of up to 3 V. While they have *relatively low energy density* (3-5 Wh/kg), they *excel in power density* (9000 W/kg), making them ideal for applications requiring *rapid charge and discharge cycles*. Supercapacitors have a *remarkable cycle life* (up to 1000000 cycles) and can *function in a wide range of temperatures*, from -40 °C to +65 °C. Their *self-discharge rate is high*, however, and their operating lifetime typically spans 10-20 years.

Lithium-ion batteries (LIBs), on the other hand, store energy through electrochemical intercalation and de-intercalation processes (Dresselhaus & Dresselhaus, 2002). These processes involve the reversible insertion and extraction of lithium ions between the electrodes, typically using materials like LiCoO₂ for the cathode and graphite for the anode. This mechanism allows for *higher energy density* (120-190 Wh/kg) than supercapacitors, making them suitable for applications like portable electronics and electric vehicles, where long-duration energy storage is critical. However, LIBs have a much *lower power density* (1000-3000 W/kg) compared to supercapacitors and are *prone to thermal runaway*, especially in high-temperature conditions. Their *cycle life is shorter* (500 cycles) compared to supercapacitors, and their *self-discharge rate is considerably lower*, meaning they can last several years without significant loss of charge. The batteries operate within a temperature range of 0-45 °C and are more sensitive to high voltage and temperature fluctuations. As depicted in a Ragone chart, the relationship between power density and energy density of various energy storage devices (Figure 1), supercapacitors as high-power systems, fuel cells are shown as high-energy systems and batteries occupy an intermediate position with respect to both power and energy capabilities. While these batteries offer high energy density and good cycle life, supercapacitors can handle more total energy over their entire cycle lifetime.

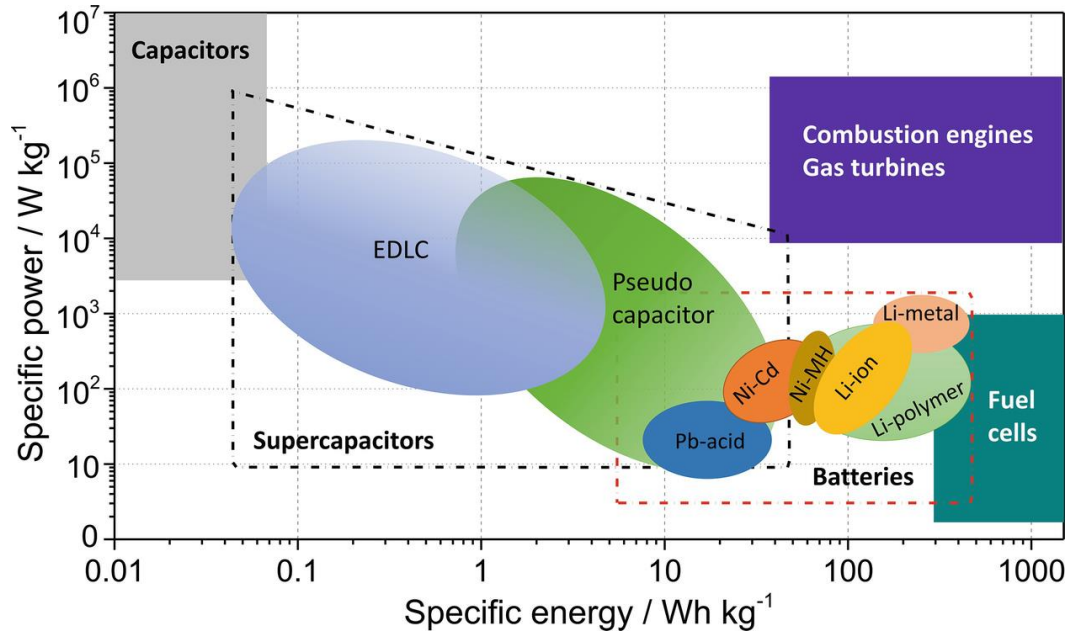


Figure 1. Ragone plot of different electrochemical energy conversion devices. Reproduced with permission from Zhen et al., 2019.

Therefore, supercapacitors and batteries serve complementary roles in the landscape of energy storage; supercapacitors are ideal for high-power, low-energy applications, such as voltage stabilization, short-term power bursts, and self-powering electronics. Recent research has aimed at enhancing their energy density, focusing on novel materials like metal oxides (MOs) (An et al.,

2019), NiCo composites (Ray et al., 2023), and doping (Zheng et al., 2022), which expands their potential in asymmetric (Ramachandran et al., 2023), hybrid (D. Gao et al., 2023), and micro-scale devices (S. Wang, Ma, et al., 2022) (Figure 2). Batteries, by contrast, prioritize high energy storage, making them suitable for long-term energy needs in applications like electric vehicles, portable electronics, and IoT devices. Advances in battery chemistry, such as lithium-ion, sodium-ion, and lithium-sulfur, are driven by the need for greater power density, improved cycle life, and higher stability. As research continues, *hybrid technologies* and applications that draw on the strengths of both supercapacitors and batteries are emerging (Paper IV), such as hybrid electric vehicles and renewable energy systems, offering a balance between high energy and high power (D. P. Chatterjee & Nandi, 2021).

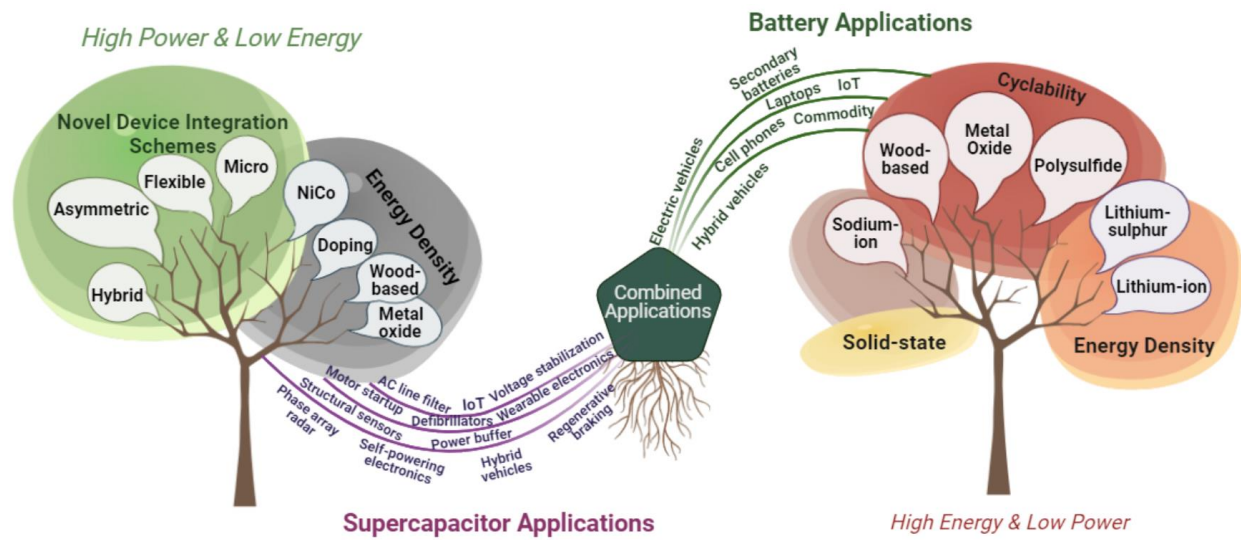


Figure 2. Supercapacitor and battery technology migration to close the energy gap is largely driven by a number of important emphasis areas (corresponding technology's most notable research-focused branches in the last 12 years). Each technique has often only been used in specialized applications. New possible applications emerge when the technologies change and converge (Paper IV).

Conventional materials used in batteries, such as lithium, cobalt, lead, and cadmium, present challenges due to their limited availability, extraction-related environmental damage, and toxicity (Gratz et al., 2014), (Kang et al., 2013). The growing global energy demand, coupled with environmental concerns over traditional energy storage devices, underscores the need for alternative *sustainable solutions*. As we transition to greener energy sources such as solar and wind, energy storage systems need to keep pace in terms of efficiency, cost-effectiveness, and environmental impact. As a result, researchers are exploring *renewable and abundant materials*, such as wood-based-lignin, -cellulose, and other bio-based materials, to engineer components for energy storage devices (Nowak et al., 2018; Tenhaeff et al., 2014). The goal of exploring greener materials for electrodes is not necessarily to replace lithium-based batteries entirely but rather to create complementary hybrid solutions that could reduce the reliance on too much lithium and mitigate its environmental impact.

2.3. Energy Storage Mechanisms in Wood-based-lignin, -cellulose Supercapacitors

Figure 3 offers a comprehensive schematic representation of the broad classification of supercapacitors based on their energy storage mechanisms, specifically focusing on wood-based lignin and cellulose materials as electrodes in the different types. The classification distinguishes between EDLC and pseudocapacitive-based materials, both of which rely on different energy storage mechanisms to store electrical energy. As outlined in **Table 2**, this classification by the

type of electrode materials significantly influences the energy storage characteristic and thereby its performance as an energy storage device.

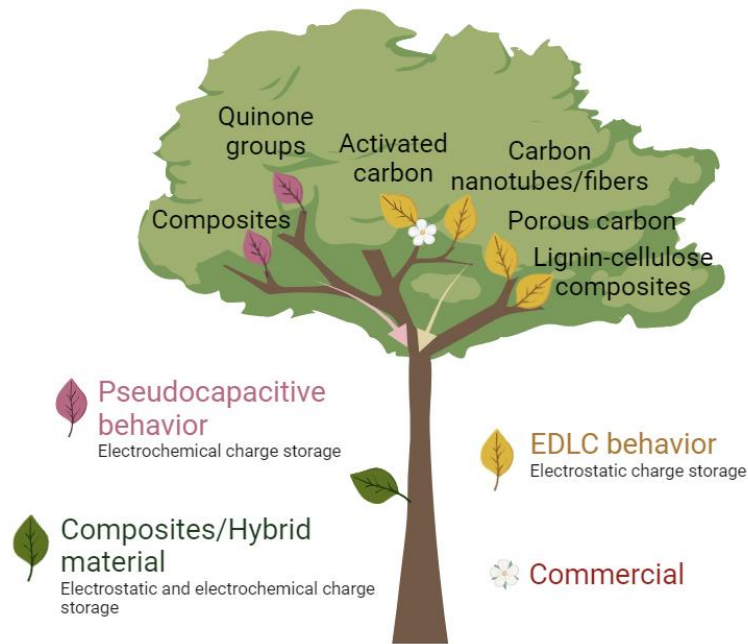


Figure 3. Broad classification of predominant types of supercapacitors being explored today from wood-derived components and their corresponding charge storage mechanisms.

Table 2: Classification of electrodes based on type of material

	EDL-capacitive	Pseudocapacitive	Composites
Standard materials	Carbon	Metal oxides (MO)	Carbon/MO
Charge storage	Electrostatic	Electrochemical	Electrostatic and electrochemical
Electronic conductivity	High	Low	Intermediate
Rate capability	High	Low	Intermediate
Specific surface area	High	Low	Depends on carbon scaffold
Pore size	Tailorable	Definite	Depends on carbon scaffold
Chemical/thermal stability	High	Low	Intermediate
Availability	Abundant	Limited (depends on MO)	Intermediate
Cost of raw material and production	Cheap	High	Intermediate
Toxicity	Low (greener)	High	Intermediate

Electrical double layer (EDL) capacitive electrodes primarily use carbonized wood-based materials, storing energy electrostatically with high electronic conductivity, excellent rate capability, and tailorable surface area and pore size, include materials such as *carbonized wood*, *activated carbon (AC)*, *carbon nanotube (CNTs)*, *cellulose nanofibers (CNFs)*, *porous carbon*, and *lignin-cellulose composites* (Adam et al., 2020; C. Liu et al., 2024; Tong et al., 2023). They are typically low in cost in terms of production and have high chemical and thermal stability, making them widely available and environmentally friendly.

On the other hand, pseudocapacitive materials offering higher capacitance at the expense of lower electrical conductivity, rate capability, and stability tend to be more expensive and less readily available. The *quinone functional groups* in lignin recognized for their pseudocapacitive behavior, offers enhanced capacitance and overall device performance compared to their only EDL capacitive counterparts (B. Zhou et al., 2019). Composites combining carbon and functional groups offer a balance between the electrostatic and electrochemical storage mechanisms, providing intermediate performance in terms of conductivity, rate capability, and stability, with moderate cost and availability.

The involvement of industrial companies in the development of wood-based carbon for energy storage devices has been pivotal in advancing sustainable and scalable solutions. Stora Enso has been developing a lignin-based anode material called Lignode, derived from wood, which is aimed to replace fossil-based graphite with activated carbon from lignin in LIBs, enhancing charging speeds, improving low-temperature performance, and ensuring safety in colder environments (Greene & Denny, 2022). Just as lignin’s unique properties enable enhanced performance in Lignode in LIBs, similar principles can be applied to their development for supercapacitor electrode materials.

2.3.1. Electrochemical Double Layer Capacitors

As depicted in Figure 4, EDLCs store energy electrostatically through the adsorption and desorption of electrolyte ions on the electrode's surface.

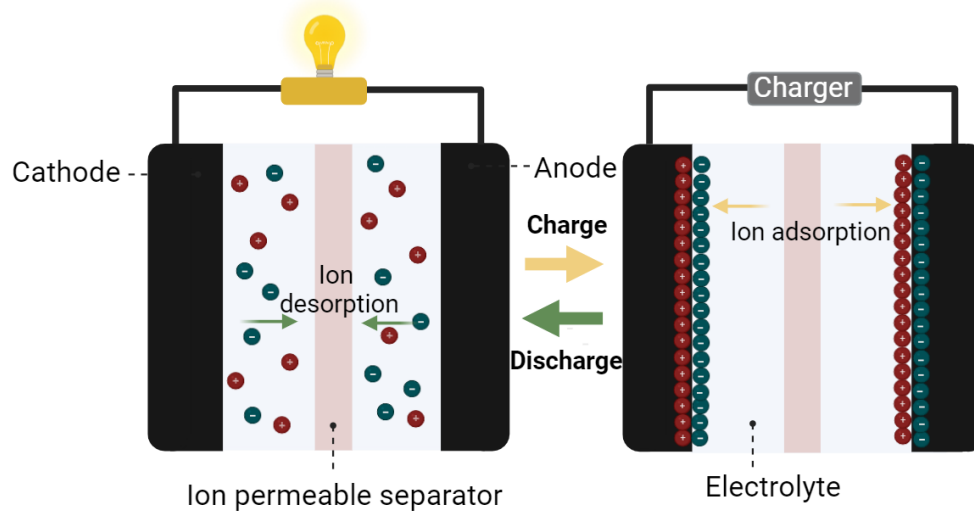


Figure 4. Schematic representation of the electrostatic charge storage mechanism during charging-discharging cycles in an EDLC device (Paper IV).

The capacitance C quantifies the electrode's ability to store charge Q per unit applied voltage V , as described in Equation 1:

$$C = \frac{Q}{V} \quad (\text{Equation 1})$$

In a supercapacitor device, the net capacitance arises from the combined contribution of the two electrodes, which act as capacitors connected in series. The net capacitance C_{net} is given by:

$$\frac{1}{C_{net}} = \frac{1}{C_1} + \frac{1}{C_2} \quad (\text{Equation 2})$$

where C_1 and C_2 are the capacitances of the individual electrodes. Achieving an optimal net capacitance requires careful balancing of the individual electrode capacitances. Any mismatch in electrode capacitances can lead to a suboptimal performance and reduced energy storage capability.

Now, the capacitance of an EDLC electrode can be expressed using the formula:

$$C_{dl} = \frac{A \cdot \epsilon}{d} \quad \text{(Equation 3)}$$

where A is the electrode's electrochemically active surface area, d is the effective electrical double layer's thickness, and ϵ is the permittivity related to the electrolyte. Therefore, by increasing the surface area of the electrode material the capacitance can be significantly increased. Typically, the capacitance value, when normalized with respect to a specific parameter such as the mass, area, or volume of the electrode material, is referred to as specific capacitance (C_{sp}). To enhance the specific capacitance of lignin-based EDLC electrodes, strategic engineering of structural designs is crucial. As illustrated in Figure 5, the development of nanoporous or nanostructured carbon materials can significantly improve performance. Innovative techniques such as templating and carefully tuned activation methods enable the creation of optimal pore structures. This systematic approach allows for precise tailoring of material properties, resulting in higher capacitance and improved overall supercapacitor performance.

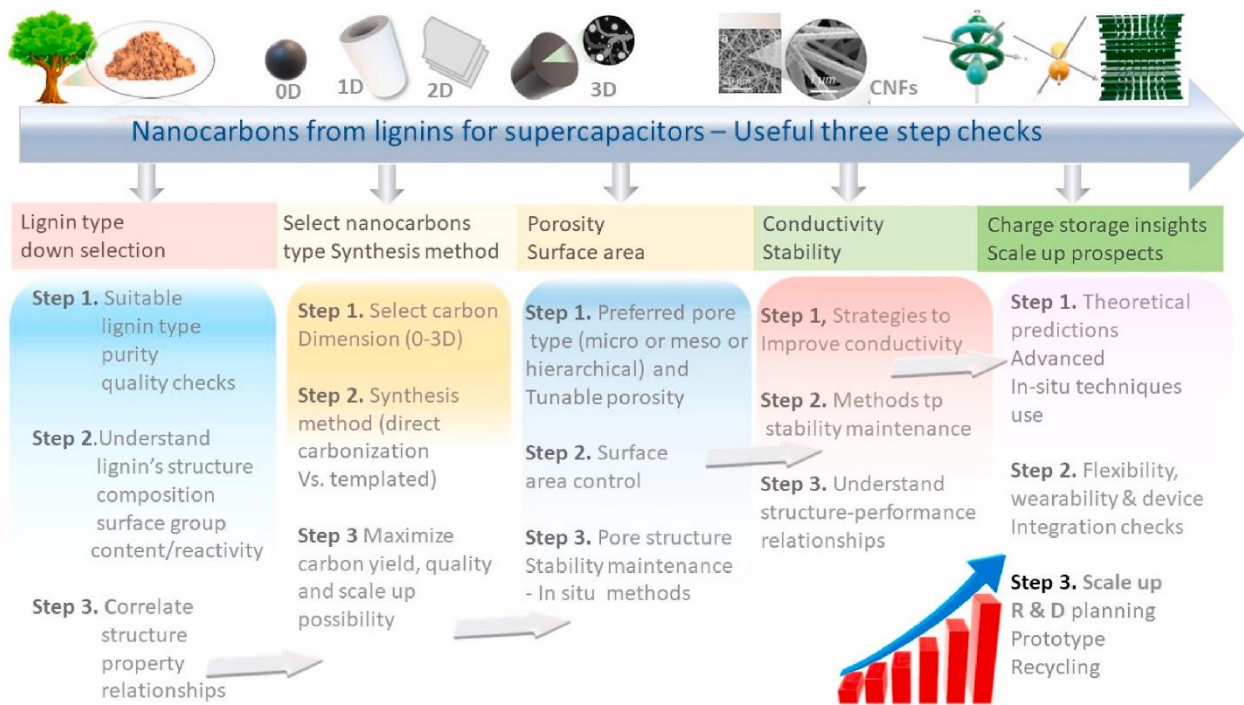


Figure 5. Processing stages proposed by Madhu et al. 2023 to produce high-quality lignin nanocarbons that can be effectively made to develop high performing supercapacitors. Reproduced with permission from the source.

Table 3 shows a list of different lignin-based electrodes for use in EDLCs, with performance characteristics varying across different types of lignin and tailoring methods. The specific capacitance values for these materials range between 500 - 100 F/g. Energy density varies among lignin-derived carbon materials, with electrolyte playing crucial roles. Kraft lignin-derived porous carbon, produced through activation, achieves the highest energy density of 78 Wh/kg when used

with a gel electrolyte. Alkali lignin-derived activated carbon and alkali kraft lignin/polyacrylonitrile (PAN) carbon fiber also offer competitive energy densities of 66 Wh/kg and 59 Wh/kg, respectively. These high energy densities can be attributed, in part, to the use of ionic electrolytes, which allow for increased operating voltages. The specific lignin source and processing method, combined with appropriate electrolyte selection, significantly influence the energy storage capabilities of these materials. In terms of power density, these lignin-based electrodes show moderate to high performance, with some achieving values up to 50 kW/kg. Cycle stability, which refers to a device's capacitance retention over a specific number of repeated charge-discharge cycles, is a feature that was observed in several lignin-based materials. For instance, the carbon fibers and activated porous carbons demonstrated excellent performance by maintaining over 90% of their initial capacitance after extensive cycling. It is interesting to highlight that the performance of these electrodes is influenced by the source of lignin, the processing methods used, and their composite structures. Overall, alkali lignin, kraft lignin, and lignosulfonate displayed good performance. Also, in a study by (Du et al., 2021), hardwood lignin/PAN outperformed softwood and cornstalk lignin in supercapacitor applications, with a specific capacitance of 340 F/g at 0.5 A/g, an energy density of 57 Wh/kg (40 W/kg), and 90% retention after 5000 cycles. As Du et al. explain, hardwood lignin's higher β -O-4 aryl ether linkages, larger molecular weight, and narrower polydispersity index (PDI) enable the production of high-quality lignin carbon nanofibers (LCNFs), enhancing electrode performance. Overall, the data suggests that lignin-based electrodes are a promising alternative to traditional materials, offering strong energy storage capabilities with good cycle stability.

Table 3 : Device performances of various lignin-based EDLC supercapacitor electrodes (Q. Cao et al., 2024; Jyothibasud et al., 2022; H. Liu, Xu, et al., 2021; Tong et al., 2023; Zhong et al., 2024)

Electrode material	Capacitance (F/g)	Energy Density (Wh/kg)	Power Density (W/kg)	Cycle Stability
CARBON FIBERS PRODUCED BY ELECTROSPINNING METHOD				
Corn stalk lignin/DMF*/PAN*	430 (1 A/g)	37	400	97% after 10000 cycles
Kraft lignin/PVA*	450 (1 A/g)	63	1250	96% after 1000 cycles
Alkali lignin/DMF*/plant protein	410 (1 A/g)	–	–	95% after 10000 cycles
Kraft lignin/H₂O/PEO*	345 (1 A/g)	8	–	96% after 5000 cycles
Alkali lignin/KOH/PEO*	345 (10 mV/s) 195 (50 mV/s)	8	–	96% after 5000 cycles
Softwood lignin/PAN*	300 (0.5 A/g)	–	–	–
Hardwood lignin/PAN*	340 (0.5 A/g)	57 (40)**	394 (5000)**	90% after 5000 cycles
Cornstalk lignin/PAN* (Du et al., 2021)	280 (0.5 A/g)	–	–	–
Kraft/DMF*/PVP*	250 (0.2 A/g)	–	–	97% after 1000 cycles

Kraft lignin/NaOH/PEO*	190 (0.1 A/g)	~8	2600	93% after 6000 cycles
Organosolv lignin/H₂O/PEO*	180 (1 A/g)	10	50000	–
Alkali Kraft lignin/DMF*/PAN*	130 (1 A/g)	59	15000	75% after 1000 cycles
Alkali lignin/DMF*/PAN*	130 (0.5 A/g) 110 (5 A/g)	4	2630	95% after 10000 cycles
Acetic acid lignin-based CNF*	120 (0.5 A/g)	–	–	90% after 1000 cycles
Alkali lignin/PVA*	65 (0.4 A/g) 50 (2 A/g)	~6	94	90% after 6000 cycles
Organosolv lignin/DMF*/PEO*	70 (0.5 A/g)	–	–	107% after 1000 cycles
PEGL* carbon fiber	85 (2 A/g)	14	422	–
PEGL* carbon fiber	95 (1 A/g)	–	–	–
Organosolv lignin/NaOH/PEO*	130 F/cm ³ (0.1 A/g)	6 Wh/L (~3 Wh/L)**	(10000 W/L)**	90% after 10000 cycles
CARBONS PRODUCED BY TEMPLATE METHOD				
Biochoice™ lignin and cellulose-nanofiber based aerogels	410 (2 mV/s)	~4	500	94% after 4500 cycles
Technical soda lignin-derived carbon aerogel/nickel binary network	240	–	–	–
Alkali lignin-derived hierarchical porous carbon monolith	210 (0.1 A/g)	0.16 mWh/cm ²	1.75 mW/cm ²	95% after 10000 cycles
Alkali lignin-derived porous carbon	170 (0.1 A/g)	–	–	–
Organic solvent lignin	140 (1 A/g)	~4	1300	87% after 5000 cycles
Organic solvent lignin [Asymmetric]	140 (1 A/g)	~6	1300 (50 000)**	–
Alkali lignin-derived hierarchical porous carbon microspheres	140 (0.05 A/g)	~25	6800	89% after 10000 cycles
Alcell lignin derived-hierarchical porous carbon (Salinas-Torres et al., 2016)	-	4.2	1300	95% after 5000 cycles
CARBONS PRODUCED BY ACTIVATION METHOD				
Alkali lignin-derived carbon	430 (1 A/g)	66	312	97% after 10000 cycles

Lignin porous carbon	420 (0.1 A/g)	23	25400	99% after 10000 cycles
Walnut lignin graphene-like nanosheets	390 (0.2 A/g)	~14 (11)**	129 (6465)**	99% after 10000 cycles
Lignin sulfonate-derived porous carbon	340 (0.5 A/g)	~10	250	95% after 5000 cycles
Organic solvent lignin-derived rod-shaped porous carbon	335 (1 A/g)	–	–	100% after 1000 cycles
Enzymatic hydrolysis lignin-derived 3D hierarchical porous carbon	325 (0.5 A/g)	18 (~6)**	458 (50400)**	100% after 5000 cycles
Alkali lignin-derived hierarchical porous carbon	285 (0.2 A/g)	9 (~6)**	52 (1900)**	–
Alkali lignin	235 (0.5 A/g)	–	–	92%
Technical lignin-derived hierarchical porous carbon	268	40	–	93%
Kraft lignin-derived porous carbon	250 (1 A/g)	78 (47)**	748 (12300)**	96% after 5000 cycles
Corn stalk lignin-derived cage-like mesoporous carbon	215 (0.5 A/g)	–	–	95% after 5000 cycles
Lignin porous carbon	175 (0.5 A/g)	55	23000	100% after 2000 cycles
Alkali lignin-derived porous carbon	170 (0.1 A/g)	–	–	–
Alkali lignin-derived 3D hierarchical porous carbon	165 (0.05 A/g)	~6 (~4)**	15 (1070)**	97% after 5000 cycles
Enzymatic hydrolysis lignin-derived hierarchical porous carbon aerogel	145 (0.5 A/g)	–	–	96% after 2000 cycles
Kraft lignin-derived mesoporous carbon	100 (2 mV/s)	–	–	–
CARBON COMPOSITES				
Lignosulfonate lignin/graphene hydrogels	550 (1 A/g)	–	–	84% after 1000 cycles
Softwood sodium lignosulfonate lignin-rGO* composite	430 (10 mV/s)	–	–	96% after 3000 cycles

Lignosulfonate-functionalized graphene hydrogels	430 (1 A/g)	14 (12)**	500 (5000)**	84% after 10000 cycles
Hardwood lignin/cellulose acetate CF*	345 (0.1 A/g)	32	400	–
Kraft lignin-modified HNO₃-treated active carbon	295 (1 A/g)	–	–	98% after 1000 cycles
Lignosulfonate lignin/single-walled CNT* hydrogel	290 (0.5 A/g)	–	–	80% after 10000 cycles
Graphene-soda bagasse lignin composite	210 (1 A/g)	–	–	88% after 15000 cycles
Alkali lignin-rGO*	190 (0.5 A/g)	–	–	87% after 10000 cycles
Kraft lignin/CNT*	145 (50 mV/s)	–	–	93% after 500 cycles
Lignin/rGO*	35 (0.1 A/g)	–	–	79% after 1000 cycles

* Where DMF is dimethylformamide, PVA is polyvinylalcohol, PAN is polyacrylonitrile, PEO is polyethylene glycol, PMMA is polymethyl methacrylate, PVP is polyvinyl pyrrolidone, PEGL is polyethylene glycol, CNT is a carbon nanotube, CF is carbon fiber, CNF is carbon nanofiber, rGO is reduced graphene oxide. ** In Table 3, the energy and power density values presented in parentheses () represent the values corresponding to the highest power density achieved at a lower energy density.

2.3.2. Pseudocapacitors

Unlike EDLCs, pseudocapacitors involve surface reversible Faradaic (redox) reactions via electron charge transfer at the electrode's reactive sites. Common pseudocapacitive materials include MOs and conducting polymers (CPs). MOs with higher oxidation states are ideal for supercapacitor electrodes, but their practical application is limited by issues such as agglomeration and surface area tailoring challenges. Faradaic processes can develop charge transfer resistances, affecting rate capabilities and cycle stability. These Faradaic redox reactions occur on the surfaces of the solid electrodes and in the bulk near those surfaces; therefore, the specific capacitances and energy densities of pseudocapacitors are much larger than those of EDLCs. The theoretical specific pseudo-capacitance of MOs is calculated as:

$$C_p = \frac{n \cdot F}{M \cdot V} \quad (\text{Equation 4})$$

where n is the mean number of electrons transferred in a one-way redox reaction, F is the Faradaic constant, M is the specific MO's molar mass, and V represents the potential window or operating voltage range over which the material is pseudocapacitive (Zhi et al., 2013).

A conventional supercapacitor cell comprises a pair of electrodes connected in series, separated by an insulating separator (Figure 6). Its electrical behavior can be modeled by an equivalent circuit, which captures the contributions of various physical processes in the cell. C_{dl} represents

the capacitance formed at the electrode-electrolyte interface due to the EDL (described by Equation 3). C_p represents capacitance due to the fast, reversible redox reactions. R_r represents the resistance to charge transfer during Faradaic reactions and is more relevant in pseudocapacitors than EDLCs. R_{ESR} represents the combined resistance of the electrolyte, electrode material, and current collectors. It limits the device's power density and determines the time constant τ .

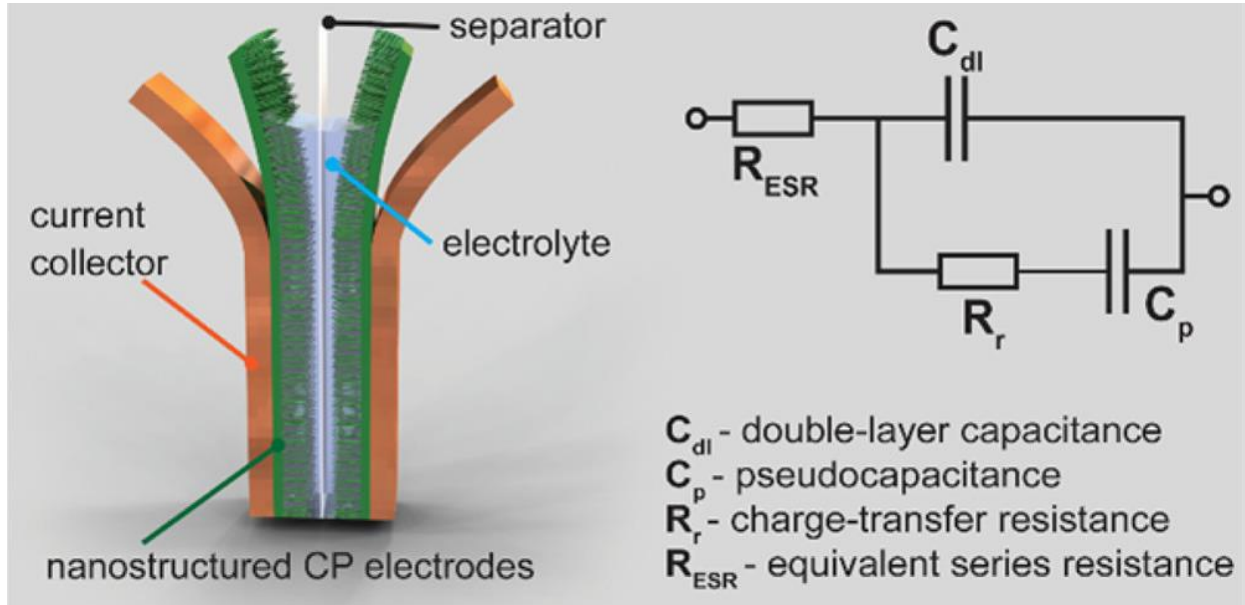


Figure 6. Representation of a symmetric pseudocapacitor with two conducting polymer (CP) electrodes separated by a separator b) an equivalent circuit diagram of a supercapacitor that models the electrical behavior of the cell. Reproduced with permission from Bryan et al., 2016.

Wood-derived carbon materials primarily act as EDLCs due to their high surface area and porous structure, offering low R_{ESR} and rapid ion transport for high power density. However, they do not exhibit pseudocapacitive behavior inherently except for certain components, particularly lignin, which show potential for pseudocapacitance under specific conditions. Lignin, in its natural state, contains quinone groups that undergo redox reactions, enabling the storage and release of both electrons and protons, which gives it pseudocapacitive properties. However, raw lignin typically exhibits low electrical conductivity and limited porosity, which restricts its ability to effectively store charge. Therefore, it is transformed through suitable carbonization processes to enhance its suitability for energy storage applications. This transformation not only improves its structural properties but also allows for the effective exploitation of its quinone groups, thereby enhancing its overall electrochemical performance. Jyothibasud et al., 2022 discusses how the quinone/hydroquinone (Q/QH₂) redox system in lignin enables the movement of two electrons and two protons during charging and discharging cycles. This reaction, described in their study on rGO-lignin composites in an acid aqueous electrolyte, is represented by the following chemical reaction:



In this context, QH_2 signifies the hydroquinone variant, Q denotes the quinone variant, and rGO serves as a reduced graphene oxide substrate providing conductivity. The redox activity takes place in acidic aqueous conditions and plays a critical role in delivering pseudocapacitive behavior in lignin-based materials. This process involves the reversible exchange of two protons and two electrons within a molecular framework containing six carbon and two oxygen atoms. It results in a theoretical charge storage capability of 2 Farads per 108 grams, translating to 18.5 mF/g, or considering a voltage of 1V capacitance translates to a charge of 1787 C/g (496 mA h/g)

(Jyothibasud et al., 2022). This dual mechanism comprising Faradaic redox reactions and EDLC enables lignin-derived materials to achieve superior charge storage performance.

Cellulose does not inherently show pseudocapacitance, but it can serve as a scaffold or precursor for creating pseudocapacitive materials when combined with other components or when being chemically modified. Wood-derived carbons, although not strictly pseudocapacitive in their minimally processed state, can exhibit some pseudocapacitive behavior due to the presence of heteroatoms like nitrogen, oxygen, and sulfur, which are inherited from the original wood structure. These carbons typically require activation or further treatment to unlock their full pseudocapacitive potential. Additionally, the natural combination of lignin and cellulose in wood forms a promising basis for pseudocapacitive behavior when processed to expose more active sites. Furthermore, the porous structure of wood can be utilized to create high-performance electrodes that combine both EDLC and pseudocapacitance when appropriately functionalized.

2.3.3. EDLC/pseudocapacitor Composites

To overcome the challenges and limitations of pseudocapacitive materials, they are often combined with high specific surface area EDLC materials making composites. These composites enhance charge transport properties and cycle stability by leveraging the high electronic conductivity and surface area of carbon materials with the high capacitance of redox-active MOs. The ion transport time constant (τ) in these composites is calculated as:

$$\tau = \frac{L^2}{D} \quad \text{(Equation 5)}$$

where L denotes the ion transport length and D is the ion diffusion constant (D.W. Wang et al. 2008). The ion transport time constant in a supercapacitor is primarily determined by the pore structure, electrolyte conductivity, and electrode material properties, all of which affect ion mobility and accessibility. For instance, a 3D hierarchical porous scaffold can greatly enhance ion transport kinetics by accommodating large amounts of electrolyte and reducing ion transportation distances, which contributes to superior performance.

Table 4: Device performances of various lignin-based composite supercapacitor electrodes (Q. Cao et al., 2024; Jyothibasud et al., 2022; Tong et al., 2023)

Electrode material	Capacitance (F/g)	Energy Density (Wh/kg)	Power Density (W/kg)	Cycle Stability (%)
LIGNIN CARBON/CONDUCTING POLYMER COMPOSITE				
PANI*/ Sodium lignosulfonate nanocomposite	1200 (1 A/g)	21 (14.5)**	279 (26000)**	87% after 15000 cycles
Ligninsulfonate /PPy*/Phosphomolibdic acid	680 (1 A/g)	–	–	70% after 2000 cycles
Functionalized porous carbon nanospheres/sodium lignosulfonate lignin/PPy* hydrogel	540 (0.5 A/g)	–	–	80% after 7000 cycles
Lignin cellulose nanofibrils/rGO*/PANI*	475 (10 mV/s)	~100 (~25)**	~900 (~11000)**	87 % after 5000 cycles
Alkali lignin/PPy*	444 (1 A/g)	–	–	–

Lignin functionalized graphene hydrogel	410 (1 A/g)	13.8	500	84% after 10000 cycles
PANI* -lignosulfonate lignin	375 (1 A/g)	–	–	74% after 10000 cycles
PANI*/kraft lignin composite	285 (0.5 A/g)	–	–	67.4% after 5000 cycles
PEDOT*/lignosulfonate biocomposite	170 (1 A/g)	–	–	80% after 1000 cycles
Kraft lignin/PEDOT*	97 (0.1 A/g)	–	–	79% after 1000 cycles
PEDOT/ Sodium Lignosulfonate lignin/ PAAQ* [Asymmetric]	75 (1 A/g)	8.2 (6.8)**	700 (5600)**	80% after 10000 cycles
Sodium Lignosulfonate lignin/PPy* hydrogel	1060 mF/cm ² (1 mA/ cm ²)	47 μWh/cm ²	400 μW/cm ²	82.1% after 5000 cycles
LIGNIN CARBON/METAL OXIDE COMPOSITE				
MCNFs@SnO₂	405 (0.5 A/g)	11.5	451	95% after 10000 cycles
Alkali lignin-derived hierarchical porous carbon nanofiber films	250 (0.2 A/g) 145 (20 A/g)	–	–	97% after 1000 cycles
Organosolv lignin-derived CNF* with Fe₃O₄ nanoparticles	215 (0.1 A/g)	43	242	97% after 10000 cycles
Alkali lignin derived carbon/ZnO	195 (0.5 A/g) 150 (20 A/g)	6.7 (5.2)**	198 (11797)**	97% after 5000 cycles
MnO₂/Methanol soluble lignin isolated from kraft lignin-derived CNF*	172 (5 mV/s) 90 (50 mV/s)	6	160	99% after 1000 cycles
MnO₂/Alkali lignin-derived CF*	130 (0.3 A/g)	15	135	–
Electrospun CNF*/MnO₂	85 (250 mA/g)	84	5720	96.5 % after 5000 cycles
MnO₂-deposited CNF* mats	65 (0.1 A/g)	6	160	99% after 1000 cycles
Al foil coated alkaline lignin/MnO₂	380 mF/cm ² (40 m A/g)	6	(355)**	80%
AC*/lignin-MnO₂ [Asymmetric]	22 mF/cm ² (10 mV/s)	–	–	90% after 700 cycles
Al foil coated alkaline lignin–NiWO₄	17 mF/cm ² (0.15 A/g)	8.5	509	84% after 2000 cycles
Al foil coated/AC*/lignin-MnO₂ [Asymmetric]	5.5 mF/cm ² (6 m A/g)	14	(1000)**	97% after 2000 cycles
FUNCTIONAL GROUP DECORATED CARBONS				
OKL*/hierarchical porous nitrogen-doped carbon	410 (1 A/g)	–	–	94% after 1000 cycles

OKL*/HNO₃-treated activated carbon composite	390 (0.5 A/g)	–	–	98% after 2000 cycles
O/N codoped organic solvent lignin-derived porous carbons	370 (10 mV/s)	–	–	100% after 30000 cycles
N doped alkali lignin-derived porous carbon	355 (0.2 A/g)	13	162	99% after 16000 cycles
O/N/S codoped enzymatic hydrolysis lignin hierarchical porous carbon	320 (0.5 A/g)	~17	249	100% after 10000 cycles
N/O lignin-based ultra-fine porous carbon nanofibers	290 (0.1A/g) 160 (20 A/g)	–	–	92% after 10000 cycles
N/S codoped lignin sulfonate porous carbon	270 (0.5 A/g)	~37	62	98% after 10000 cycles
N/S co-doped activated carbon nanofibers	265 (5 mV/s) 150 (50 mV/s)	9	493	99% after 10000 cycles
N/S doped lignin sulfonate-derived porous carbon	240 (1 A/g)	27	10000	95% after 3000 cycles
N/O doped alkali lignin-derived hierarchical porous carbon	235 (0.5 A/g)	~15	450	92% after 10000 cycles
S doped calcium lignosulfonate- derived micro/mesoporous bio-carbon	225 (0.5 A/g)	–	–	99% after 10000 cycles
O doped enzymatic hydrolysis lignin-derived nanoporous carbon	180 (0.5 A/g) 140 (10 A/g)	–	–	–

*Where PANI is polyaniline, PPy is polypyrrole, rGO is reduced graphene oxide, PEDOT is Poly (3,4-ethylenedioxythiophene), PAAQ is poly(aminoanthraquinone), CF is carbon fiber, CNF is carbon nanofiber, AC is activated carbon, OKL is Oxidized Kraft lignin. **In Table 4, the energy and power density values presented in parentheses () represent the values corresponding to the highest power density achieved at a lower energy density.

Table 4 presents the electrochemical performance of various lignin-based composite and functional group-decorated supercapacitor electrodes, organized in descending order of specific capacitance alongside their corresponding energy density, power density, and cycle stability. Across the composites, the capacitance varies widely, with some high-performance materials such as polyaniline (PANI)/lignin and Ligninsulfonate/polypyrrole (PPy) composites achieving capacitance values of 1200 F/g and 680 F/g, respectively, indicating that the addition of CPs can significantly enhance capacitance. However, cycle stability, an essential metric for longevity, with CPs are compromised making them less attractive for long-term applications. Meanwhile, lignin-based carbon/MO composites exhibit remarkable retention (above 95%) over thousands of cycles. In terms of power density, most composites featuring MOs like MnO₂ or CPs (e.g., PANI, PPy) typically show enhanced performance due to improved ion transport and conductivity. However, composites with functional group decorated lignin or single additives like PEDOT show lower energy density and power output, suggesting that multi-component systems are generally more effective for energy storage applications.

Overall, the table indicates that lignin-based composites offer enhanced capacitance and energy density compared to lignin-based EDLC electrodes in **Table 3**, attributed to the inclusion of conductive polymers, MOs and functional groups that introduce pseudocapacitive behavior. However, EDLC electrodes generally maintain higher power densities and, in some cases, slightly better cycle stability. This variability underscores the versatility of lignin as a base material and the importance of composite design in optimizing supercapacitor performance.

2.4. Classification of Supercapacitors Based on Device Configuration

Supercapacitors can also be classified based on device configurations into symmetric, asymmetric, and hybrid supercapacitors.

2.4.1. Asymmetric Supercapacitors

Symmetric supercapacitors consist of identical EDL-capacitive or pseudocapacitive electrodes, while asymmetric supercapacitors pair different EDL-capacitive and pseudocapacitive electrodes. Asymmetric configurations are efficient in extending the cell voltage by using electrolytes with highly stable potential windows or MOs with higher overpotentials.

One strategy to increase the working voltage in an EDLC system involves using imbalanced electrode masses, as demonstrated in the following equations:

$$Q_+ = Q_- \quad (\text{Equation 6})$$

$$\frac{V_+}{V_-} = \frac{m_- C_-}{m_+ C_+} \quad (\text{Equation 7})$$

where Q represents the charges, V the potential windows, C are the specific capacitances, and m are the masses of the positive and negative electrodes, respectively (J. Li et al., 2017). The positive (+) and negative (-) indices signify the two electrodes in the supercapacitor, where the positive electrode undergoes oxidation (electron loss), and the negative electrode undergoes reduction (electron gain) during charge/discharge. The equations outlined here emphasize the importance of carefully balancing the masses and capacitances of the positive and negative electrodes to optimize supercapacitor performance. Specifically, Equation 7 reveals that the voltage distribution between the two electrodes can be controlled by adjusting the ratio of their respective masses and capacitances. This balance is crucial for maximizing the working voltage of the supercapacitor avoiding overpotential effects that might lead to electrolyte decomposition or electrode degradation. By tuning the electrode masses, especially in asymmetric configurations, the system can take advantage of materials with different electrochemical properties such as pairing a high-capacitance material (e.g., AC) with a material capable of operating at a wider potential range (e.g., MOs or CPs) while maintaining charge balance (as shown in Equation 6). This strategy allows for the extension of the supercapacitor's voltage window, enabling better energy storage capabilities. Additionally, this approach offers a practical means to optimize the performance of supercapacitors for specific applications, whether the focus is on maximizing energy density, improving power density, or extending cycle life, based on the needs of the end-use application.

Table 5 provides a comparative analysis of lignin-based asymmetric supercapacitor systems, highlighting how differences in anode-cathode electrode material and mass differences influence key performance metrics such as capacitance, energy density, power density, and cycle stability. A key takeaway from the analysis is that while lignin-based materials offer promising performance, the overall performance metrics vary significantly depending on the materials used

Table 5: Device performances of various lignin-based asymmetric supercapacitors (Q. Cao et al., 2024; Jyothibasud et al., 2022; Tong et al., 2023)

Electrode material	Capacitance (F/g)	Energy Density (Wh/kg)	Power Density (W/kg)	Cycle Stability (%)
Enzymatic-hydrolysis lignin-derived 3D HPC[*]//AC[*]	432 (0.5 F/g)	34 (16) ^{**}	237 (14300) ^{**}	87% after 10000 cycles
PEDOT[*]+ Lignin/PAAQ[*]// PEDOT[*]/PAAQ[*] (Ajjan et al., 2017)	420 (1 A/g)	8.2 (6.8) ^{**}	700 (5600) ^{**}	80% after 10000 cycles
O/N/S codoped HPC[*]//AC[*]	318 (0.5 A/g)	~17	249	99.6% after 10000 cycles
Al/AC[*]/lignin-MnO₂// Al/AC[*] (Jha, Mehta, Chen, Ma, et al., 2020)	173 (10 mV/s)	14	1000	99% after 1000 cycles
HPC[*] with different electrode masses (Salinas-Torres et al., 2016)	137	6.3	1300	100% after 5000 cycles
Lignin/PEDOT[*]// partially rGO[*]	35 (0.5 A/g)	–	–	79% after 1000 cycles
Al foil/alkali lignin/MnO₂//Al foil/AC (Jha, Mehta, Chen, Likhari, et al., 2020)	379 mF/cm ² (40 mA/g)	6	355	80% after 3000 cycles

^{*} Where HPC indicates hierarchical porous carbon, AC is activated carbon, PEDOT is Poly (3,4-ethylenedioxythiophene), PAAQ is poly(aminoanthraquinone), CNFs are carbon nanofibers. ^{**} In Table 5, the energy and power density values presented in parentheses () represent the values corresponding to the highest power density achieved at a lower energy density.

in this configuration of the supercapacitors. For instance, enzymatic hydrolysis lignin-derived 3D hierarchical porous lignin (HPC)//AC (432 F/g and 34 Wh/kg) show notable capacitance and reasonable cycle stability (87% after 10000 cycles, respectively), also their energy densities are reasonably high even at a higher power density of 14300 W/kg likely due to the use of ionic electrolytes and interconnected porous structure that enhances ion transport kinetics. The O/N/S codoped HPC//AC device demonstrates relatively lower capacitance (318 F/g) and energy density (~17 Wh/kg) but achieves an outstanding 99.6% stability after 10000 cycles, emphasizing the desirable performance longevity in asymmetric systems. Devices such as HPC with electrodes of differing masses exhibit remarkable cycle stability 100% after 5000 cycles. However, this performance comes at the cost of reduced capacitance and energy density, likely attributable to the intrinsic properties of the materials. The PEDOT+Lignin/PAAQ//PEDOT/PAAQ (where PAAQ

stands for poly(aminoanthraquinone)) device demonstrates relatively low capacitance in acidic aqueous electrolyte medium (74 F/g) and retains 80% stability after 10000 cycles. This outcome suggests that the PEDOT-lignin composite delivers only moderate performance, emphasizing the critical need to optimize the material combinations for the anode, cathode and electrolyte to fully leverage the benefits of an asymmetric assembly. Since also the research with it is limited, further exploration and optimization of the electrode designs from lignin-based materials will be crucial to strike an effective balance between high performance and long-term reliability.

The main difference between composite electrodes and asymmetric devices lies in their material configurations. Composite electrodes combine various materials, such as conductive carbons, MOs, and CPs, to enhance energy and power densities by leveraging the strengths of each electrode. Asymmetric devices, in contrast, use two electrodes with different materials that allow them to achieve a more optimal energy-power trade-off. However, while asymmetric devices often offer superior performance, they may not always incorporate sustainable materials in both electrodes. Composite electrodes, particularly those based on renewable materials like lignin, provide a more environmentally friendly alternative with some compromised performance, making them a preferable option when sustainability is a key consideration.

2.4.2. Hybrid Supercapacitors

Hybrid supercapacitors combine the strengths of both batteries and traditional supercapacitors by utilizing distinct electrode materials. Unlike conventional LIBs, which use graphite as the negative electrode, hybrid supercapacitors employ a carbon-based electrode (typically AC) for capacitive storage and a battery-type electrode (often lithium-based) for Faradaic reactions. While both hybrid and asymmetric supercapacitors use different electrode materials, hybrid systems combine battery-type and capacitive electrodes. This unique configuration allows hybrid supercapacitors to achieve higher energy density than traditional supercapacitors while maintaining rapid charge and discharge capabilities. The carbon-based electrode in hybrid supercapacitors is optimized for surface area and pore structure to maximize ion adsorption, whereas the graphite in LIBs is designed for lithium intercalation. The battery-type electrode in hybrid supercapacitors, usually composed of MOs or other lithium-intercalating materials, provides higher energy storage capacity through redox reactions. This asymmetric design enables hybrid supercapacitors to bridge the gap between the high-power density of supercapacitors and the high energy density of batteries, offering a balance of both properties in a single device. The result is a more versatile energy storage solution that can deliver quick bursts of power while still maintaining a higher overall energy capacity compared to traditional supercapacitors.

Lithium-ion capacitors (LICs) exemplify the innovative approach of hybrid supercapacitors, leveraging the strengths of both battery and capacitor technologies. These devices typically employ a lithium-based cathode (such as LiCoO_2 or LiFePO_4) paired with an AC anode, enabling high energy density and rapid charge-discharge cycles. The use of ionic liquids or organic electrolytes in LICs allows for operation at higher voltages compared to aqueous systems, further enhancing energy density. While metal oxides like nickel cobalt oxide (NiCo_2O_4) are also common in hybrid systems, LICs specifically utilize lithium-based cathodes to optimize energy storage. This configuration capitalizes on the EDL formation at the carbon electrode and the Faradaic reactions at the lithium-based electrode, resulting in a synergistic effect that enhances overall performance

In the literature, many research and review articles often conflate the terms composite supercapacitors and hybrid supercapacitors, leading to significant confusion. This distinction is critical, as hybrid systems inherently involve a combination of battery-like Faradaic behavior with capacitor-like EDLC behavior, whereas composites typically refer to materials designed to enhance specific properties of a single electrode or system. To clarify, hybrid supercapacitors must

Table 6: Device performances of various lignin-based hybrid supercapacitors (Tong et al., 2023)

Electrode material	Capacitance (F/g)	Energy Density (Wh/kg)	Power Density (W/kg)	Cycle Stability (%)
NiCo ₂ O ₄ @CNFs//N-rGO* (Lei et al., 2017)	1757 (2 mA/cm ²)	48	800	138% after 5000 cycles
Bimetallic Ni ₃ Co ₁ WO ₄ nanoparticles/enzymatic-hydrolysis lignin-derived 3D HPC*//AC*	1084 (0.5 A/g)	106	400	81% after 10000 cycles
Lignin-derived CNFs* - NiMnS//AC* (Ranjith et al., 2021)	652 C/g (1 A/g) (~400 F/g)	52	800	91% after 5000 cycles
N-doped kraft lignin derived porous carbon//NiCo layered double hydroxide (Kim et al., 2022)	301 (1 A/g)	78 (47)**	748 (12294)**	91% over 20000 cycles
AILCFN* - 3//AILCFN*/Ni-Co-S (M. Zhou et al., 2021)	279 (0.14 A/g)	31	800	99% after 10000 cycles
Zn//Lignin-derived HPCs* (L. Zhao et al., 2022)	298 (0.1 A/g)	135	101	97% after 8000 cycles
ZIHC* in air with lignin-derived HPCs*//Zn foil as an anode (L. Wang et al., 2024)	292 (0.1 A/g)	97 (40)**	79 (7500)**	95% after 12000 cycles
Lignin/NiCoWO ₄ /AC*	862 mF/cm ²	5.8	(855)**	100% after 2000 cycles

* Where HPC indicates hierarchical porous carbon, AC is activated carbon, AILCFN stands for activated interconnected lignin-derived carbon fibrous network, ZIHC is Zinc-ion hybrid capacitor, CNFs is carbon nanofibers. ** In Table 5, the energy and power density values presented in parentheses () represent the values corresponding to the highest power density achieved at a lower energy density.

include at least one electrode with battery-like behavior, such as intercalation or surface redox reactions over a broader potential range, while composites improve the physical or electrochemical properties of a given electrode without introducing distinct battery-like behavior.

As noted by (Brousse et al., 2015), Ni(OH)₂ electrode types exhibit battery-like behavior in terms of their redox mechanisms, despite being commonly grouped under asymmetric configurations in the literature (Y. Wang et al., 2016). In this thesis in **Table 6**, NiCo-based systems like NiCo₂O₄@CNFs//N-rGO and Ni₃Co₁WO₄//AC are categorized as hybrid supercapacitors. This classification is justified by their exceptionally high values of capacitance, energy density, and power density, which surpass typical asymmetric configurations. For instance, NiCo₂O₄@CNFs//N-rGO achieves a capacitance of 1757 F/g, an energy density of 48 Wh/kg, and a cycle stability of 138% after 5000 cycles. The increase in capacitance to 138% has been attributed to the gradual activation of the active materials on the working electrode during the repeated charge-discharge process. Similarly, Ni₃Co₁WO₄ nanoparticles//enzymatic-hydrolysis lignin-derived 3D HPC delivers 1084 F/g, 106 Wh/kg energy density, and 81% stability after 10000 cycles. The N-doped kraft lignin-derived porous carbon//NiCo lignin-derived hybrid device

Table 6, besides displaying NiCo-based electrodes, highlights the performance metrics of lignin-based hybrid supercapacitor systems, primarily zinc-ion hybrid capacitors (ZIHCs), showcasing their strengths in high capacitance, energy density, and stability over extensive cycles. Systems like lignin-derived CNFs-NiMnS//AC demonstrate peak capacitance (400 F/g), while Zn//LHPCs leads in energy density (135 Wh/kg), though with relatively low power density. All systems show strong cycle stability, with activated interconnected lignin-derived carbon fibrous network (AILCFN)-3//AILCFN/Ni-Co-S retaining 99.6% capacitance after 10000 cycles, indicating excellent durability for sustainable energy storage applications. However, studies remain limited for ZIHCs and other hybrid systems at this point, suggesting potential need for further exploration and optimization in materials integration.

2.5. Performance of Wood-based Supercapacitors in the Energy Landscape

To analyze the electrochemical performances of the prominent supercapacitor types their Ragone plots were shown in [Paper IV](#), where our analysis observed distinct clusters of energy density vs power density across different supercapacitor technologies, with the dotted black box highlighting the 'prime region' enveloping most of the data.

As shown in the top-left plot (Figure 7), hybrid and asymmetric supercapacitors perform well in terms of energy density, with a dense prime region. These supercapacitors achieve higher energy density with only a moderate compromise on power density, leveraging material combinations to maximize energy storage capacity while retaining sufficient power output. In fact, the cluster of devices with higher energy density is larger in this category of devices even beyond the prime region. This balance positions them well for applications that require high energy density with reasonable compromise on power.

In comparison, wood-based supercapacitors fall somewhat short of reaching higher energy density levels beyond prime region achieved by hybrid, asymmetric, and other advanced supercapacitors. While devices in the prime region seem to exhibit a balanced profile in terms of energy density and power density, they do not achieve the superior values needed for high-performance applications, highlighting the need for improvement. Enhancing the energy density of wood-based supercapacitors will require controlled engineering of these materials, focusing on creating optimized structures and channels that promote efficient energy storage. By refining the

microstructure, it may be possible to increase the accessible surface area, improve ion transport, and enhance capacitance.

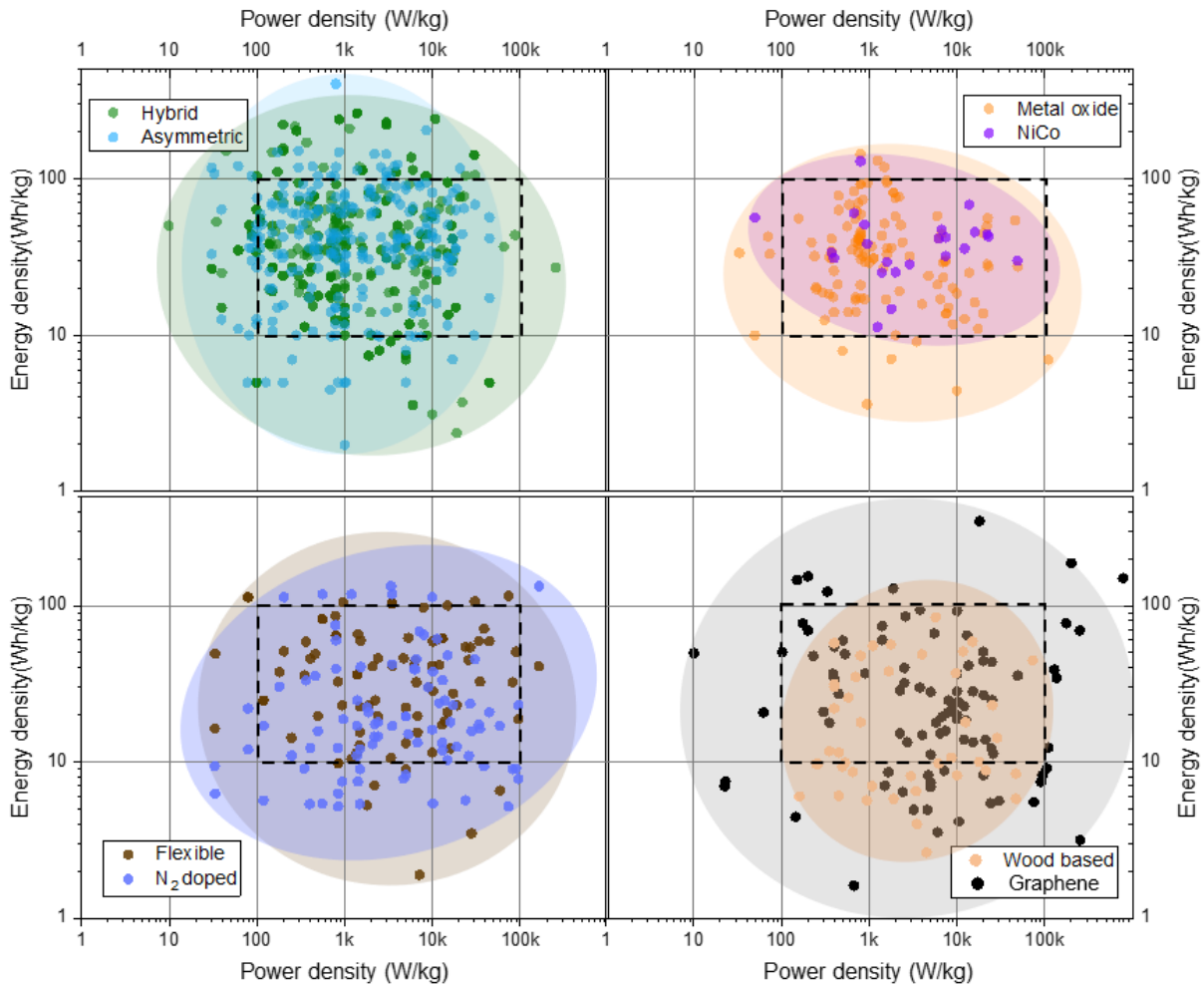


Figure 7. Ragone plot comparing various lab-scale supercapacitor technologies developed over the past two decades (Paper IV).

Outliers in the non-dense zone of the data may indicate that certain samples exceed typical performance ranges, which may result from specific material optimizations or testing conditions. These outliers are valuable for identifying best-case scenarios but may not represent consistent performance across all samples.

In other categories, MO and NiCo supercapacitors (top-right plot) achieve high power density but lower energy density, suitable for short, high-power applications. Flexible and nitrogen-doped supercapacitors (bottom-left) and graphene-based supercapacitors (bottom-right) show varying performance, with graphene achieving some of the highest energy density and power density values. Wood-based supercapacitors, although below the peak energy density and power density of these advanced materials, stand out for their sustainability.

2.6. Deconvolution of Different Capacitive Behaviors

Deconvoluting different capacitive behaviors, such as EDLC and pseudocapacitance, is key to engineer supercapacitor electrodes and for device design. By isolating the specific contributions from each mechanism, researchers can optimize materials for target characteristics: enhancing

energy density through pseudocapacitive materials or achieving cycle stability with EDLC materials. This level of distinction also enhances device modeling accuracy, allowing prediction of supercapacitor performance across various conditions and applications, from delivering short, high-power bursts to providing stable, long-term energy storage. Additionally, deconvolution improves the testing and characterization process and helps in evaluating and comparing materials objectively by isolating each contribution.

The observable differences between EDLC and pseudocapacitive/battery-like materials arise primarily from their distinctly different thermodynamic and kinetic properties. To evaluate these differences, numerous electrochemical techniques have been developed to deconvolute the contributions from basic charge storage mechanisms, that originate from EDL formation and redox reactions or diffusion-controlled processes (such as ion intercalation).

The general dependence of measured peak current (i_p) from a cyclic voltammogram measurement at different scan rates (v) is given by:

$$i_p = k \cdot v^b \quad (\text{Equation 8})$$

For pseudocapacitive materials, which undergo fast surface or bulk redox reactions that are not diffusion-controlled, the peak current varies linearly with scan rates, as demonstrated by (Conway & Kannangara, 1987; T. -C. Liu et al., 1998). In this case, b in the equation is near 1. When the storage process is purely diffusion-controlled, b is equal to $1/2$.

For systems exhibiting both forms of storage behavior (i.e., hybrid energy storage), J. Wang et al., 2007 proposed a method to deconvolute the contributions by correlating voltage-dependent current with scan rates:

$$i_p = k_1 v + k_2 v^{1/2} \quad (\text{Equation 9})$$

k_1 (capacitive) and k_2 (diffusion controlled) are proportionality constants determined from the slope and Y-intercept of the plot of $i_p/v^{1/2}$ versus $v^{1/2}$ as shown in Figure 8.

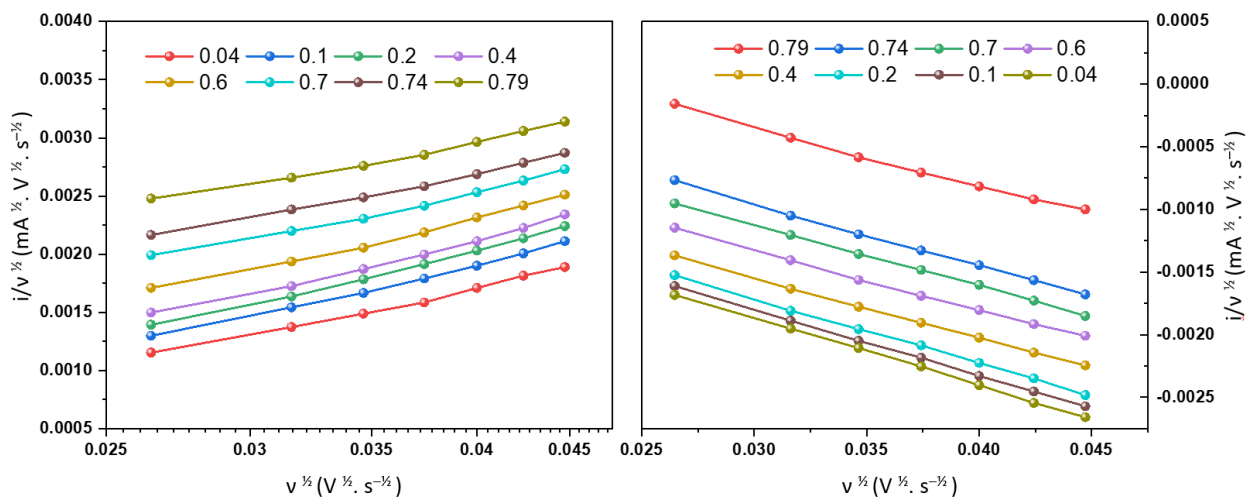


Figure 8. Linear fitting of the anodic and cathodic CV scan rates at different voltage points (Paper I).

Trasatti et al. proposed another method by observing the relationship of cyclic voltammetry charge with varying scan rates (Ardizzone et al., 1990). In this method, the dependence of surface (Q_s) and bulk (Q_b) charge contributions were measured as the total charge Q_t ,

$$Q_t = Q_s + Q_b \quad (\text{Equation 10})$$

The surface charge Q_s here is independent of the scan rate v , representing fast, surface-confined processes. In contrast, the bulk charge Q_b arises from diffusion-controlled processes governed by Fick's laws of diffusion. While the diffusion-controlled current in cyclic voltammetry increases with the square root of the scan rate (scales as $v^{1/2}$), the corresponding charge contribution decreases with $1/v^{1/2}$. This is because, at higher scan rates, there's less time for diffusion processes to contribute to the total charge. Consequently, the total charge $Q_t(v)$ exhibits a characteristic dependence on scan rate v , expressed as:

$$Q_t(v) = Q_s + c_1 v^{-1/2} \quad (\text{Equation 11})$$

Here c_1 is a constant related to the bulk diffusion-controlled charge contribution. This equation represents that while the diffusion-controlled current increases with the square root of the scan rate, the corresponding charge contribution decreases with the square root of the scan rate due to the shorter time available for the diffusion process at higher scan rates.

Q_s is determined from the extrapolation of $Q_t(v)$ as $1/v^{1/2} \rightarrow 0$ using Equation (11). At very high scan rates ($v \rightarrow \infty$), the bulk charge contribution becomes negligible ($1/v^{1/2} \rightarrow 0$) leaving only the surface charge: $Q_t(v) \rightarrow Q_s$. At lower scan rates, $1/v^{1/2}$, becomes significant, and the total charge includes both surface and bulk contributions. Thus Equation (11) effectively separates these two contributions by exploiting their distinct scan rate dependencies.

As a data-fitting strategy, an alternative to Equation 12 can be employed as below to fit specific empirical plots.

$$\frac{1}{Q_t(v)} = \frac{1}{Q_t} + c_2 v^{1/2} \quad (\text{Equation 12})$$

Here $Q_t(v)$ is the total charge at a specific scan rate v , Q_t is the expected limiting total charge as the scan rate approaches zero ($v \rightarrow 0$), where bulk contributions dominate, and c_2 is a proportionality constant related to the material's response to the scan rate.

The equation representing the reciprocal charge dependence on scan rate derives from two key assumptions where at low scan rates ($v \rightarrow 0$), $Q_t(v)$ approaches Q_t , where bulk storage dominates. A term proportional to $v^{1/2}$ is included to account for diffusion-limited contributions to bulk charge. The equation is thus attempting to model the transition from pure surface charge behavior to a regime dominated by bulk contributions as v changes. Plotting $1/Q_t(v)$ against $v^{1/2}$ allows for the extrapolation of $1/Q_t$ (i.e., the intercept), which corresponds to the maximum storage capacity due to bulk processes. When the system exhibits both forms of storage behavior, it is considered hybrid, making it easier to distinguish. However again, this method is also suitable only for a limited range of smaller scan rates.

Gibson & Donne, 2017 proposed a different method based on the current response from each potential step as a function of time. This method relies on the difference in equilibration time depending on the type of material. Materials exhibiting EDL behavior equilibrate quickly, while diffusion-limited behavior equilibrate slowly. This approach is particularly useful for understanding diffusion-induced processes and studying the efficiency of diffusion in electrodes with higher mass loadings. The Step Potential Electrochemical Spectroscopy (SPECS) model

includes currents representing the generation of an EDL at the geometric (i_{DL1}) and porous surface (i_{DL2}), as well as a current associated with the diffusion-limited (i_D) and residual processes (i_R).

The total current i_T of SPECS data is calculated as follows:

$$i_T = i_{DL1} + i_{DL2} + i_D + i_R \quad (\text{Equation 13})$$

Shao et al., 2019 proposed Multiple Step ChronoAmperometry (MUSCA) to reduce the ohmic drop contribution from SPECS, allowing for accurate investigation of the electrochemical kinetics of pseudocapacitive electrodes. MUSCA computes ohmic drop-corrected cyclic voltammograms of pseudocapacitive electrodes at various potential scan rates. The surface and bulk process current contributions are then effectively recovered using Wang's methods by showing current-voltage curves with a reduced ohmic drop at various scan speeds. The difference in charge storage mechanisms between supercapacitors and batteries varies largely because of their differences in thermodynamics and kinetics. As a result, for the convenience of evaluation numerous electrochemical techniques for deconvoluting the contributions from basic charge storage mechanisms such as the EDL and diffusion-limited processes have been devised.

2.7. Classification of Supercapacitor Configuration Based on Application

2.7.1. Micro-supercapacitors

Micro-supercapacitors (MSCs) represent a cutting-edge solution in the realm of energy storage, specifically tailored for applications demanding compact size and high-power density. These miniature devices find extensive use in portable and wearable electronics, in biomedical implants, in sensors for the IoT and in other miniaturized devices where rapid energy delivery and long-term stability are crucial (Bu et al., 2020; Xu et al., 2024).

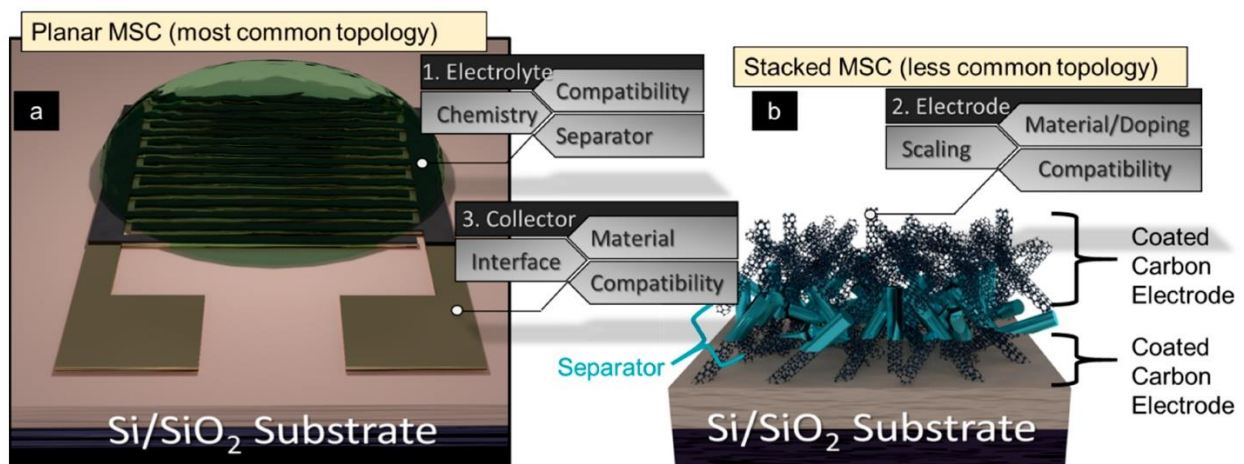


Figure 9. Schematic of MSCs designs - (a) planar and (b) stacked - illustrating the three primary areas for performance improvement: electrolyte, electrode, and current collector. Each area comprises three subset groups offering opportunities for optimization, which are the focus of this overview. Reproduced with permission from Smith et al., 2019.

Fabrication of MSCs involves sophisticated microfabrication techniques to achieve their small footprint with optimized performance. Electrodes are typically constructed using methods like photolithography or inkjet printing, allowing precise deposition of materials such as activated carbon or graphene onto substrates. Their topologies are typically planar or stacked (Figure 9).

Solid-state or gel electrolytes are integrated to enhance safety and compactness, filling the micro-gaps between electrodes.

Micromachining and additive manufacturing offer precise micrometer-scale control over electrode placement and electrolyte distribution, enabling the fabrication of MSCs with charge and discharge

Table 7: Device performances of various lignin-based micro-supercapacitors

Electrode material	Electrolyte	Capacitance (mF/cm ²)	Energy Density (mWh/cm ²)	Power Density (mW/cm ²)	Cycle Stability (%)
L-LSG*/Mn₃O₄-3 (Remesh, Loganathan, et al., 2024)	PAAS*/K ₂ SO ₄	136 (0.08 mA/cm ²)	~0.011	0.27	93% after 5000 cycles
L-LSG*/Mn₃ (Remesh, Loganathan, et al., 2024)	PAAS*/K ₂ SO ₄	40 (0.08 mA/cm ²)	~0.003	0.25	89% after 5000 cycles
Black liquor lignin/Mg-Al LDH* composite (Remesh, Vasudevan, Sivakumar, et al., 2023)	PAAS*/K ₂ SO ₄	40 (0.08 mA/cm ²)	~0.003	0.055	89% after 5000 cycles
L-LSG* (Remesh, Vasudevan, Perumal, et al., 2023)	PAAS*/K ₂ SO ₄	31 (0.08 mA/cm ²)	~0.002	0.25	88% after 5000 cycles
L-LSG*/SS/K⁺ (Remesh, Vasudevan, et al., 2024)	PAAS*/K ₂ SO ₄	22 (0.08 mA/cm ²)	~0.002	0.25	83% after 5000 cycles
3D- LSG (W. Zhang et al., 2018)	PVA/H ₂ SO ₄	25	1 mWh/cm ³	2 W/cm ³	99% after 12000 cycles
Lignin/PAN (S. Wang et al., 2019)	PVA/H ₂ SO ₄	6.7 (0.9 F/cm ³)	–	–	–
3HPC/WO₃ (Shi et al., 2021)	PVA/H ₂ SO ₄	432 F/g (0.5 A/g)	34 Wh/kg (16 Wh/kg)	14 W/kg (237 W/kg)	87% after 10000 cycles

* Where L-LSG is lignin-derived laser scribed graphene, LDH is layered double hydroxide, PAAS is sodium polyacrylate, HPC is hierarchical porous carbon. ** In Table 7, the energy and power density values presented in parentheses () represent the values corresponding to the highest power density achieved at a lower energy density.

rates on the order of 200 to 1000 mV/s and cycle stability exceeding 10000 cycles (Dinh et al., 2023). Consequently, MSCs will play a crucial role in driving the miniaturization of next-generation energy-efficient electronics

Current research focuses on improving energy density, developing solid-state electrolytes, and enhancing fabrication techniques for large-scale production. The field is moving towards 3D architectures, novel materials, and integrated systems combining energy harvesting and storage capabilities (Dinh et al., 2023; Shen et al., 2017).

Table 7 provides a comparative analysis of energy density, power density, and cycle stability across various lignin-based MSCs, revealing the influence of material compositions and configurations on performance. The lignin-derived laser scribed graphene (L-LSG)/Mn₃O₄-3 configuration offers a performance uncompromised profile, with an energy density of 0.011

mWh/cm² and high cycle stability (93% retention over 5000 cycles), demonstrating both durability and performance. The 3D-LSG structure stands out for its exceptional cycle stability of 99% after 12000 cycles, underlining the effectiveness of 3D architectures in prolonging device lifespan. Other materials, like laser scribed graphene and Mg-Al layered double hydroxide (LDH), show moderate energy and power densities but strong cycle retention, reflecting their endurance in applications where longevity is key. Overall, lignin-based MSCs exhibit versatile performance profiles, with specific configurations excelling in energy or stability metrics, though achieving optimal performance across all parameters with more materials should continue as a research focus.

2.7.2. Flexible and Wearable Supercapacitors

Flexible and wearable supercapacitors are another rapidly advancing class of energy storage devices designed to meet the growing demand for portable and wearable electronics. These supercapacitors are characterized by their need to maintain high performance under mechanical deformation, making them suitable for integration into flexible substrates. Key to the development of flexible supercapacitors is the use of innovative materials and fabrication techniques. Carbon-based materials, such as activated carbon fibers, graphene, and CNTs, are frequently employed due to their excellent electrical conductivity, mechanical flexibility, and high surface area. These materials are often combined with CPs or MOs to enhance capacitive performance.

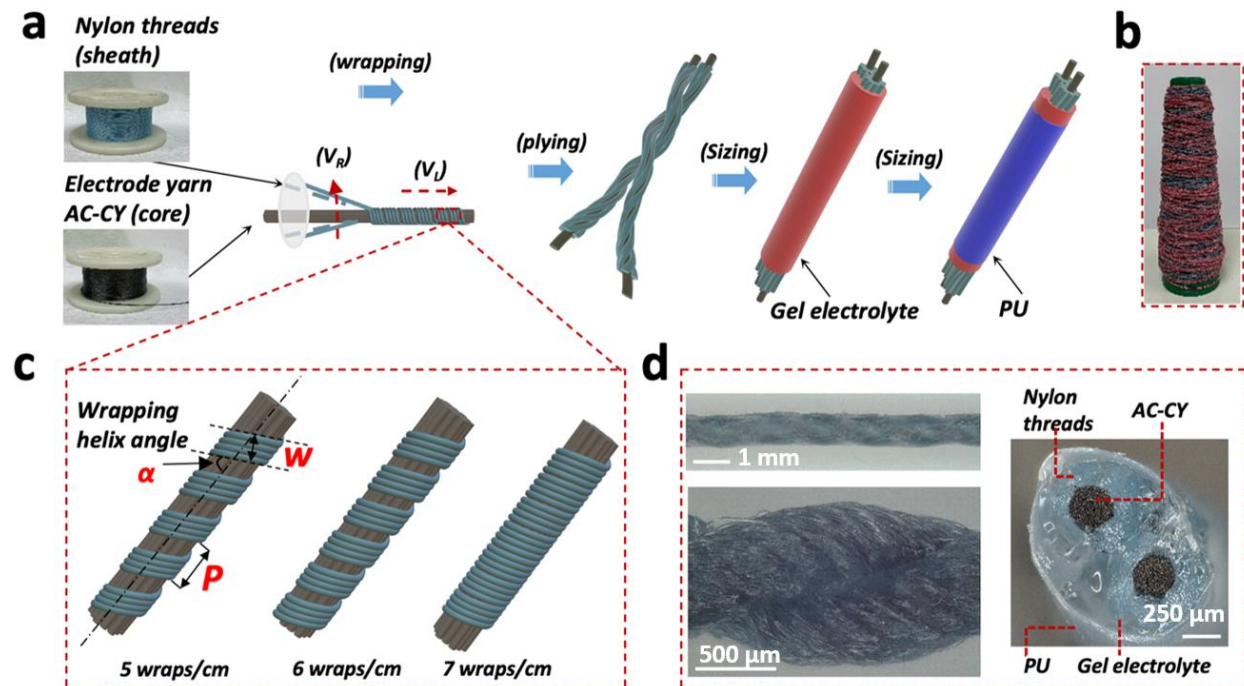


Figure 10. (a) Schematic illustration of the fabrication process for thread-based yarn capacitors (TYCs) incorporating separator threads. (b) Photograph of tens of meters-long TYCs wound on a spool, with different colors arising from the incorporation of various nylon separator threads. (c) Schematic representation of the wrapping density of separator threads in activated carbon-based yarn capacitors (AC-CYs). (d) Optical microscopic images showing the side and cross-sectional views of the TYCs. Reproduced with permission from He et al., 2022.

A notable advancement in this field is the development of spin yarn supercapacitors (Figure 10). These devices involve spinning carbon-based fibers into yarns that are then woven into textiles. Spin yarn supercapacitors retain the flexibility of the fiber while providing substantial energy

storage capacity. They can be seamlessly integrated into clothing and other wearable items, powering various small electronic devices and sensors embedded in smart textiles.

Qu et al. (2022) developed a PAN/lignin-based carbon fiber (LCF) from industrial lignin using an economical and scalable melt-spinning process. This LCF shows excellent strength and flexibility, making it a promising alternative to PAN-based carbon fibers for structural applications. The material achieved a high areal specific capacitance of 0.14 F/cm² at 0.19 mA/cm² and retained this capacitance even when subjected to bending and twisting. In fiber-based supercapacitors, capacitance reported as F/cm² typically refers to the outer, macroscopic surface area of the fiber or yarn. This is calculated using the cylindrical surface area ($2\pi \cdot r \cdot h$) of the fiber, providing a standardized way to compare performance across different fiber-based devices, regardless of their internal structure or porosity. Besides such macro-fibers or yarns, most other flexible electrode materials from lignin include carbon fiber or nanofiber mats.

Table 8: Device performances of various lignin-based flexible carbon fiber mat electrodes for supercapacitors

Electrode material	Capacitance (F/g)	Energy Density (Wh/kg)	Power Density (W/kg)	Cycle Stability (%)
Kraft LCNFs (<i>Singh et al., 2021</i>) (all-solid-state supercapacitor)	451 (1 A/g)	63	1250	99% after 10000 cycles
Lignin-based multi-channels CNFs@SnO₂ nanocomposites (<i>M. Cao et al., 2020</i>)	406 (0.5 A/g)	11 (7)	451 (18514)	95% after 10000 cycles
LCNFs -Pluronic	339 (0.1A/g) 290 (5 A/g)	57	339	91% after 5000 cycles
N/O co-doped lignin-based ultra-fine porous CNFs	289 (0.1 A/g)	–	–	92% after 10000 cycles
N/S co-doped graphene modified lignin/PAN CNFs (<i>Dai et al., 2019</i>)	267 (5 mV/s)	9	~493	97% after 5000 cycles
Lignin-based porous CNFs (<i>C. Ma et al., 2018</i>)	248 (0.2 A/g)	–	–	97% after 1000 cycles
CNFs consisting of PAN and enzymatic hydrolysis lignin (<i>X. Wang et al., 2018</i>)	217 (1 A/g)	–	–	89% after 2000 cycles
CNFs@Fe₃O₄ (<i>Butnoi et al., 2021</i>)	216 (0.1 A/g)	43	242	97% after 1000 cycles
Lignin/PAN composite nanofiber membrane (<i>Wu et al., 2022</i>)	201 (0.5 A/g)	–	–	–
Microporous ACF (<i>García-Mateos et al., 2020</i>)	240	8	650	85% after 5000 cycles
MnO₂ deposited LCNF mats (<i>Youe et al., 2018</i>)	172 (5 mV/s)	6	160	99 % after 1000 cycles

P doped electrospun LCF (<i>García-Mateos et al., 2022</i>)	150	–	–	–
O doped LCF (<i>Schlee et al., 2019</i>)	155 F/g (0.1 A/g)	~10 W/cm ³	~0.001 Wh/cm ³	4% after 6000 cycles
MnO₂-deposited LCF (<i>Guo et al., 2020</i>)	131 (0.3 A/g)	~15	135	
Lignin/PAN nanofiber (<i>Park et al., 2019</i>)	129 (0.5 A/g)	49 (3.8)	252 (2630)	95% over 10000 cycles
Modified LCFs (<i>M. Zhu et al., 2020</i>)	106 (0.5 A/g)	37	400	97% after 10000 cycles
Lignin nonwoven CF (<i>Thielke et al., 2022</i>)	103 (0.25 A/g)	2.7	60	97% after 1000 cycles
ECNF/MnO₂ (<i>X. Ma et al., 2016a</i>)	83	84	5700	75% after 10000 cycles
Lignin/PVA CFs (<i>Lai et al., 2014</i>)	64 (400 mA/g)	~6	94	90% after 6000 cycles

*Where CNFs are carbon nanofibers, PAN is polyacrylonitrile, LCF is lignin carbon fiber, ACF is activated carbon fiber, ELCHF is electrospun lignin carbon fibers, ECNF IS electrospun carbon nanofiber.

**In Table 8, the energy and power density values presented in parentheses () represent the values corresponding to the highest power density achieved at a lower energy density.

The summarized account of device metrics in **Table 8** emphasizes lignin's versatility as a sustainable precursor for high-performance, flexible supercapacitor electrodes, especially when combined with functionalization methods and compositional modifications. Various lignin-based carbon fiber composites, including those doped with nitrogen and sulfur or modified with MOs like MnO₂ and SnO₂, display enhanced energy density, power density, and cycle stability. For instance, SnO₂-decorated lignin-based carbon nanofibers showed excellent cycling stability, maintaining 95% retention after 10000 cycles. Similarly, nitrogen- and sulfur-co-doped graphene-modified lignin/PAN CNF electrodes achieved only a moderate energy and power density while it retained its superior capacitance with almost 97% capacity over 5000 cycles. Materials with enhanced functionalization such as N/S doping, MnO₂ deposition, or SnO₂ nanocomposites typically seem to outperform standard lignin-based carbon fibers, showing higher capacitance even over prolonged cycling due to the introduced additional pseudocapacitive contributions. Nevertheless, standard EDLC based kraft lignin-based carbon nanofibers, tested in solid-state devices, also achieved an impressive 63 Wh/kg energy density and 99% stability of its high capacitance of 451 F/g over 10000 cycles, indicating lignin's feasibility for advanced, durable flexible supercapacitor applications.

2.2. Major Wood Components

Wood is composed of three key biopolymers - cellulose, hemicellulose and lignin, each offering distinct properties that contribute to energy storage applications. The following section provides a brief background of these precursors for sustainable material design.

2.2.1. Lignin

Lignin is a complex, naturally occurring biopolymer found in the cell walls of plants, particularly in wood, where it provides crucial structural support and rigidity. It is a macromolecule, composed of phenolic compounds, primarily derived from three monolignols: p-coumaryl alcohol, coniferyl

alcohol, and sinapyl alcohol. The structural complexity of lignin stems from its radical-driven polymerization process, resulting in its intricate, branched, and highly heterogeneous macromolecular structure. This complexity can vary significantly depending on the wood species and even the growth conditions within the same species. This inherent variability in lignin influences its chemical properties and performance, making it a versatile material for applications ranging from biofuels to high-performance composites.

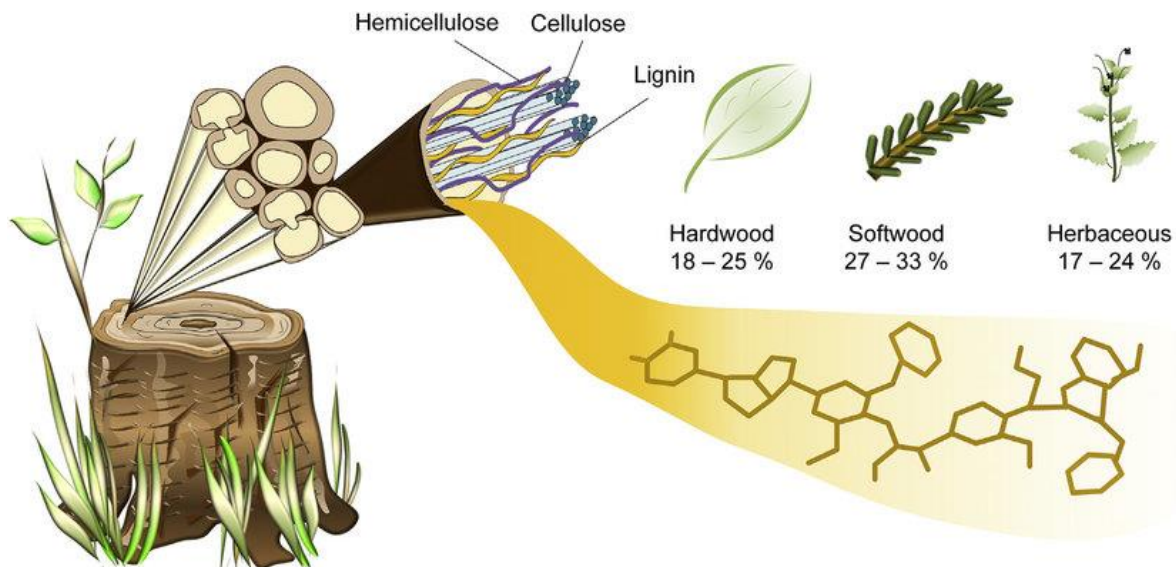

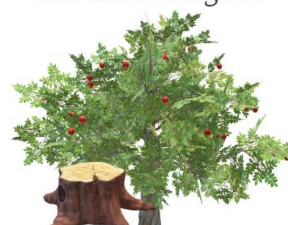


Figure 11. Wood is composed of lignin, cellulose, and hemicellulose. The amount of lignin varies depending on the source of wood. Reproduced with permission from Becker & Wittmann, 2019.

Lignin is found in both hardwood and softwood (Figure 11), but it can differ in properties (Table 9) due to their distinct botanical origins.

Table 9: Compositional and performance variance of lignin from softwood and hardwood isolated using the LignoBoost process (Schlee et al., 2020)

Softwood lignin	Hardwood lignin
	
Carbon content: 66%	Carbon content: 62%
Carbohydrate: 0.31%	Carbohydrate: 0.4%
Molecular weight: 8600 g/mol	Molecular weight : 1900 g/mol
Polydispersity Index (PDI): 2.8	PDI: 1.5
Glass transition temp. (Tg):184 °C	Tg :154 °C
Aliphatic to phenolic OH groups:0.5	Aliphatic to phenolic OH groups : 0.3

Hardwood lignin is generally more complex, containing a higher proportion of syringyl (S) units, which result from the polymerization of sinapyl alcohol. These S units contribute to a more linear and less condensed structure due to their methoxy groups, which reduce the number of crosslinking sites. As a result, hardwood lignin is less prone to forming dense, rigid networks, making it more amenable to chemical processing and depolymerization. In contrast, softwood lignin predominantly consists of guaiacyl (G) units derived from coniferyl alcohol. The G units possess

fewer methoxy groups, leading to a higher degree of crosslinking and a more condensed, rigid structure. This makes softwood lignin more challenging to process.

The differences in the S/G ratio between hardwood and softwood lignin are influenced by the biosynthetic pathways of the plants, which depend on the enzymes involved in lignin precursor synthesis. For hardwood lignin, the syringyl (S) units contribute to greater solubility and reactivity due to their fewer crosslinking sites and higher β -O-4 linkages. This makes hardwood lignin more suitable for applications requiring easier depolymerization or chemical modification, such as biorefinery processes or functionalized materials. In contrast, softwood lignin's composition of guaiacyl (G) units, which form more C-C linkages, results in a denser and more rigid structure. This structural robustness makes softwood lignin typically preferable for applications requiring high mechanical strength, such as carbon fibers or structural composites. Nevertheless, the properties of lignin are significantly influenced by the extraction method used. For instance, mild methods like milled wood lignin extraction preserve the intrinsic structure of lignin, while harsher methods like Kraft or Klason processes lead to higher yields but can alter its chemical composition and thermal properties. These factors further determine the suitability of hardwood or softwood lignin for specific applications in materials science, energy storage, and biorefinery processes.

The primary distinction between hardwood Kraft lignin (HKL) and softwood Kraft lignin (SKL) lies in their content of β -O-4 ether bonds, which constitute 63% of total linkages in HKL compared to only 35% in SKL (Schlee et al., 2020). This higher proportion of β -O-4 bonds in HKL enhances its reactivity and processability, making it more suitable for applications like carbon fiber production (Q. Li et al., 2021). In contrast, SKL's greater stability due to a higher content of C-C bonds results in a more rigid structure, advantageous for applications requiring thermal stability (Figure 12). Additionally, while fewer hydroxyl groups in HKL can contribute to superior mechanical properties in carbon fibers, the role of hydroxyls in forming hydrogen bonds should also be considered (Q. Li et al., 2021). Overall, the structural differences between HKL and SKL significantly influence their suitability for various applications in materials science.

In (Böhm et al., 2018), they highlighted the minimum Young's modulus and tensile strength needed for CFs in applications such as steel replacement and concrete reinforcement. While commercially available and experimental CFs, primarily derived from PAN or pitch, meet the stiffness criteria for steel replacement, lignin-based CFs require further enhancement of their mechanical properties to compete in these demanding applications.

From one of our preliminary studies, which involved a comparative analysis of the mechanical properties of lignin-cellulose composite carbon fibers derived from both HKL and SKL, we observed that the decomposition temperature (T_d) of HKL was lower (280 °C) compared to SKL (360 °C) (Figure 12). We speculate that the increased β -O-4 content improves the alignment of lignin polymers and strengthens the lignin-cellulose interactions, leading to the development of a more structured pre-pyrolytic carbon. This aligns with previous studies on maple wood and SKL (Q. Li et al., 2021), reinforcing our hypothesis that composite carbon fibers made from HKL-lignin and cellulose may exhibit enhanced mechanical performance compared to those made from SKL (Figure 12).

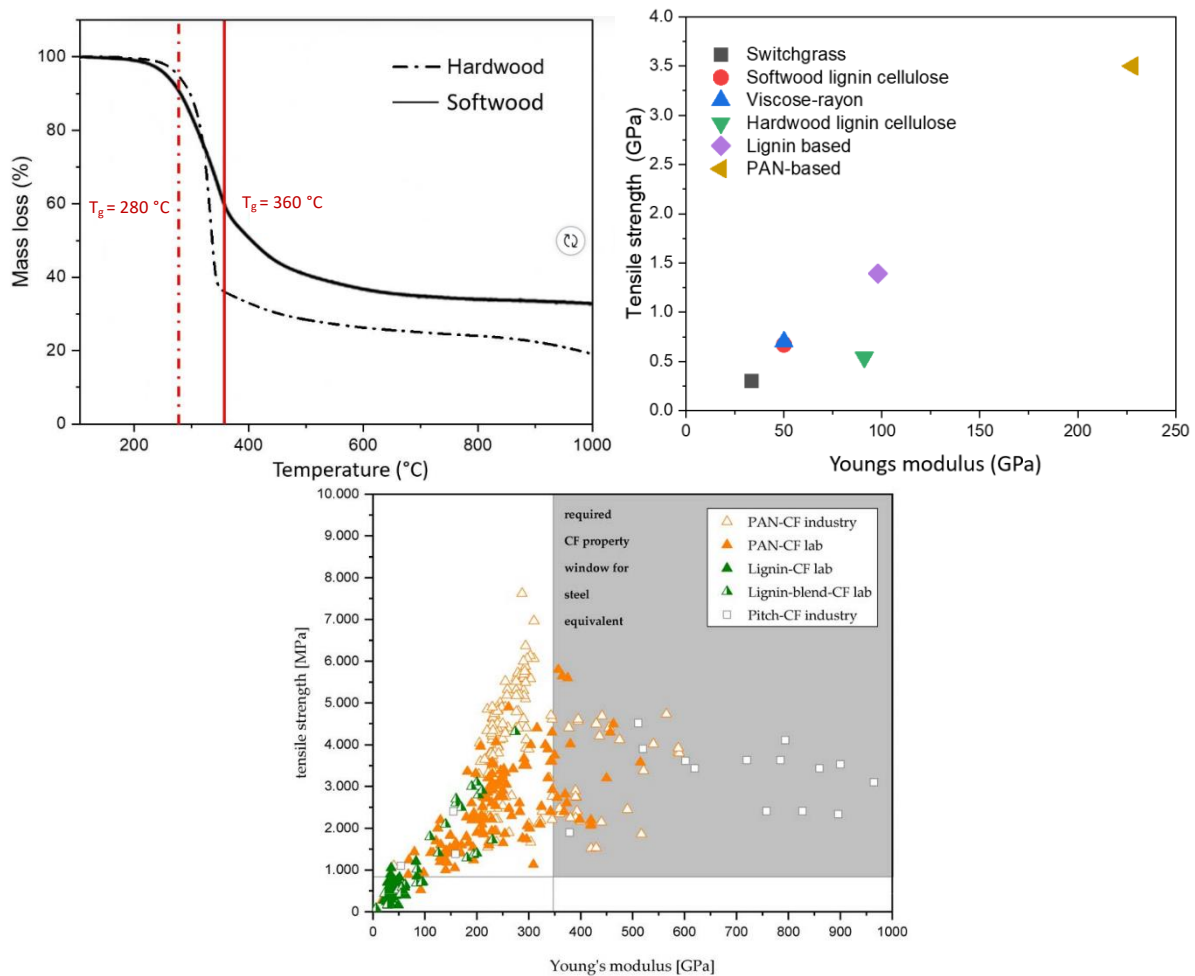


Figure 12. Thermogravimetric analysis (TGA) curve of HKL and SKL, Mechanical performance comparison of carbon fibers derived from different wood and other biomass sources, it becomes evident that their mechanical strength is generally similar among themselves, yet significantly falls short of the mechanical strength achieved by PAN-based fibers. Reproduced data and figure with permission from the sources A. Bengtsson, 2022 & Böhm et al., 2018, respectively.

This diversity in lignin structure across different types of wood and sometimes within the same species is critical for its potential use in various industrial applications, including energy storage devices like supercapacitors.

Black liquor

Black liquor, a high-aromatic carbon bioresource, rich in lignin, is primarily obtained as a byproduct of the Kraft pulp process and is emerging as a significant material for engineering applications. Stora Enso pulp mill in Sunila, Finland, utilizing the LignoBoost process by Valmet - a Swedish-patented separation method developed by researchers at Chalmers and RISE in the 2000s - extracts about 35-45% of lignin from black liquor (Kienberger et al., 2021). Now a Södra pulp mill is set to introduce a lignin production system based on Andritz's LignaRec lignin recovery process, which is the largest of its kind in the world. This system will be implemented at Södra's Mönsterås mill and is expected to begin operations in 2027 (*Södra Signs Agreement to Supply UPM with Kraft Lignin from World-Leading New Plant*, 2024). The process involves recovering lignin from the black liquor generated during the pulping process, with the goal of creating a product that can replace fossil-based materials in various applications, such as biofuels and chemicals. This will be an advantage for the global lignin market grown given that it is projected to grow at an annual rate of 2% from 2020 to 2027, reaching over USD 1 billion by

2027. This growth is driven by increasing demand for animal feed and natural products, with Europe contributing to 40% of global commercial lignin production as of 2019 (*Lignin Market Size, Share & Trends Analysis Report By Product (Ligno-Sulphonates, Kraft, Organosolv), By Application (Macromolecule, Aromatic), By Region, And Segment Forecasts, 2020 - 2027, 2020*).

Over the past decade, research has identified this source of lignin as a promising precursor for a range of carbon materials. In Europe and China, ongoing research is focused on black liquor-derived lignin's potential in developing carbon fibers, nanocarbons, composites, and bio-asphalt, which can replace oil-based products in various sectors, including automotive, construction, coatings, plastics, and pharmaceuticals. Despite challenges in modifying and functionalizing these lignin-based materials due to their chemical and physical heterogeneity the potential for lignin derivatization (Balakshin et al., 2021) and mass production remains vast and offers exciting opportunities for applications.

2.2.2. Cellulose

Cellulose is a carbohydrate polymer made up of over 10000 glucose molecules linked by β -(1,4)-glycosidic bonds. As the most prevalent natural polysaccharide, cellulose is the main component in the primary cell wall in trees, plants (Figure 13), algae, and fungi. The main sources of cellulose in nature include wood (40 -50%) and plant materials (30 -75%) due to their high availability and low cost.

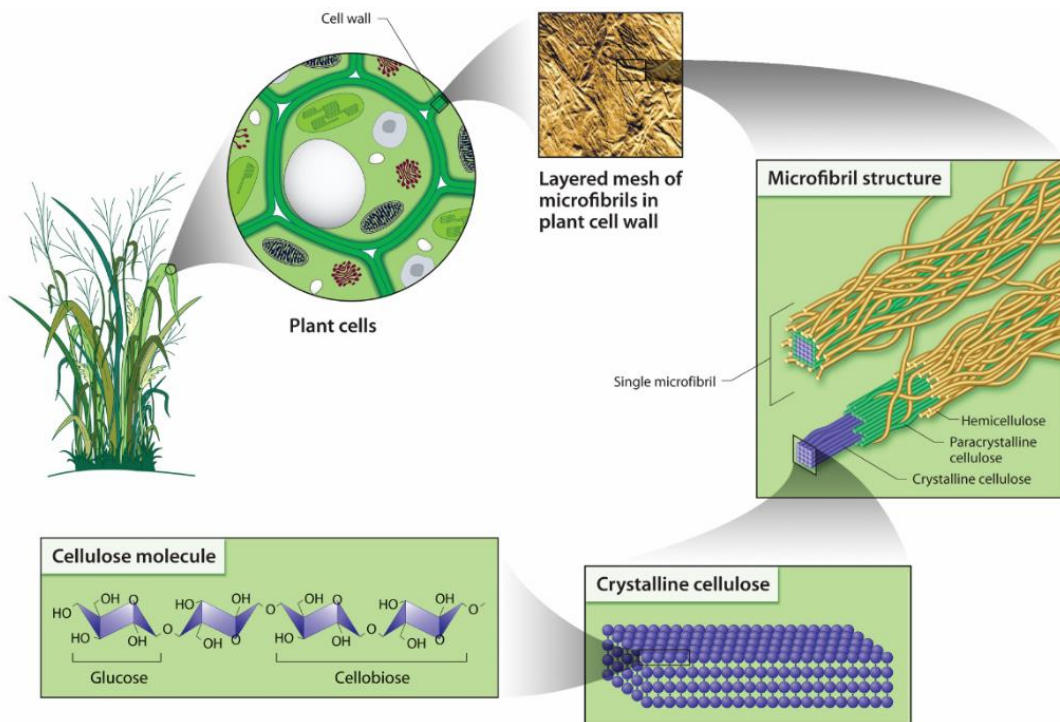


Figure 13. Chains of cellulose molecules combine with other polymers within the plant cell wall to produce linear structures with great tensile strength known as microfibrils. The cell wall is made up of layers upon layers of microfibrils. Each microfibril has a diameter of 10 to 20 nm and can include up to 40 cellulose chains. Source: (US DOE. 2005. *Genomics:GTL Roadmap, DOE/SC-0090, U.S. Department of Energy Office of Science. (p. 204), n.d.*).

Cellulose from wood and cotton are the primary raw materials in the textile, construction, paper-pulp, and food industries. The largest use of cellulose is in various paper and board products, but in addition to this industrial use also includes garments (cotton, linen, rayon), electronics

(nitrocellulose), and films (cellulose acetate). Also, its strong biocompatibility and suitable physical and chemical properties make cellulose relevant for biomedical applications such as wound dressings, tissue engineering, and drug delivery systems (Seddiqi et al., 2021).

Diverse cellulose derivatives are produced through chemical treatments or functionalization for various applications. Processes such as acid hydrolysis, solvent dissolution, and bacterial fermentation reduce cellulose pulp into nanofibers. The properties of cellulose derivatives depend on the type and degree of substitution and the functionalization pattern along the polymer chain. Modifying cellulose is challenging due to its insolubility in most conventional solvents and the steric hindrance posed by its bulky main chain. The hydroxyl group serves as the primary target for derivatization through esterification or etherification, altering the chemical structure of the cellulose molecules. These modifications impact properties such as polarity, moisture sorption, water interaction, surface activity, and solubility (Seddiqi et al., 2021).

2.2.3. Hemicellulose

Hemicelluloses, a group of heterogeneous polysaccharides comprising 15-35% of hardwood and 30-32% of softwood dry weight, play crucial roles in wood cell wall structure and mechanical properties (Abik et al., 2023). However, their exploration for supercapacitor applications has been limited compared to cellulose and lignin. This could primarily be due to their lower stability, higher susceptibility to chemical and thermal degradation, and increased hydrophilicity, which can compromise electrode stability in electrolytes (Mehta et al., 2020). Additionally, hemicelluloses lack the aromatic structures found in lignin that contribute to electrical conductivity, a critical factor in supercapacitor performance. Nevertheless, some studies demonstrate the potential of hemicellulose-derived carbons for high-performance supercapacitor electrodes when properly activated and modified (Y. Wang, Lu, et al., 2022; Z. Zhang et al., 2022). Further research is needed to optimize and fully explore the potential of hemicellulose as electrodes or other components for energy storage applications.

2.3. State-of-the-Art in Wood-Derived Components: Lignin and Cellulose for Supercapacitors

This section introduces and discusses lignin and cellulose as promising renewable and sustainable materials in the form of electrodes or other components (such as binders, separators, and electrolytes) of a supercapacitor device.

2.3.1. Electrode

Supercapacitor electrodes are typically thin coatings coupled to a conductive current collector. Ideal electrode materials should possess good conductivity, high-temperature stability, long-term chemical stability, corrosion resistance, and primarily high surface area per unit mass or volume. Additionally, low-cost material extraction and production, as well as environmental friendliness, are advantageous properties.

Carbon electrodes with high surface area morphology such as pores of varying sizes (micro-, meso- and macro-pores) offer enhanced charge storage through EDLC compared to planar carbon surfaces. Even better EDLC formation is achieved in interconnected carbon fiber or aerogel networks, which allow higher migration rates of electrolyte ions into deeper layers (Figure 14). However, electrodes with high mass loadings may not always achieve high capacitance because a significant portion of the inactive material may become inaccessible to electrolyte ions. This inaccessibility increases the electrical resistance between the electrode and the current collector, negatively impacting the rate capability and specific power performance of the electrode.



Figure 14. Schematic representation of a coin cell and its different components with some of their different electrode forms.

Lignin-based carbon electrodes, as discussed in previous sections 2.3 to 2.6, demonstrate the versatility of engineering electrodes and have garnered significant interest due to their competitive electrochemical properties compared to commercial electrode materials. These electrodes can be produced in various forms, including porous carbons, carbon fibers, and even thin films.

Cellulose has also been explored extensively for supercapacitor applications in the form of carbonized cellulose nanofibers; particularly those derived from electrospun cellulose acetate fibers offer promising results due to their high surface area and high electrical conductivity. When combined with conductive materials like carbon nanotubes or graphene (Z. Wang et al., 2017), cellulose nanocrystal (CNC) composites demonstrate superior electrochemical performance (X. Yang et al., 2015), including high capacitance and enhanced cycling stability. Another noteworthy development is activated carbon paper (ACP) electrodes derived from cellulose fibers extracted from waste wood, which provide an alternative method to produce flexible electrodes with high specific surface areas (J. J. Lee et al., 2023). These cellulose-based materials are advantageous in terms of sustainability, scalability, and performance, making them competitive alternatives to traditional activated carbon electrodes.

Also, the combination of lignin and cellulose into composite electrodes brings together advantages of both materials, resulting in synergistic effects that enhance performance (Le et al., 2020; Trogen et al., 2021). Lignocellulosic biomass-derived carbon electrodes, which exploit the natural combination of lignin and cellulose exhibit enhanced mechanical strength and increased carbon yield compared to only lignin or cellulose-derived materials ([Paper III](#)) (Nasri et al., 2023).

2.3.2. Separator

The primary function of the separator is to prevent electrical short circuits by keeping the electrodes apart while allowing the transfer of ionic charge carriers necessary for current flow in the electrochemical cell. In addition, separators must fulfill several functional requirements to operate efficiently (Figure 15). Various polymer membranes and cellulose-based separators are utilized in supercapacitors today (L. Li et al., 2018; Z. Wang et al., 2016). Cellulose filter paper membranes, used as separators in [Papers I](#) and [II](#), are favored for their low cost, high flexibility, excellent thermal, mechanical, and chemical stability, surface hydroxyl groups, and strong wettability. These properties make cellulose ideal for use as separators in supercapacitors, where they demonstrate superior ionic conductivity, low resistivity, high electrolyte absorptivity, and even higher temperature tolerance compared to commercially available separators (D. Zhao et al., 2017).

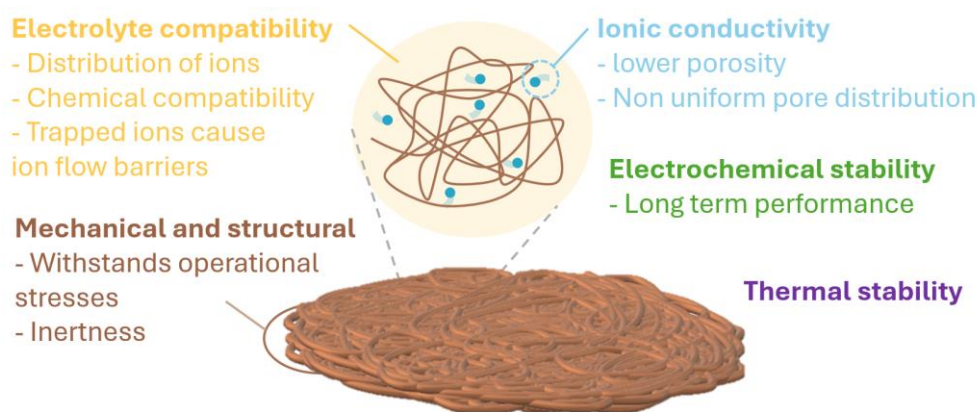


Figure 15. Desirable functionalities of a separator for supercapacitors.

Performance and Stability of Lignin-Based Separators in Supercapacitors

The potential of lignin-based fibers as separators in supercapacitors needs to gain recognition, building on foundational research in LIBs and other energy storage systems. Lignin offers intrinsic advantages such as excellent thermal stability, flame retardancy, and favorable electrolyte wettability (A. Liu et al., 2022). Prior studies have shown that electrospun lignin/PVA and lignin/PAN composite separators improve electrolyte absorption, compatibility, and porosity, leading to enhancements in ionic conductivity, rate capability, and cycling performance (C. Song et al., 2023; Yerkinbekova et al., 2022). Moreover, lignin-coated separators have shown significant promise in lithium-sulfur batteries, highlighting their versatility and potential applicability in diverse energy storage systems (Uddin et al., 2017).

In one of our non-extensive studies, the electrochemical behavior of electrospun lignin-based fibers as separators was analyzed in a coin cell configuration, employing activated carbon-polytetrafluoroethylene (AC-PTFE) electrodes and various electrolytes, with a focus on KOH. Lignin fiber separators derived from hardwood and softwood kraft lignin were systematically compared with cellulose nonwoven separators to assess their electrochemical performance, thermal stability, and overall suitability for supercapacitor applications.

The investigation into lignin-based separators for supercapacitors reveals both promising characteristics and potential challenges. A key advantage of these separators is their enhanced thermal stability compared to cellulose nonwovens, attributed to lignin's inherently robust aromatic structure. This thermal resilience is particularly beneficial for supercapacitors, where heat accumulation during rapid charge-discharge cycling can be significant. Lignin's aromatic backbone provides superior resistance to thermal degradation, potentially improving the structural integrity of separators under operational conditions.

Electrochemical performance evaluations demonstrated that lignin fiber separators can match or exceed the performance of traditional cellulose separators. Specific capacitances of 174 F/g and 170 F/g were achieved with hardwood and softwood lignin separators respectively, comparable to cellulose nonwovens at 173 F/g. Notably, lignin nonwovens outperformed both with a specific capacitance of 187 F/g. This enhancement can be partially attributed to the high electrolyte wettability and porosity of lignin-based separators, facilitating improved ionic conductivity and electrode-separator interactions. The softwood separator, in particular, exhibited superior rate capability and charge retention across various scan rates, aligning with its robust thermal and morphological characteristics.

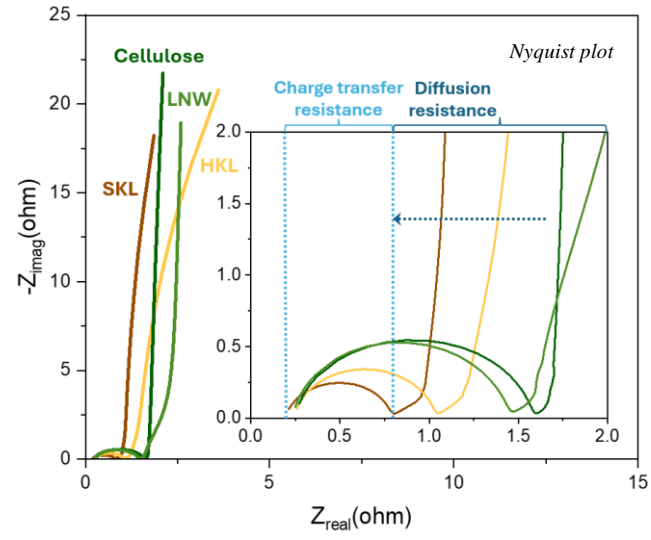
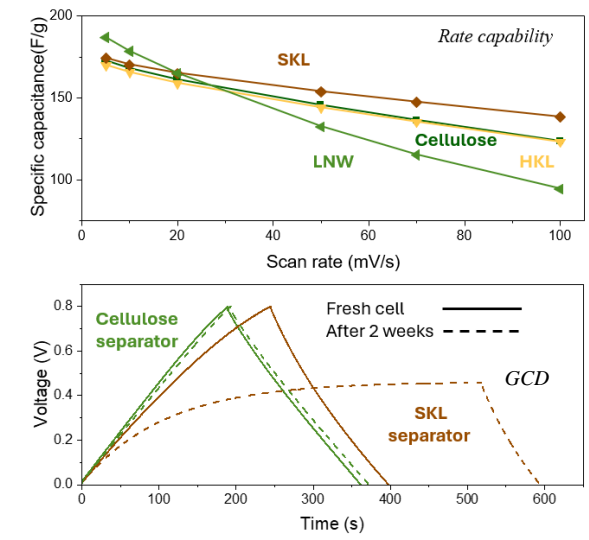
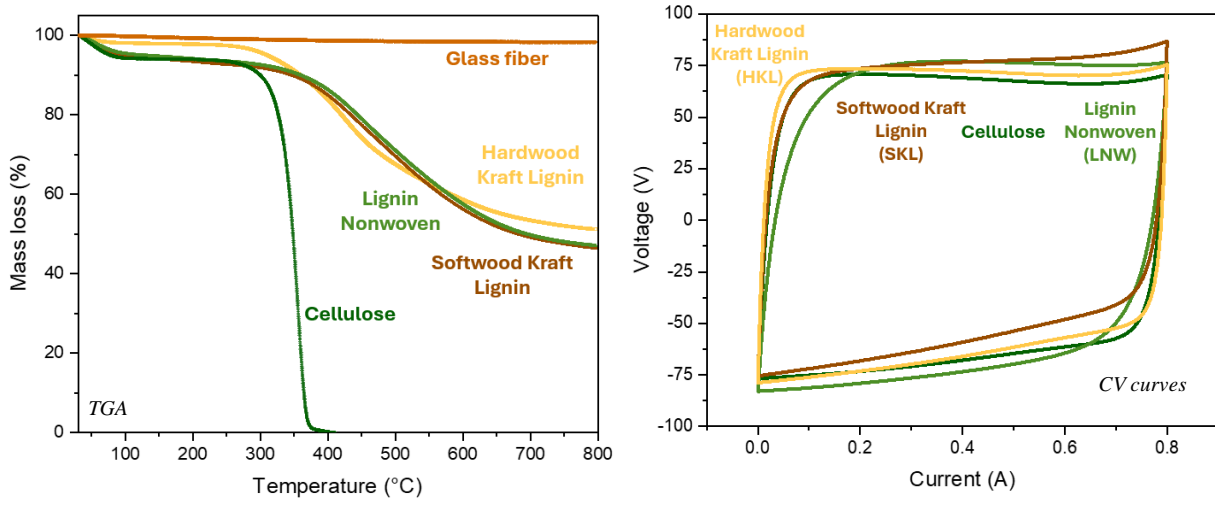
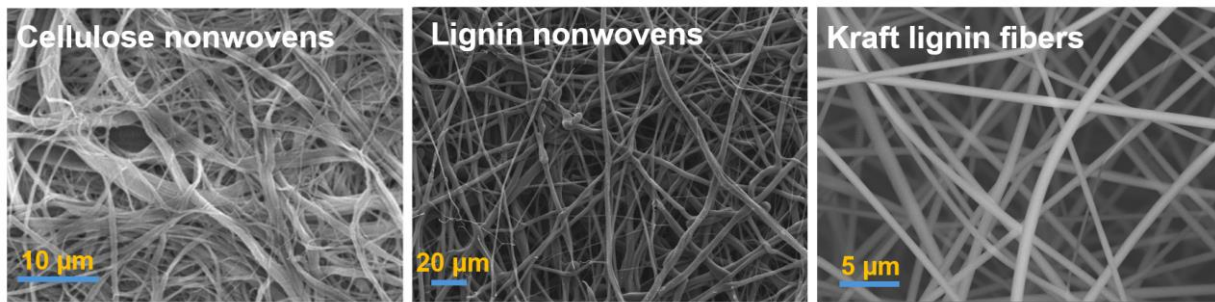


Figure 16. Morphological, thermal, and electrochemical analysis of various separators (arranged top to bottom, left to right) SEM images alongside their TGA curves. Following these, electrochemical characterizations of the cells using AC electrodes with 6M KOH electrolyte are presented, including CV profiles, rate capability, GCD curves, and EIS responses.

Initial GCD profiles revealed that the SKL fiber separator delivered superior performance with higher specific capacity and lower internal resistance compared to cellulose separators. This was attributed to lower charge transfer resistance and more efficient ion transport in the SKL separator (Figure 16, Nyquist plot). However, a significant caveat emerged during extended testing: performance deterioration was observed from the GCD curves over a two-week cell storage period. This decline suggests that unmodified lignin-cellulose materials may not be entirely inert, particularly in alkaline media. Further insights were gained through preliminary XPS analysis of

SKL and cellulose nonwoven separators after operation in a 6M KOH electrolyte. Notable differences in chemical states were observed, indicating degradation and reflecting the impact of the basic electrolyte on surface chemistry. These changes potentially affect the long-term performance of the separators in supercapacitor devices.

While lignin-based separators show promise in terms of thermal stability and initial electrochemical performance, the observed degradation in alkaline conditions highlights a critical area for future research. Addressing this limitation, possibly through surface modifications or protective coatings, will be crucial for realizing the full potential of lignin-based separators in supercapacitor applications.

Limitations of Glass Fiber Separators in Alkaline Electrolytes

The XPS analysis of fresh glass fiber and glass fiber exposed to 6M KOH electrolyte revealed a significant degradation of the separator material in the basic electrolyte (**Table 10**), contributing to the observed dissolution and loss of physical separation between electrodes in the device. Fresh glass fiber displays a strong Si-O peak (53%), indicating a stable silica-based structure, with minor organic contamination represented by C-C (10.5%) and C-O (1%). However, after exposure to the 6M KOH electrolyte, the Si-O peak intensity decreases to 30.5%, and new peaks for Na⁺ (13%) and K⁺ (10%) emerge, indicating that the silica network is being attacked by the concentrated hydroxide ions, leading to structural breakdown and the dissolution of the glass fiber. In contrast, glass fiber exposed to 1M KOH shows less degradation, with the Si-O content remaining higher (62%), indicating that the lower concentration of KOH causes less aggressive interaction with the silica structure. The XPS results suggest that higher concentrations of KOH accelerate the dissolution of the silica network, whereas acidic electrolytes like 1M H₂SO₄ show minimal degradation, as the silica structure remains largely intact. This analysis highlights the critical influence of electrolyte concentration and pH on the long-term stability of glass fiber separators, with more aggressive basic electrolytes, especially at higher concentrations, leading to substantial separator material degradation.

Table 10: Qualitative assessment of chemical states from high-resolution XPS scans in glass fiber and post operated glass fiber materials in various electrolytes.

Binding energy (eV)	C1s					O1s			F1s	Na1s	Si2p _{3/2}	S2p _{3/2}	K2p _{3/2}		
	284.8	286.5	287.5	289.5	530.5	531	532.5	534	537	689	1072.5	101.5	103	169	293-294
Possible chemical states	C-C	C-O	C=O	COO-	M-O	M-OH/ C=O	C-O Si=O S=O	Si-O	H ₂ O	F-	Na ⁺	Si-O	Si=O	SO ₄ ²⁻	K ⁺
Fresh glass fiber	10.5%	1%	0.5%	-	-	7.5%	53%	1%	1%	-	4.5%	-	19%	-	1%
Glass fiber (1M H ₂ SO ₄)	5.5%	2%	0.5%	-	-	-	62%	-	-	-	-	-	19.5%	<1%	-
Glass fiber (1M Na ₂ SO ₄)	8%	1.5%	<0.5%	-	-	4%	58%	-	1%	-	4.5%	-	18%	2%	0.5%
Glass fiber (1M KOH)	11%	1%	-	1.5%	11.5%	30.5%	13.5%	-	-	-	1.5%	-	13%	-	10%
Glass fiber (6M KOH)	10%	-	1%	2%	26%	14.5%	-	3%	-	7.5%	-	8.5%	-	-	13.5%

2.3.3. Electrolyte

The predominant types of electrolytes used in supercapacitors today are aqueous electrolytes, organic electrolytes, ionic liquids, and redox electrolytes. Aqueous electrolytes are favored for their low cost and excellent conductivity. While ionic liquids and organic electrolytes expand the potential window, they suffer from reduced conductivity and the hazardous nature of organic solvents (C. Zhao & Zheng, 2015). Hence, the choice of electrolyte is as crucial as selecting the right electrode material to enhance or control supercapacitor performance and device's sustainability. Also, customizing and engineering electrolytes based on the electrode type is essential to maximize efficiency.

Table 11: Device performances of various lignin-based electrolytes for supercapacitors

Electrolyte	Conductivity (mS/cm)	Capacitance (F/g)	Energy Density (Wh/kg)	Power Density (W/kg)	Cycle Stability (%)
Ag-Lignin nanoparticles into polyacrylamide network (D. Wang, Yang, et al., 2022)	85	299 (10 mV/s)	13.7 (11.4)	201 (4714)	90% after 10000 cycles
Double cross-linked sarcosine lignin hydrogel (C. Gao et al., 2022)	57	231 (0.1A/g)	106	164	98% after 5000 cycles
Double cross-linked lignin hydrogel (T. Liu et al., 2020)	800	190 (0.25 A/g)	15 (~9)	95 (~2160)	91% after 10000 cycles
Lignin/PEGDGE/3.3 M KOH (Park et al., 2019)	10	129 (0.5 A/g)	4.5 (3.8)	252 (26300)	95% after 10000 cycles
Lignin grafted on PEG (H. Liu, Mulderrig, et al., 2021)	0.14	-	-	-	-
Organosolve lignin derived hydrogel (Muddasar et al., 2024)	-	41 (0.5 A/g)	-	-	-

*Where PEGDGE is poly (ethylene glycol) diglycidyl ether and PEG is polyethylene glycol. **In Table 11, the energy and power density values presented in parentheses () represent the values corresponding to the highest power density achieved at a lower energy density.

Lignin has been explored as an additive and a base for creating advanced supercapacitor electrolytes due to its redox-active quinone (Q-type) moieties, enhancing capacitance through Faradaic reactions at the electrode/electrolyte interface. Studies show lignosulfonate as an additive to an aqueous acidic liquid electrolyte can increase capacitance by up to 33% through reversible redox activity on the positive electrode (Lota & Milczarek, 2011). Although redox-active lignin electrolytes improve capacitance, they can increase self-discharge rates due to redox-active species migration. Lignin derived from corncob based hydrogel electrolytes produced by (T. Liu et al., 2020) have also shown promise. Using ring-opening polymerization and cross-linking, lignin

hydrogels achieved high ionic conductivity and mechanical stability, enabling flexible supercapacitors with retained capacitance and durability under bending stress. A double-crosslinking approach further improved the mechanical strength and ionic conductivity (up to 800 mS/cm) in devices with PANI deposited carbon cloths as electrodes, providing high specific capacitance (190 F/g) and energy density (15 Wh/kg). **Table 11** gives an account of a few other lignin-based hydrogel electrolytes that have been explored for supercapacitors.

Cellulose on the other hand (such as MCC: Microcrystalline Cellulose, BC: Bacterial Cellulose, CMC: Carboxymethyl Cellulose) as a renewable and biodegradable biopolymer offers a sustainable alternative to conventional electrolyte materials (Bai et al., 2021; Pérez-Madriral et al., 2016; Sun et al., 2021). Its high aspect ratio, porosity, and high mechanical flexibility make it ideal for flexible supercapacitor applications (Sun et al., 2021; P. Zhang et al., 2023). Cellulose similarly like lignin can be processed into hydrogel electrolytes, creating a quasi-solid-state system that combines the benefits of both solid and liquid electrolytes (X. Lin et al., 2023; P. Zhang et al., 2023). These hydrogels provide good ionic conductivity, facilitating efficient ion transport between electrodes, while their mechanical robustness and flexibility enable the fabrication of flexible and wearable supercapacitors (X. Lin et al., 2023). Additionally, the abundant hydroxyl groups in cellulose allow for chemical modifications, enhancing properties like ionic conductivity and mechanical strength to meet specific requirements (Ding et al., 2024).

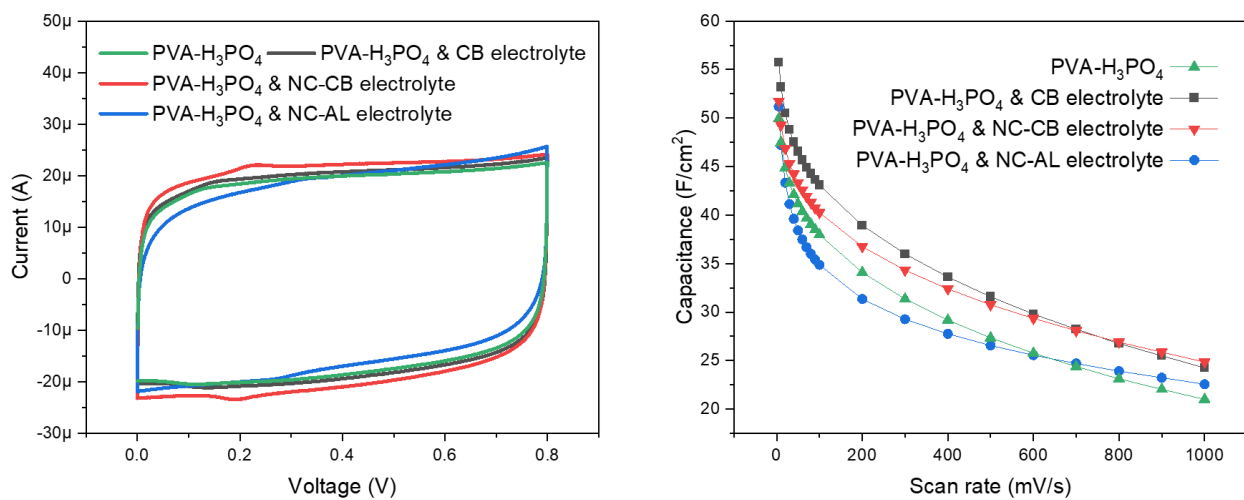


Figure 17. CV and rate capability curves of IrO₂ MSCs in different gel-based electrolytes.

We have explored the electrochemical performance of IrO₂ MSCs fabricated with cellulose-based gel electrolytes. Specifically, we analyzed devices utilizing two different electrolyte formulations: one incorporating nanocellulose (NC) with CB into the PVA/Phosphoric acid matrix and another with alkali lignin (AL) combined with NC in the same matrix. Based on previous studies, the incorporation of NC into gel electrolytes is speculated to be a key factor for increasing ionic conductivity, as NC introduces polar functional groups that act as channels for ion transport, facilitating ion hopping across the electrolyte matrix (W. Wang, Li, et al., 2022). Also, CMC nanofibers can enhance ionic conductivity in ionic liquid-based gel electrolytes from 0.26 mS/cm to values as high as 0.94 mS/cm. Supercapacitors using 1-ethyl-3-methylimidazolium dimethyl phosphate (EMIMP) with CMC nanofiber ionogel electrolytes with AC electrodes have demonstrated increase in capacity (160 F/g at 1 mA/cm²) and decrease on ESR compared to only EMI MP electrolyte (González-Gil et al., 2022). Our preliminary observations align with these observations, as the device containing NC in the PVA/KOH electrolyte showed a higher current response in the CV curves and improved rate capability (Figure 17), suggesting improved ionic

transport and decreased ESR within the electrolyte. In devices where CB was added, CB serves as a conductive agent within the electrolyte, effectively lowering internal resistance. This effect is reflected in prior research, where supercapacitors using PVA-KOH-carbon black electrolytes achieved specific capacitances up to 227 F/g at a current density of 0.5 A/g (Momodu et al., 2017). Devices with the PVA-KOH-carbon black gel electrolyte in another study exhibited a maximum energy density of 15.5 Wh/kg, the improvement is attributed to carbon black's high conductivity and ability to enhance ion mobility across the electrolyte matrix, which is critical for achieving higher energy density and power output in supercapacitors (Barzegar et al., 2015).

2.3.4. Binders and Additives

Typically, activated or porous carbon powders are combined to form an electrode using suitable binders and conductive additives like carbon black (CB) to enhance electrical conductivity. To create robust, free-standing electrodes with an environmentally friendly binder, microfibrillated cellulose (MFC) was tested (in [Paper II](#)), considering the environmental and biological hazards of commonly used binders like polyvinylidene fluoride (PVDF), polytetrafluoroethylene (PTFE), and N-methyl-2-pyrrolidone (NMP). However, electrodes using MFC binders were prone to cracking upon drying, especially at higher mass loadings, leading to reduced flexibility and poor device stability. A study by (Landi et al., 2021) investigated activated carbon electrodes using CMC as a binder material where the electrode resulting in electrodes with uniform, dense surfaces and minimal holes or cracks. The device with CMC binder demonstrated significant pseudocapacitive behavior, accounting for over 70% of the total capacitance, with diffusion-controlled processes being dominant in overall capacitance. Remarkably, devices with CMC showed a capacitance increase of some 40% after 1000 cycles, along with an approximate 20% increase in capacitance by the end of the cycling process. This study highlighted that the pseudocapacitive behavior at the electrode interface in supercapacitors is influenced by the binder type, underscoring the role of CMC in enhancing device stability and performance.

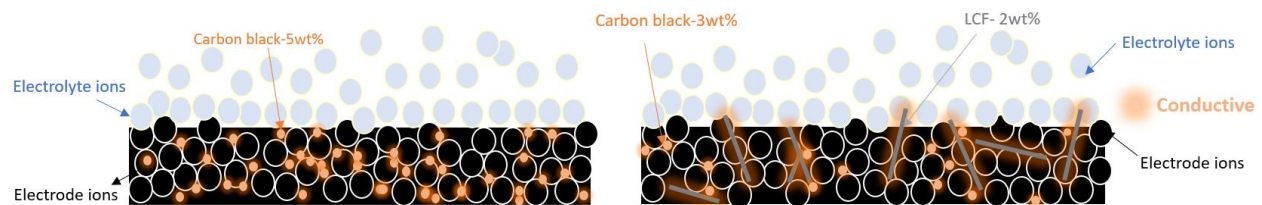


Figure 18. Comparison of electrodes with only CB additive vs LCF+CB additives (acting as conductive pathways) ([Paper II](#))

In [Paper II](#), the incorporation of longitudinal lignin carbon fiber alongside conductive carbon black into an activated carbon matrix as conductive additive enhanced supercapacitor electrode performance, particularly in thicker electrode matrices, which could be explained as follows:

1. Improved electron transport: Longitudinal carbon fibers may create a direct pathway for electron flow within the thick electrode structure, decreasing resistance. This can improve the overall conductivity of the matrix, reducing internal resistance and enabling faster charge and discharge rates (Figure 18).
2. Enhanced mechanical stability: Carbon fibers may offer structural reinforcement in the electrode matrix, which helps to maintain the integrity of thicker electrodes. This stability prevents cracking or mechanical degradation over repeated cycling, which is especially valuable for high-performance applications requiring durability.

3. Better ion transport and accessibility: Carbon fibers, due to their length and alignment, may create interconnected pathways within the electrode. This structure helps ions move more easily throughout the electrode, reducing diffusion limitations that commonly arise in thicker electrodes. As a result, it improves the accessibility of activated carbon surfaces for charge storage, enhancing specific capacitance.

These combined benefits significantly improve the capacitance, charge-discharge rates, and cycling stability of the supercapacitors, addressing the typical performance trade-offs associated with thicker electrodes.

Chapter 3

Methodology

3.1. Extraction and Purification Techniques

There are various existing techniques such as kraft pulping, sulfite pulping and organosolv processes for extracting and purifying lignin from lignocellulosic biomass sources.

3.1.1. Kraft Pulping Process

Kraft pulping is the predominant method in the chemical pulping industry, accounting for 80% of the market. This process involves digesting debarked wood chips at temperatures ranging from 150 to 180 °C for 2 to 4 hours under high pressure in an aqueous solution of sodium hydroxide (NaOH) and sodium sulfide (Na₂S), known as white liquor. During this digestion, various chemical bonds, primarily ether bonds, are broken, and the high pH ionizes the phenolic hydroxyl groups in lignin, effectively dissolving the lignin that binds cellulose fibers together (Ahmad & Pant, 2018). Following digestion, the liberated cellulose fibers are removed from the cooking liquor and washed. The remaining cooking liquor, now rich in solubilized lignin, is referred to as black liquor (BL). This black liquor is then concentrated in an evaporator train and used in boilers to generate steam. The composition of black liquor can vary depending on factors such as the source of the wood raw material, the composition of the white liquor, and post-storage conditions. Typically, before evaporation, black liquor consists of an aqueous mixture with lignin residues, hemicellulose, inorganic chemicals used in the process, and 15% w/w solids -10% of which are organic and 5% inorganic. The organic content includes 30%-45% aliphatic carboxylic acids, 35%-45% lignin, and 5%-15% other organic compounds (Bonhivers & Stuart, 2013; *Report on Other Components and Polymers Present in the Black Liquors*, n.d.).

3.1.2. Extraction of Lignin from Black Liquor

The LignoBoost process (Figure 19) is a patented method for extracting lignin from kraft black liquor that comprises of two main steps: precipitation and purification. During the precipitation step, BL is taken from the evaporation plant, and CO₂ is added to lower the pH, causing lignin to precipitate out of the liquor. The precipitated lignin is then separated using a filter press, producing a crude lignin filter cake. In the purification step, the crude lignin filter cake is washed with an acidic solution, such as sulfuric acid, to remove impurities. The washed lignin is then dewatered using a second filter press, resulting in purified lignin. In lab-scale preparation, lignin is recovered from BL at a pH of 9-11, causing its precipitation. The filtrate, after fine filtering, contains most inorganic compounds. The precipitated lignin is then washed with sulfuric acid at pH 2 for further purification. To maximize the yield of dried lignin solids, repeated washing is avoided.

The LignoBoost process is advantageous because it allows for the optimization of conditions for precipitation and purification separately. A gas handling system uses CO₂ from the purification step to acidify incoming black liquor. Additionally, the advanced filter press design ensures high lignin quality and process reliability. A sulfuric acid plant can also be integrated to control the mill's sulfur balance, allowing for the extraction of up to 25% of lignin without major mill modifications, or up to 70% with increased pulp production (“LignoBoost® - the Process,” n.d.; W. Zhu, 2015).

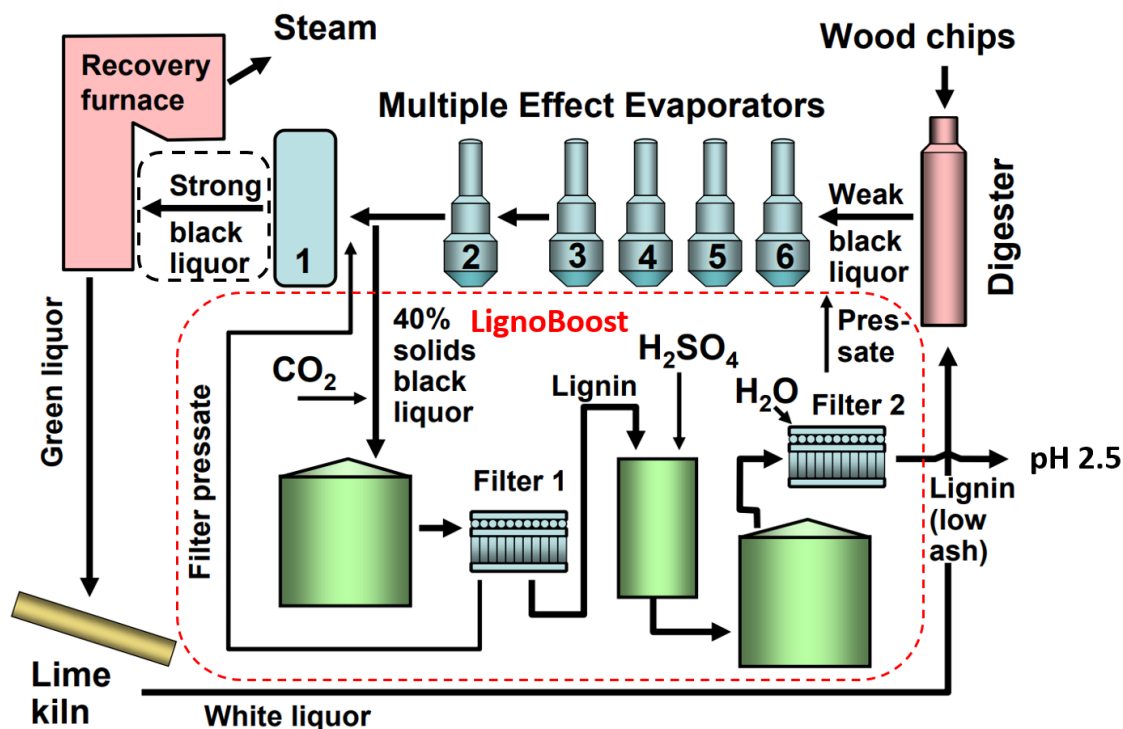


Figure 19. The sequence of steps conducted during lignin extraction from black liquor by LignoBoost method. Reproduced with permission from Hubbe et al., 2019.

The extracted lignin can be used as a renewable solid biofuel or as a raw material for producing biochemicals, materials, and other value-added products. This makes the LignoBoost process not only efficient but also aligns with the increasing demand for sustainable and environmentally friendly materials in numerous industries.

3.2. Synthesis Methods for Lignin Fibers

This section will outline the synthesis methods used to prepare lignin-based fibers for supercapacitors. It will begin with a key procedure for fractionating lignin to obtain the desired molecular weight. Subsequently, various techniques, such as solution spinning and electrospinning, will be discussed. These methods were specifically employed in our study to produce lignin-based fibers, which are later subjected to heat treatments to manufacture self-standing and flexible carbon fiber electrodes.

3.2.1. Lignin Fractionation

Technical lignin, such as LignoBoost lignin, typically has a lower molecular weight than polymers such as PAN, which makes electrospinning of the former challenging without co-polymerization with other major fossil-based polymers. Therefore, the lignin is either modified or fractionated based on molecular weight. Lignin fractionation is the process of dividing heterogeneous lignin into fractions of different molecular weight with lower PDI, and these fractions have distinct molecular weight distributions. The fraction with a greater molecular weight is preferable for spinning into carbon fibers. The fractionation procedure described by Baker et al. was practiced for electrospinning ELCF in [Paper 1] (O. Hosseinaei & D. A. Baker, n.d.). The quantified molecular weight of lignin following the procedure is 8600 g/mol with a PDI of 2.8. This high molecular weight lignin blended with polymers demonstrated significantly stronger interface connection bonds, boosting the spinnability of lignin-based polymers that

furthermore improved the mechanical elastic modulus, tensile strength, and elongation characteristics of the fiber (Pang et al., 2021).

3.2.2. Spinning Methods

Unmodified lignin has been used as a low-cost precursor for carbon fiber production (S. M. Yang et al., 2023). To enhance spinnability, this lignin is blended with other polymers like PAN (Jiang et al., 2018) or cellulose (Paper III). Chemical modifications, such as methylation and phenolation, have been investigated to tailor the structure of lignin before carbonization (S. Chatterjee, Clingenpeel, et al., 2014; Kadla et al., 2002).

Traditional fiber spinning methods, such as the solution spinning technique, have been used to produce lignin-based precursor fibers. More recently, electrospinning has gained prominence as a versatile technique for creating lignin-based carbon nanofibers with high surface areas. The scalability of electrospinning has been improved through needleless setups, enabling the continuous production of lignin carbon fiber mats (Thielke et al., 2022). Additionally, coaxial or core-shell fiber structures, with lignin serving as the core or sheath, can be fabricated to enhance specific properties or functionalities (Lallave et al., 2007). Beyond spinning, composite and hybrid structures have been developed by coating lignin fibers with conductive polymers or integrating them with carbon materials like CNTs to improve conductivity (S. Wang, Bai, et al., 2022).

Solution spinning

Solution spinning, such as wet-spinning and dry-jet wet spinning, are versatile manufacturing techniques used to produce fibers from polymer solutions (J. Bengtsson, 2021; S. M. Yang et al., 2023). In these processes, a polymer is dissolved in a suitable solvent to form a spinning solution. The solution is then extruded through a spinneret, a device with multiple small holes, into a coagulation bath where the solvent is removed, and the polymer solidifies into a fiber.

Solution spinning is particularly advantageous for creating macro fibers that are flexible and uniform in diameter. These fibers serve as precursors for carbon fibers, where the flexibility and structural integrity obtained during the spinning process are crucial. Once formed, these precursor fibers undergo carbonization, where they are heated to high temperatures in an inert atmosphere to eliminate non-carbon atoms, resulting in carbon fibers.

The ability to tailor the spinning parameters allows for control over the fiber's characteristics, such as diameter, strength, and orientation, which are critical for the performance of carbon fibers in various applications. Solution spinning thus plays a fundamental role in the production of high-quality carbon fibers used in aerospace, automotive, and renewable energy sectors, among others, due to their lightweight, high strength, and excellent thermal and electrical conductivity properties.

Solution spinning like dry-jet wet spinning is also suitable for producing fibers from blends of lignin and cellulose as in Paper III. By combining these materials in varying ratios and dissolving them in suitable solvents, solution spinning enables the creation of homogeneous spinning solutions. This process enhances the spinnability of lignin-cellulose blends, leveraging the synergistic effects of lignin's structural complexity and cellulose's molecular arrangement. The resulting fibers benefit from improved mechanical properties, such as enhanced strength and flexibility, making them suitable for a range of applications. Moreover, using lignin, a by-product of pulp and paper industry, promotes environmental sustainability by valorizing waste materials. These fibers serve as valuable precursors for carbon fibers, where their controlled spinnability and optimized properties can be potential for producing sustainable materials.

Melt-blowing

Melt-blowing is a specialized technique used to create nonwoven fabrics by extruding molten polymer through fine nozzles into high-speed air streams, forming microfibers that accumulate randomly to form a web-like structure (Drabek & Zatloukal, 2019). When applied to lignin, melt-blowing presents unique opportunities for producing eco-friendly nonwoven materials. Challenges include the need for specialized equipment and precise processing conditions to melt and extrude lignin, given its high molecular weight. By leveraging lignin's natural properties, such as its thermal stability and antioxidant effects, it is possible to create nonwovens with improved durability, heat resistance, and chemical resistance. Applications for lignin-based nonwovens span filtration, insulation, packaging, and composite materials, contributing to sustainable practices by utilizing biomass waste and reducing reliance on petroleum-derived materials.

Electrospinning

Since lignin is made up of randomly dispersed aromatic units separated by aliphatic chains, dissolving lignin in non-polymeric solvents for electrospinning does not allow for adequate chain entanglements, resulting in particle electro-spraying. For lignin to be electro-spinnable, it is either blended with a secondary polymer, or solvent fractionated to eliminate low molecular weight fractions. Although the first approach improves fiber properties, it raises the product cost. Hence the latter method involves fractionated parts of high molecular weight lignin mixed with an organic solvent as described in [Paper I](#). To obtain a defined morphology of the carbon fibers, the tuning of processing parameters such as the voltage, ambient humidity, needle size, needle distance from the collector, and spinning solution feed rate are critical (Nasouri et al., n.d.).

3.3. Synthesis of Lignin-based Carbon Electrode Materials

The development of engineering lignin-based carbon materials as electrodes has seen significant progress, focusing on synthesis methods and material preparation strategies. Various morphologies such as porous carbons, carbon fibers, carbon aerogels, and nanostructured carbons have been synthesized from lignin precursors by controlling carbonization conditions and utilizing templating or self-assembly approaches (P. Li et al., 2024). Notable structures achieved include 2D carbon nanosheets, 3D porous carbon architectures, and hierarchical porous structures, all designed to enhance electrochemical performance (W. Zhang et al., 2022).

Modifications of lignin precursors involve blending with other biomass components like cellulose or combining with conductive additives such as graphene oxide to improve properties before carbonization. Chemical modifications of lignin have also been explored to tailor its structure for better carbonization outcomes (P. Li et al., 2024). The carbonization temperature significantly impacts the degree of graphitization, porosity, and conductivity of the resulting carbon materials, with activation methods like physical and chemical activation increasing surface area and porosity (Yao et al., 2022).

Additionally, the inherent oxygen and nitrogen functionalities in lignin facilitate heteroatom doping in the carbon materials, enhancing their electrochemical activity ([Paper I](#), Thielke et al. 2022). For upscaling and continuous production, techniques such as electrospinning and needleless electrospinning have been employed to produce lignin-based carbon fibers and mats continuously (Thielke et al., 2022). These advancements contribute to sustainable and low-cost synthesis routes for producing lignin-based carbon materials.

3.3.1. Thermostabilization

Thermostabilization is a critical process in the production of lignin-based carbon fibers, preparing the fibers for subsequent carbonization. This step involves heating lignin fibers in an oxidative atmosphere, such as air or oxygen, at temperatures around 200-300 °C (Figure 20). During oxidative stabilization, dehydrogenation reactions occur, forming carbon-carbon double bonds and crosslinking between lignin molecules (J. Lin et al., 2012). Cleavage of bonds like β -O-4 ether linkages generates free radicals, further facilitating crosslinking and condensation reactions (Braun et al., 2005). Additionally, oxidation reactions introduce oxygen-containing functional groups, increasing the molecular rigidity of the lignin.

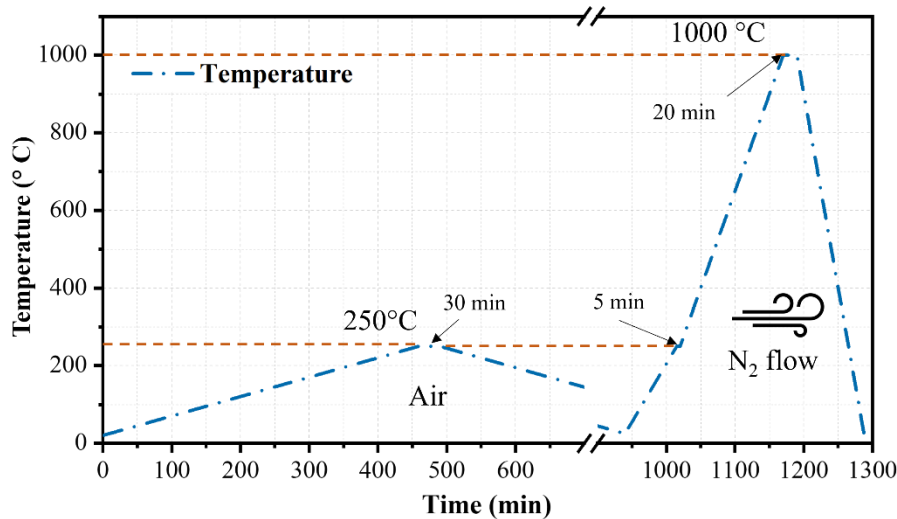


Figure 20. ELCFs carbonization profile; stabilization using Nabertherm box furnace and carbonization using Thermolyne - Open Tube/1600 °C furnace).

The thermostabilization process also removes the fusion tendency of lignin fibers, making them infusible and preventing them from melting or fusing together during the high-temperature carbonization stage. Crosslinking and condensation reactions increase the glass transition temperature (T_g) of the lignin, enhancing its thermal stability to endure the harsh carbonization conditions (Hosseinaei et al., 2017). Controlled heating rates, typically between 0.05-5 °C/min, are employed to ensure uniform oxidative reactions throughout the fibers.

Typically, softwood lignin has higher cross-linking than hardwood lignin, which results in lower spinnability but achieves thermostabilization in a shorter duration (Norberg et al., 2013). Additionally, lignin's higher carbon content makes the thermostabilization of lignin fibers less energy and time-intensive compared to PAN fibers, reducing the process time from 16 hours to less than 2 hours at 250 °C (A. Bengtsson et al., 2019). In this thesis work ([Paper I](#), [Paper II](#), [Paper III](#) and for the lignin separator study) most lignin-based fiber materials were thermostabilized at 250 °C with a slow heating rate of 0.5 °C/min in an open-air atmosphere.

3.3.2. Carbonization

The carbonization process converts lignin-based precursor fibers into carbon fibers. This involves heating the stabilized lignin fibers to high temperatures, typically between 800-1500 °C, in an inert atmosphere such as nitrogen or argon. This high-temperature treatment removes non-carbon elements and increases the fraction of carbon content.

During carbonization, the stabilized lignin fibers undergo significant structural transformations. Pyrolysis reactions remove remaining hydrogen, oxygen, and other heteroatoms, forming a turbostratic carbon structure with increasing graphitic character as the temperature rises. This process also leads to the development of porous structures in the resulting carbon fibers, with higher temperatures generally producing higher porosity and surface area (Rennhofer et al., 2021).

The carbonization process enhances the thermal stability and electrical conductivity of the fibers due to the increased carbon content and formation of graphitic structures (S. Chatterjee, Saito, et al., 2014; F. Liu et al., 2022). It also results in significant weight loss, typically 30-50%, and densification of the fibers due to the removal of non-carbon elements and structural rearrangement (Poursorkhabi et al., 2020). Controlled heating rates, usually between 1-10 °C/min, are employed to prevent defects and maintain the fiber morphology (Poursorkhabi et al., 2020). Compared to PAN precursor fibers, lignin fibers generally require shorter carbonization times (1-2 hours) due to their higher carbon content and lower stabilization requirements (F. Liu et al., 2022).

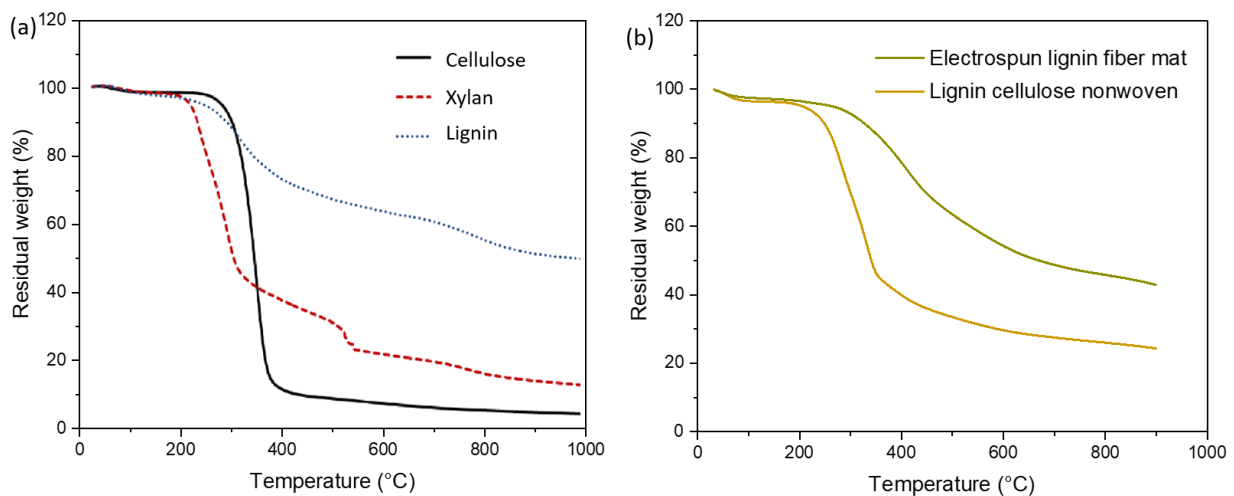


Figure 21. a) Weight loss profile from TGA of the major wood components. Reproduced with permission from Pasangulapati et al., 2012, and b) lignin fiber and lignin cellulose composite nonwovens in a nitrogen atmosphere at a heating rate of 50 °C/min.

The conditions of carbonization, such as temperature, heating rate, and atmosphere, significantly influence the final properties of lignin-based carbon fibers, including their mechanical strength, electrical conductivity, and surface characteristics. TGA is performed prior to establishing a thermal treatment profile, determining the thermal stability and measuring the loss of volatile components by their changing weight profile (Figure 21 a). At lower temperatures around 105 °C, moisture is removed, followed by the breakdown of hydroxyl groups up to 600 °C. Between 190 °C and 800 °C, CO and CO₂ gases are produced from the thermal decomposition of carbonyl and carboxyl groups, and ether cleavage (Yan et al., 2018). At temperatures from 500 °C to 1000 °C, hydrogen gas evolves due to the breakage and depolymerization of aliphatic and aromatic hydrocarbon bonds, leading to the formation of aromatic carbon structures. Above 1000 °C, the tensile strength decreases due to defects and reduced fiber diameter (A. Bengtsson et al., 2020). Across all our carbon fiber studies ([Paper I](#), [Paper II](#), and [Paper III](#)), the fibers were carbonized at 1000 °C, as optimized by previous studies (A. Bengtsson et al., 2020; Thielke et al., 2022). Additionally, the development of functional porous morphologies with a broad pore size distribution can be fine-tuned by carefully controlling the carbonization profile and selecting appropriate secondary polymers (S. Wang, Bai, et al., 2022).

In the case of ELCF spun without any fossil-based secondary polymer, a wide distribution of pores is observed (Figure 22 a), predominantly comprising mostly micro- (diameter less than 2 nm) and mesopores (diameter between 2 nm to 50 nm). Further advancements in pore engineering can be achieved through alternative methods such as templating and chemical activation, which involve the use of various chemicals to define pore structures (Figure 22 b).

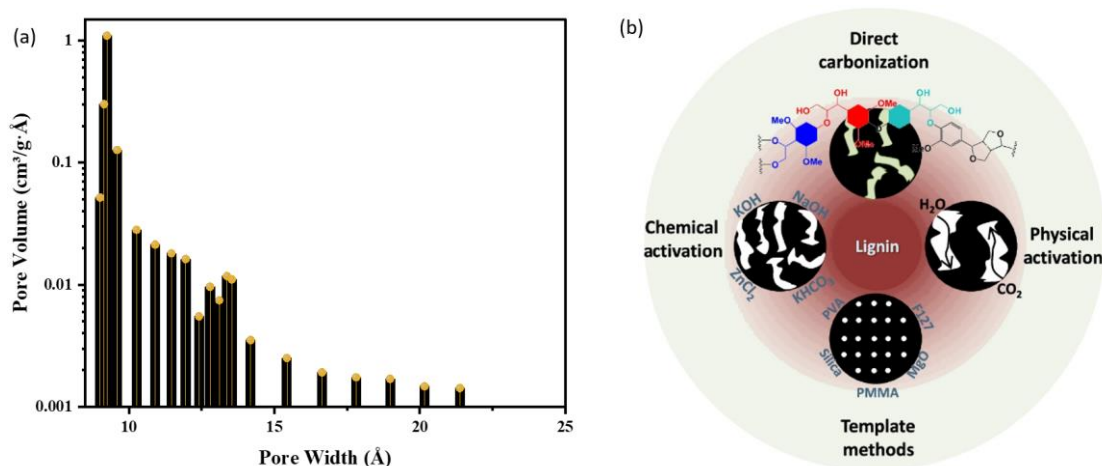


Figure 22. a) Pore size distribution in ELCF sample, b) Different pore engineering strategies for lignin-derived porous carbons. Reproduced with permission from W. Zhang et al., 2022.

3.3.3. Activation

Activation of lignin-based carbon fibers is a crucial step aimed at enhancing their structural and chemical properties for various applications. Recent research highlights significant progress in the activation of lignin-based carbon fibers, focusing on enhancing their porosity and surface area for improved performance as electrode materials. After carbonization, various activation methods, including physical activation with gases and chemical activation using oxidizing agents, are employed to create porous structures within the fibers (Karume et al., 2023). Physical activation involves carbonization followed by thermal activation in the presence of gases like CO₂ or steam. This process etches the carbon surface creating new pores and widening existing ones through specific carbon-gas reactions (Liang et al., 2020), significantly enhancing the material's surface area and adsorptive properties (W. Zhang et al., 2022). Chemical activation, on the other hand, employs agents like H₃PO₄ (García-Mateos et al., 2020), KOH (M. Song et al., 2019), NaOH (Hu & Hsieh, 2013), ZnCl₂, or a combination of them (Prauchner et al., 2016) to impregnate raw materials, facilitating pyrolytic breakdown and generating a highly porous carbon structure. Some studies have explored one-step activation during carbonization by impregnating lignin precursor fibers with activating agents like KOH, streamlining the production process (Hu & Hsieh, 2013). By carefully controlling activation conditions such as temperature and activating agent concentration, researchers can tailor the pore size distribution and microstructure to meet specific functions. Moreover, activation facilitates heteroatom doping (e.g., nitrogen, oxygen), further improving the fibers' electrochemical properties (J. Zhang et al., 2024).

3.3.4. Graphitization

Graphitization of lignin-based carbon fibers involves heating the lignin-based carbon fibers to temperatures above 1800 °C to induce structural rearrangement and order within the turbostratic carbon structure, forming stacked graphene layers. This process significantly enhances thermal stability, electrical conductivity, and mechanical strength (Torres-Canas et al., 2020). Catalytic graphitization using metal catalysts at lower temperatures (around 1200-1500 °C) is known to

accelerate this transformation (Farid et al., 2023; L. Zhou et al., 2023). Surface graphitization techniques like chemical vapor deposition can selectively enhance graphitic content on fiber surfaces (Ge et al., 2022). In the presence of oxidizing gases during thermal treatments, processes such as atom rearrangement in amorphous carbon are accelerated, breaking bonds in disordered regions and promoting interconnection between stacked planes or sections. This process can lead to the formation of nanocrystalline graphite, observed to improve mechanical properties at temperatures exceeding 1600 °C (A. Bengtsson et al., 2020; Youe et al., 2016). Achieving high graphitization levels remains challenging due to inherent defects and impurities in lignin-based carbon fibers, yet enhancing graphitic properties is crucial for superior performance in applications like energy storage electrodes and structural composites.

3.4. Characterization Techniques

This section provides a background to the various characterization methods used to examine the properties of the different materials treated in the appended papers and this thesis work. Furthermore, we provide a nuanced understanding of their different roles in characterizing lignin-based materials, emphasizing both the personal technical hurdles and the strategies employed to overcome them.

3.4.1. Scanning Electron Microscopy

Scanning Electron Microscopy (SEM) is an essential technique for the detailed morphological and structural analysis of carbon and carbon fiber materials used in our studies. SEM utilizes a focused beam of high-energy electrons to generate high-resolution images, revealing the surface topography and composition of the material. It provides detailed images of surface morphology, allowing for the observation of the microstructure and nanostructure of the carbon materials, including fiber diameter, surface roughness, and porosity. SEM helped identify the distribution and alignment of carbon fibers, as well as any defects or irregularities in the material, which is vital for correlating structural characteristics with electrochemical performance.

The key challenges faced while SEM imaging of lignin fibers and lignin carbon fibers during our analysis:

1. Sample preparation and charging effects

- Challenge: Lignin fibers (such as-spun in [Paper I, III](#) and thermostabilized fibers used for separators), being non-conductive, often require a conductive coating to prevent charging during SEM imaging. The gold coating prevents this charge build-up, ensuring high-quality imaging. As charging accumulates electrons under the electron beam it can distort images of lignin fibers, leading to inaccurate interpretations of fiber diameter and surface texture. An article (“Fiber Analysis – Using SEM for the Quality Analysis of Fibers,,” 2024) discusses specific challenges in imaging non-conductive fibers, including charging effects and sample preparation techniques. It provides practical solutions like low vacuum imaging and conductive coating methods to overcome these issues.

- Interpretation and mitigation strategy: In our experiments, using low-vacuum modes of 5 kV reduced charging but sometimes at the cost of resolution. This trade-off was carefully managed to ensure accurate characterization. Also, optimizing the coating thickness was crucial to balance conductivity with image clarity. As excessive coating masks surface features, while insufficient coating leads to charging artifacts (“How Does Coating Thickness Affect SEM Imaging?,” n.d.). We employed a 5 nm gold layer sputtered onto the samples to enable our standard morphological analysis.

2. Resolution and surface detail

- Challenge: While SEM provides high-resolution images, capturing the cross sections ([Paper III](#)) and true surface morphology of lignin fibers was difficult due to their complex, irregular structures.

- Interpretation and mitigation strategy: adjusting imaging parameters like working distance and accelerating voltage helped enhance visibility.

3. Artifacts from sample preparation

- Challenge: As the carbon fibers are quite delicate (especially lignin-cellulose CFs ([Paper III](#))) it made mechanical handling during sample preparation difficult as it introduced defects or alter the fiber structure if handled without care, affecting SEM analysis (Agrawal et al., 2024).

- Interpretation and mitigation strategy: We took special care in mounting and sectioning samples to minimize mechanical stress. However, some deformation was unavoidable, highlighting the need for gentle handling techniques.

4. Quantitative analysis limitations

- Challenge: Automated software for measuring fiber dimensions from SEM images can struggle with complex morphologies like meshed ELCF ([Paper I](#)), leading to inaccuracies. The study by (Götz et al., 2020) examines the capabilities and limitations of automated fiber diameter analysis using DiameterJ software on SEM images. It highlights issues with segmentation algorithms and potential misinterpretation of data, especially for complex fiber morphologies.

- Interpretation and mitigation strategy: Therefore, in our study, manual verification of automated measurements was necessary to ensure accuracy, particularly for fibers with non-uniform cross-sections.

3.4.2. Raman Spectroscopy

Raman spectroscopy is a powerful analytical technique crucial for characterizing carbon electrodes derived from lignin. Raman spectroscopy is based on the inelastic scattering of light by molecules, where a small fraction of incident photons interacts with molecular vibrations, resulting in scattered light with shifted energy. This technique provides a unique "chemical fingerprint" of materials by measuring the intensity and wavelength of the scattered light, allowing for the identification and characterization of chemical structures and molecular interactions (Agarwal, 2019). This technique offers detailed structural insights, revealing the degree of graphitization and the presence of graphitic (G band) and disordered (D band) structures in the carbonized fibers. The intensity ratio of these bands (I_D/I_G) served as a key indicator of the carbon material's quality ([Paper III](#)). Additionally, it helps assess the crystallinity and disorder within the carbon matrix, which directly influence the electrochemical properties of the electrodes. Raman spectroscopy is generally non-destructive, preserving the sample for further analysis or practical use, and it detects various carbonaceous phases and functional groups, elucidating the chemical modifications that carbon undergoes after carbonization or even surface modification.

1. Sensitivity of laser power

- Challenge: Carbon-based materials, typically dark in color, absorb significant energy from lasers, making them highly sensitive to laser intensity. For single lignin-cellulose carbon fibers ([Paper III](#)), exposure to a 532 nm laser wavelength resulted in burning due to the beam's intensity, necessitating careful tuning of laser power.

- Interpretation and mitigation strategy: careful optimization of the laser wavelength and power settings, along with manually optimized exposure times, was crucial to balance between achieving

a strong Raman signal and preserving the structural integrity of the sample, ensuring reliable and accurate measurements.

3.4.3. X-ray Photoelectron Spectroscopy

X-ray Photoelectron Spectroscopy (XPS) is a vital technique for analyzing the chemical composition and surface features of carbon electrodes derived from lignin, particularly in identifying functional groups. XPS operates by irradiating the sample with X-rays, causing the emission of photoelectrons whose energies are measured to provide detailed information about the elemental composition and chemical states of the atoms within the top few nanometers of the surface (Moulder et al., 1995). This technique was especially useful for detecting and quantifying various functional groups and surface oxides, providing insights into the chemical modifications that lignin undergoes during carbonization and surface modification via treatments like plasma exposure (in [Paper I](#)). By analyzing the binding energies of the emitted photoelectrons, XPS can identify specific functional groups such as hydroxyl, carbonyl, and carboxyl, which play crucial roles in the electrochemical properties of the electrodes. Furthermore, XPS can offer information on the surface oxidation states and the presence of heteroatoms like nitrogen or sulfur, which can also enhance the electrodes' performance. In [Paper I](#), potassium content and components were analyzed to examine the effects of the KOH electrolyte on the electrodes after 10000 cycles, offering valuable insights into the interaction between the aqueous KOH electrolyte and the fiber surfaces. An analysis was also conducted for discussion in section 2.3.2 to examine the impact of electrolytes on lignin-based and glass-fiber separators.

1. XPS Analysis of non-conductive fibers

- Challenge: The analysis of non-conductive lignin fibers using XPS presents significant challenges due to the tendency of these materials to accumulate charge during measurement. This charging effect can distort the spectral data, leading to inaccurate interpretations of surface functional groups and chemical states.

- Interpretation and mitigation strategy: To address this challenge, the use of the argon method for surface treatment is practiced (Baer et al., 2020). By applying an argon ion beam prior to XPS analysis, the surface of the lignin fibers can be rendered conductive, thereby minimizing charging effects during measurement. This method allows for a more accurate assessment of surface functional groups, as it facilitates better electron emission and enhances the quality of the XPS spectra obtained.

3.4.4. X-Ray Diffraction

X-Ray Diffraction (XRD) is a crucial technique for determining the crystallinity, phase composition, and surface structure of lignin-based carbon electrodes. XRD operates by directing X-rays at the material and measuring the intensity and angles of the diffracted beams, providing insights into atomic arrangements within the carbon matrix. This technique is particularly effective in identifying crystalline phases, and can quantify the degree of crystallinity or if it is amorphous carbon (Qin et al., 2012). This is essential for understanding the material's structural order, which directly impacts electrochemical performance, as more crystalline structures generally offer enhanced conductivity.

XRD also provides valuable information about the surface composition of the electrodes, including the presence of residual inorganic phases or impurities that could affect their functionality. By analyzing the diffraction patterns, details such as interlayer spacing, crystallite size, and overall structural integrity can be derived, helping to some extent to assess surface composition ([Paper II](#)) and ensure a consistent, high-quality carbon structure for improved electrochemical behavior.

1. Analysis of solution-spun individual carbon fibers

- Challenge: Conducting XRD on solution-spun individual carbon fibers presented significant challenges due to their small diameter and the potential for sample misalignment during measurement. The inherent flexibility and fragility of these fibers made it difficult to obtain stable, reproducible diffraction patterns, leading to unreliable data regarding their crystallinity and phase composition. Additionally, the presence of amorphous regions in the fibers complicated the interpretation of XRD results, as the overlapping peaks could obscure critical information about the crystalline structure.

- Interpretation and mitigation strategy: To address the challenge, Small-Angle X-ray Scattering (SAXS) was employed instead of XRD. SAXS, which is a subset of XRD, allows for the investigation of nanoscale structures and provides valuable information about the size, shape, and distribution of scattering entities within the carbon fibers (Torres-Canas et al., 2020). By utilizing SAXS, we could effectively analyze the structural characteristics of the solution-spun carbon fibers without the complications associated with traditional XRD measurements. This approach not only mitigated the issues related to sample alignment and stability but also offered insights into both crystalline and amorphous phases at a different scale, enhancing the understanding of the overall structure of these fibers (J. Liu et al., 2023) and carbon fiber's as in our preliminary studies provided in the supplementary material related to [Paper III](#).

3.4.5. Thermogravimetric Analysis

Thermogravimetric Analysis (TGA) is a critical technique for evaluating the thermal properties and stability of carbon electrodes derived from lignin. TGA measures the change in mass of a sample as it is heated, providing insights into the material's thermal stability, composition, and decomposition patterns. This analysis is crucial for understanding the thermal behavior of lignin-based carbon, including the temperatures at which various components decompose or react. TGA can reveal the presence of residual lignin or other organic compounds that may impact the performance of the carbon electrodes (Nowak et al., 2018).

In our studies, TGA characterization is employed to assess the thermal profiles of various lignin-based materials in their fresh state before undergoing thermostabilization and carbonization. By analysing the thermal degradation patterns of lignin at different temperatures, we can determine the optimal conditions for carbonization that enhance the structural integrity and electrical conductivity of the resulting carbon fibers. For example, TGA results can reveal specific temperature thresholds at which significant mass loss occurs, which may vary depending on the source of the lignin (Figure 11) or lignin-cellulose blend. While these temperature ranges help inform the carbonization process, in our study, we applied a consistent carbonization temperature of 1000°C across all cases to evaluate the resulting material properties ([Paper III](#)).

3.4.6. Carbon Hydrogen Nitrogen Sulfur (CHNS) Analysis

Chemical characterization through CHNS analysis is essential for understanding the elemental composition of carbon fibers derived from lignin. This analytical technique quantitatively measures the amounts of carbon, hydrogen, nitrogen, and sulfur present in the fibers, offering insights into their chemical makeup and purity. By identifying residual elements from the lignin precursor and any introduced impurities during processing, CHNS analysis helps optimize manufacturing processes to enhance fiber quality by understanding their influence on physiochemical features which might influence their performance as electrodes in supercapacitors (Mishra et al., 2023). Also, this information could be pivotal for quality control, ensuring consistency in electrode composition across production batches.

3.4.7. Mechanical Testing

Mechanical testing, including tensile strength and Young's modulus analysis, using a Universal Testing Machine (UTM) with fiber grips, is used for assessing the structural integrity and flexibility of carbon electrodes derived from lignin.

Tensile Strength Analysis

Tensile strength testing involves applying a controlled tensile load to the sample using the UTM. The fiber grips securely hold the electrode material in place while gradually increasing the load until the material fractures. This test determines the maximum stress the material can withstand before breaking

Young's Modulus Analysis

Young's modulus testing assesses the stiffness or elasticity of the material. It involves measuring the material's response to applied stress within its elastic deformation range. Using the UTM with fiber grips ensures precise control and measurement of the applied force and resulting deformation. Young's modulus is calculated as the ratio of stress to strain in the linear elastic region of the material's stress-strain curve. This parameter is critical for understanding how much a lignin-based carbon electrode will deform under loading and provides insights into its structural flexibility and resilience.

3.4.8. Electrical Conductivity

The four-point probe method provides a precise means of assessing the conductivity of a material by avoiding the impact of high contact resistances. This method is particularly useful for measuring the conductivity of lignin-derived carbon fibers as understanding the electrical conductivity of lignin-based carbon fibers is critical as it directly influences their performance in electrochemical applications.

Using the formula derived from (Rebouillat & Lyons, 2011):

$$\rho = \frac{\pi \cdot d^2 \cdot R}{4 \cdot L} \quad (\text{Equation 14})$$

where d is the average diameter, ρ is the resistivity, measured resistance from the four-point probe is R , and length of the fiber is L . This equation is particularly applicable when dealing with cylindrical fibers, as the term $\pi \cdot d^2/4$ represents the cross-sectional area of the fiber. This geometric consideration is critical for accurately calculating the electrical resistivity of the material. The diameter of the fiber directly influences its electrical properties; thus, precise measurement of this parameter is essential.

While the four-point probe method offers a reliable approach to measuring conductivity, several challenges can arise during interpretation, particularly related to variations in fiber diameter among samples.

1. Variability in diameter

- Challenges: If there are significant variations in the diameters of the carbon fibers being tested, this can lead to discrepancies in resistivity values. For example, a thinner carbon fiber will typically have higher conductivity compared to a thicker fiber, despite its smaller cross-sectional area. This is due to factors such as better crystallite alignment, higher surface area to volume ratio, and potentially fewer defects per unit length in thinner fibers, which enhance electron transport and

reduce resistivity. This variability complicates direct comparisons between different fibers or batches. In [Paper III](#), the assessment of different lignin-cellulose carbon fibers involved a sample set with varying diameters. Given this variability, it became essential to employ statistical methods to account for these differences. Averages alone may not accurately represent individual fibers, particularly when some fibers are significantly larger or smaller than others. This discrepancy can lead to misleading conclusions regarding the overall conductivity of the batch.

- Interpretation and mitigation strategy: To address this challenge, conductivity measurements were taken from a diverse set of fibers with varying diameters, resulting in a spread of conductivity values as detailed in the appended [Paper III](#). By utilizing statistical analysis on this broader dataset, we can better understand the impact of diameter variations on conductivity and ensure that our interpretations are robust and reflective of the entire sample population. This approach helps mitigate the risk of drawing incorrect conclusions based on potentially skewed averages, ultimately leading to a more accurate assessment of the electrical properties of lignin-based carbon fibers.

3.5. Electrochemical Testing Procedures

This section will outline the procedures for evaluating the electrochemical performance of the electrode materials in supercapacitor configurations. The techniques used were cyclic voltammetry (CV), galvanostatic charge-discharge (GCD), and electrochemical impedance spectroscopy (EIS) which yield information on specific capacitance, energy density, power density, and cycling stability.

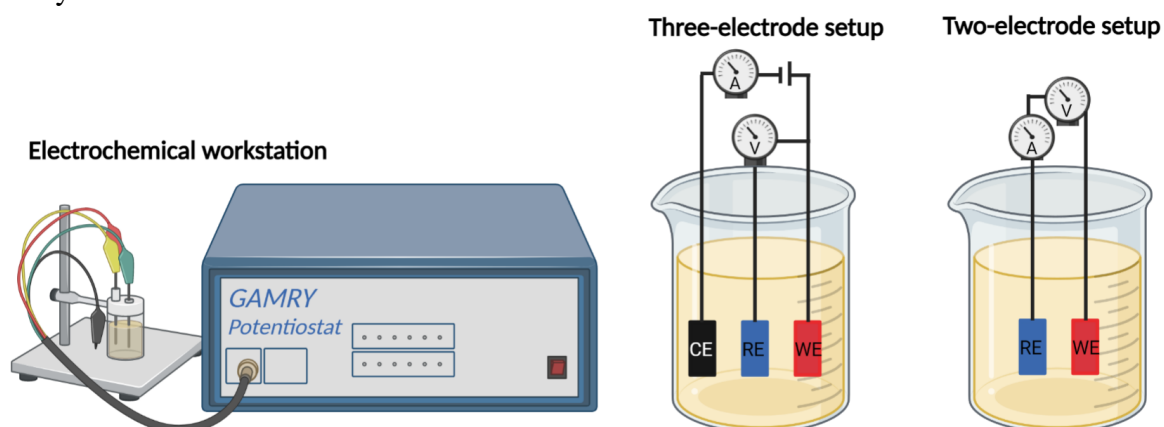


Figure 23. Schematic representation of an electrochemical workstation and the three and two-electrode setups used for electrochemical testing of supercapacitor electrode materials.

In most of our studies, electrochemical analysis was conducted using a two-electrode setup in a coin cell configuration (Figure 23). This setup involves applying a potential difference between the positive and negative electrodes immersed in the electrolyte, with the measured voltage representing the entire cell voltage. The coin cell configuration is widely used for practical evaluations as it simulates real-world device performance. However, a limitation is that it does not allow for separate monitoring of the potential changes at individual electrodes, which can obscure detailed mechanistic insights into the electrochemical behavior of specific electrode materials. By contrast, a three-electrode setup offers distinct advantages for more controlled and detailed analyses. In this arrangement, current flows only between the working electrode (WE) and the counter electrode (CE), while the voltage at the WE is monitored relative to a reference electrode (RE). This allows precise measurement of the WE's potential, independent of the CE, providing deeper insights into the electrode's behavior. Common CEs include Pt or Au, while REs often use saturated calomel electrodes (SCE), Ag/AgCl, or Hg/HgO, which maintain constant half-reaction

potentials. The three-electrode setup's primary advantage lies in its ability to isolate and study half-cell reactions, enabling a detailed understanding of processes occurring at the WE. In contrast, the two-electrode coin cell setup, while less detailed, is better suited for practical performance evaluations, making it the more appropriate choice for this study's objectives.

Most of the electrochemical measurements were conducted using a Gamry Reference 3000AE electrochemical workstation, employing a coin cell device system with electrolyte solutions prepared under ambient conditions. Additionally, custom-built devices in our laboratory were utilized to evaluate the performance of cellulose-based supercapacitors, specifically analyzing lignin-cellulose carbon fibers with PVA-KOH electrolyte and IrO₂ microsupercapacitors with cellulose-based electrolytes.

3.5.1. Fabrication of Test Cells and Experimental Configurations

The fabrication and testing of various two-electrode configurations were key aspects of this study, exploring the potential of wood-derived materials in supercapacitor applications. Below, the assembly methods, choice of electrolytes, and testing conditions for the different cell setups used across the papers are summarized to complement the detailed discussions in the respective studies.

Coin Cell Configurations

Paper I: Freestanding electrospun lignin carbon fiber (ELCF) electrodes were paired with glass fiber (GF) separators and evaluated using three electrolytes: 6M KOH, 1M H₂SO₄, and 1M Li₂SO₄. These tests assessed the influence of electrolyte type on the electrochemical performance of the electrodes.

Paper II: Composite electrodes composed of activated carbon (AC), carbon black (CB), and lignin-carbon fibers (LCF) were fabricated using microfibrillated cellulose (MFC) as a binder. GF separators and a 6M KOH electrolyte were used in the coin cell configuration to study the electrochemical behavior of the composites.

Device assembly details of other supplementary studies discussed in this thesis:

Separator study: AC and CB electrodes were fabricated using PTFE as a binder. Separators included thermostabilized SKL fibers, thermostabilized HKL fibers, lignin nonwovens, cellulose nonwovens, and GF. For the GF separators, devices were assembled in a coin cell configuration using various aqueous electrolytes, including 6M KOH, 1M KOH, 1M Na₂SO₄, and 1M H₂SO₄.

MnO₂ study: Hydrothermally treated freestanding MnO₂-coated lignin carbon fiber (M-ELCF) electrodes were paired with GF separators. These devices were tested with a 6M KOH electrolyte.

On-Plane Fiber Macrosupercapacitor Configuration

Paper III: A custom macrosupercapacitor device was fabricated on a glass slide using lignin-cellulose carbon fibers as the active material. The fibers were aligned and secured with silver paste serving as current collectors, while polyvinyl alcohol (PVA)-KOH gel acted as the electrolyte. Although primarily a material characterization study, this configuration demonstrated the practical feasibility of on-plane devices.

MSC Study with Gel Electrolytes

MSCs were developed using cellulose-based gel electrolytes composed of nanocellulose/PVA/CB, paired with IrO₂ electrodes. This configuration emphasized the integration of renewable gel electrolytes in micro-scale energy storage devices.

3.5.1. Experimental Conditions

The performance of supercapacitor devices was evaluated under selected experimental conditions to ensure reliable and comparable results across all configurations. The potential windows for the devices were typically set between 0 - 1 V, depending on the specific electrolyte used. This voltage range was chosen to remain within the electrochemical stability limits of the materials and to prevent electrolyte decomposition.

Scan rates and rate capability: Depending on study to study scan rates varied from 1 mV/s to 1000 mV/s during CV tests. The scan rate directly impacts the rate capability of the device, with lower rates providing insights into the material's full capacitance and higher rates reflecting its ability to maintain performance under rapid charge-discharge conditions. The resulting CV curves plotted across this range help evaluate the capacitance retention and efficiency at different charging speeds. Additionally, in [Paper I](#), lower scan rates were used to conduct deconvolution studies following the method proposed by Dunn et al (J. Wang et al., 2007). These studies at slower scan rates allow for a more detailed analysis of the charge storage mechanisms and the separation of capacitive and diffusion-controlled processes (see Section 2.6). Rate capability in supercapacitors refers to their ability to maintain high capacitance and power delivery at various charge-discharge rates.

Current densities: Current densities were varied between 0.1 to 20 A/g during GCD testing. Low current densities allow for the assessment of the device's maximum energy storage capability, while high current densities test its power handling ability. This range was tailored to optimize the evaluation of the electrode-electrolyte combinations used in the study.

Cycle stability and coulombic efficiency: Cycling stability was evaluated over a maximum of 10000 charge-discharge cycles, serving as a standard benchmark for assessing the long-term performance of the devices. This parameter specifically reflects the ability of the electrode and electrolyte to maintain stable capacitance over repeated cycling. Capacitance retention is the primary measure of cycling stability, indicating how much of the initial capacitance is preserved after extensive cycling use.

Coulombic efficiency, on the other hand, is defined as the ratio of discharge capacity to charge capacity in each cycle and provides insights into the efficiency of charge storage and retrieval. A high coulombic efficiency, typically close to 100%, signifies minimal energy losses during operation. However, it is essential to note that cycling stability (capacitance retention) and coulombic efficiency are independent metrics. While both are critical for evaluating device performance, the percentage values listed in the tables in this thesis are explicitly for cycling stability, measuring capacitance retention.

Test environment: All experiments were conducted at room temperature to ensure consistent and realistic evaluation conditions.

These independent performance metrics: rate capability, energy and power density, cycling stability, and coulombic efficiency collectively provide a comprehensive understanding of the supercapacitor's performance.

3.5.1. Voltammetric and Galvanostatic Charge-discharge Methods

Cyclic voltammetry (CV) is a potentiodynamic electrochemical technique where the potential of the analyzed electrode is ramped linearly versus time. During CV when the set potential is reached, the working electrode's potential ramp is inverted. This inversion occurs multiple times during an experiment as per the number of cycles given as input to run. The current of the working electrode is plotted versus the applied voltage to get the CV plot. In a three-electrode setup, this plot can be interpreted to identify electrochemical processes such as oxidation (positive current peak) and reduction (negative current peak) occurring specifically at the working electrode. However, in a two-electrode coin cell configuration, the CV plot reflects the net electrochemical behavior of both electrodes in the cell.

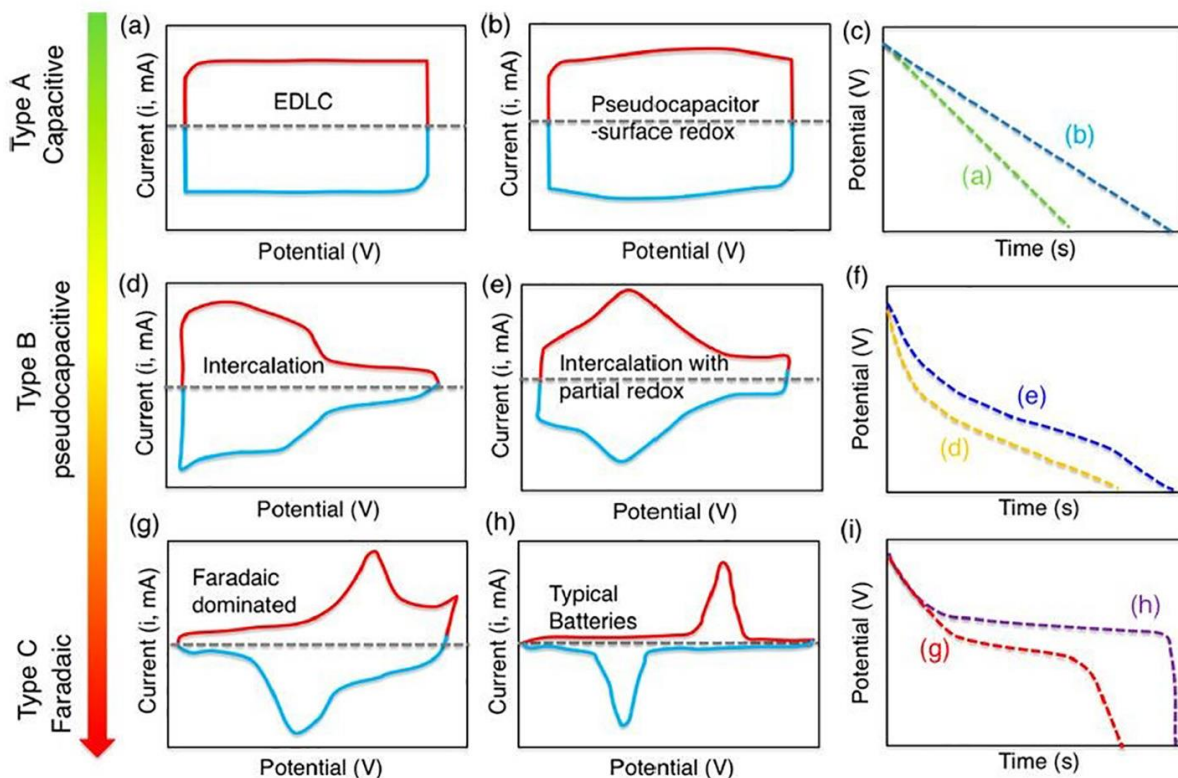


Figure 24. Schematic CV a), b), d), e), g) and h) with corresponding charge discharge profiles c), f), and i) curves for EDLC (Type A), pseudocapacitor (Type B) and battery (Type C) materials, respectively. Capacitive trend in pseudocapacitive materials is mostly either from (b) surface redox reactions or (d) intercalation-type. Also, there is a third special type with intercalation-type materials with broad redox peaks that are electrochemically reversible. Reproduced with permission from Gogotsi & Penner, 2018.

In an EDLC, the specific capacitance remains constant over the full potential range, resulting in a characteristic rectangular shape in the CV curve that reflects linear charge and discharge behavior. In fact, an EDLC capacitive behavior typically has a CV curve of rectangular shape as in Figure 23 a, whereas in pseudocapacitive materials potential-dependent redox reactions occur showing features in the characteristic curves Figure 24 b. EDLCs show constant rate of discharge whereas for pseudocapacitors the discharge rate depends on the redox reaction rate affected by potentials in Figure 24 c. Differences in CV for EDLCs from pseudocapacitors are very different when intercalation (or diffusion-controlled behavior) comes into the picture (Figure 24 d and e). During GCD, the supercapacitor is charged and discharged at a constant applied current between two defined voltage points. The voltage recorded signifies the reactivity window of the device and the time for charging/discharging gives the rate of charging/discharging. Also, this method is known

to resemble real-world performance more closely than CV. In Type C, battery like materials, two distinct peak currents can be observed in the CV where redox reactions occur.

3.5.2. Electrochemical Impedance Spectroscopy Method

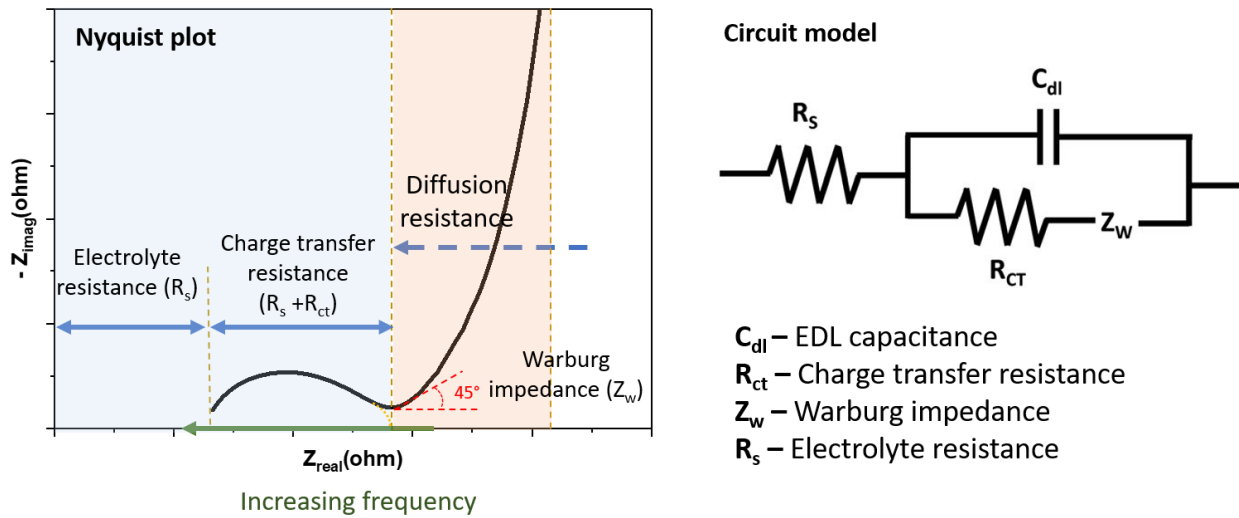


Figure 25. Nyquist plots of the impedance of a Randles circuit with Warburg impedance when the scale is orthonormal, and the low-frequency angle is 45° . Reproduced with permission from Choi et al., 2020.

Electrochemical Impedance Spectroscopy (EIS) is a versatile and widely used technique for investigating the electrical properties of electrochemical systems. By applying a small amplitude AC signal across a range of frequencies, EIS provides insights into the dynamics of processes occurring at electrode interfaces (Perdana et al., 2024). The Nyquist plot (as shown in Figure 25), a graphical representation of EIS data, offers several key indications:

- Charge transfer resistance: The semicircle diameter at high frequencies reveals charge transfer resistance, reflecting the ease or difficulty of electron transfer at the electrode surface.
- EDL-capacitance: The low-frequency region displays a linear segment indicating double-layer capacitance, which relates to the EDL formed between the electrode and electrolyte.
- Warburg impedance (Z_w): At the low-frequency end, Warburg impedance reflects diffusion processes within the electrolyte, offering insights into mass transport limitations.

Randles Circuit

To interpret these phenomena, one commonly applied model is the Randles circuit (Choi et al., 2020; Randles, 1947). This equivalent circuit typically includes:

- Electrolyte resistance (R_s): Represents the resistance of the electrolyte solution through which ions travel.
- Charge transfer resistance (R_{ct}): Corresponds to the resistance encountered during electron transfer at the electrode surface.
- Double layer capacitance (C_{dl}): Accounts for the capacitance associated with the formation of the electric double layer at the electrode/electrolyte interface.

The notion of an "electrode resistance" often refers to the equivalent series resistance (ESR), which includes contributions from both conduction through the electrolyte and the electrodes and current collectors. Conversely, "electrolyte resistance" is more accurately described as an interfacial

resistance, dependent on interactions between the electrode and electrolyte. In the modified Randles circuit (Figure 25), the R_s replaces the ESR, representing the ionic conductivity of the electrolyte solution. The pseudo-capacitance component is replaced by Z_w which models diffusion-related processes at the electrode-electrolyte interface.

Warburg Impedance

Z_w is characterized by its frequency-dependent behavior, which arises from diffusion-controlled processes in electrochemical systems. It typically appears as a straight line in the Nyquist plot at low frequencies, indicating that mass transport limitations are influencing the overall impedance. This behavior can be quantified using (Mei et al., 2018):

$$Z_w = \frac{\sigma}{j\omega} \quad (\text{Equation 15})$$

where σ is the Warburg coefficient, j is the imaginary unit, and ω is the angular frequency. A comprehensive understanding of Warburg impedance is crucial for analyzing systems where diffusion plays a significant role in electrochemical reactions.

Z_w is characterized by a 45° line in the Nyquist plot at low frequencies, indicating diffusion-controlled reactions. This modification emphasizes diffusion processes over fast Faradaic reactions typically associated with pseudocapacitors. The circuit's behavior now more closely resembles a classic Randles circuit, with R_s dominating at high frequencies and Z_w becoming significant at low frequencies. This altered model may be more suitable for systems where diffusion is a key factor, but it may not fully capture the unique voltage-dependent capacitance of pseudocapacitive materials.

The analysis of Nyquist plots through EIS provides a holistic view of electrochemical behavior, essential in fields such as battery research, corrosion analysis, and sensor development. By incorporating concepts like the Randles circuit and clarifying resistive contributions from both electrodes and electrolytes, we can achieve a more accurate interpretation of EIS data and its implications for system performance.

Chapter 4

Enhancement of Electrode Materials

This chapter describes selected approaches to enhance the performance of the lignin derived materials for supercapacitor applications. CFs made from lignin precursors have a large specific surface area, decent mechanical flexibility, moderate electrical conductivity, and beneficial surface functions compared to particulate (such as AC) morphology counterparts. ELCFs are freestanding and useful as both a current collector and an active material, minimizing device contact resistance. In addition to electrostatic charge storage, which contributes to EDL capacitance, they exhibit contributions from the Faradaic reaction of their surface functional groups, which provides pseudocapacitance. But the functional groups that contribute to capacitance are typically lost during high-temperature carbonization, also affecting the device's electrode-electrolyte interactions. To improve the electrochemical performance of the supercapacitor, the active material's surface can be plasma treated to add controlled functional groups to the carbon matrix [[Paper I](#)].

4.2. Performance Enhancement of Electrode Materials

Beyond high-temperature carbonization, achieving superior performance in lignin-based electrode materials involves adjusting various synthesis parameters. This section will delve into strategies such as surface modification of carbon fibers by introducing functional groups, enhancing capacitance by decorating MOs, and blending lignin with cellulose to create composite electrode materials aimed at improving overall performance.

4.2.1. Surface Modification

The performance of EDLC materials is characterized by their high power densities, which however is at risk of significantly diminishing if there are obstacles to ion accessibility, such as tortuous microporosity or non-graphitic carbon wall structures that create ionic resistance. Surface modification of porous carbon materials becomes essential to ensure effective adsorption and desorption of electrolyte ions both on the electrode surface and within its bulk, thereby mitigating such accessibility issues. While redox processes in pseudocapacitive materials are inherently rapid, the specific surface conditions are crucial for maximizing the utilization of surface-confined reactions. Moreover, altering the electrode/electrolyte interface by designing passive layers on the carbon surface can elevate the cell voltage, shifting electrolyte reduction and oxidation processes to higher over-voltages (Y. Zhu & Fontaine, 2022).

During the initial charge-discharge cycles, a solid electrolyte interphase (SEI) naturally forms on the carbon surface of EDLC anodes. This SEI layer, developed in the first cycle, obstructs electrolyte ion penetration into the underlying carbon layers while preventing further electrolyte reduction (Y. Zhu & Fontaine, 2022). Customizing the characteristics of the carbon surface, such as introducing hydrophobic or hydrophilic groups, could substantially increase over-voltage and expand the electrochemical stability window of the electrolyte. However, modifying the carbon/electrolyte interface poses challenges as it must not impede ion access to the porous carbon structure in the electrolyte. Careful and successful development of an artificial SEI-like layer on the porous carbon surface would markedly enhance the performance of EDLCs.

Doping represents a straightforward method to tailor the fundamental properties of electrodes and improve their compatibility with electrolytes. Common heteroatoms used for doping into carbon frameworks include oxygen, nitrogen, boron, sulfur, phosphorus, fluorine, silicon, and chlorine (Feng et al., 2021). These dopants introduce defects that serve as redox centers, thereby amplifying inherent pseudocapacitive contributions.

Nitrogen doping and oxygen functionalization are widely employed techniques to convert predominantly hydrophobic carbon surfaces to hydrophilic ones. This surface modification does not alter the material's intrinsic properties but modifies the polarity of the surface charge, thereby enhancing electrode wettability to electrolytes. Optimal wettability is crucial, as inadequate wetting of electrolytes can lead to inconsistent reactions due to unstable formation of the EDL interface. Nitrogen can be incorporated into the carbon matrix through post-processing with nitrogen-rich components such as ammonia or urea, or by starting with a nitrogen-rich precursor like polyaniline or polypyrrole. Similarly, oxygen can be introduced into the carbon matrix through non-destructive methods such as plasma treatment to derive plasma-treated LCF (PLCF) (as in [Paper I](#)).

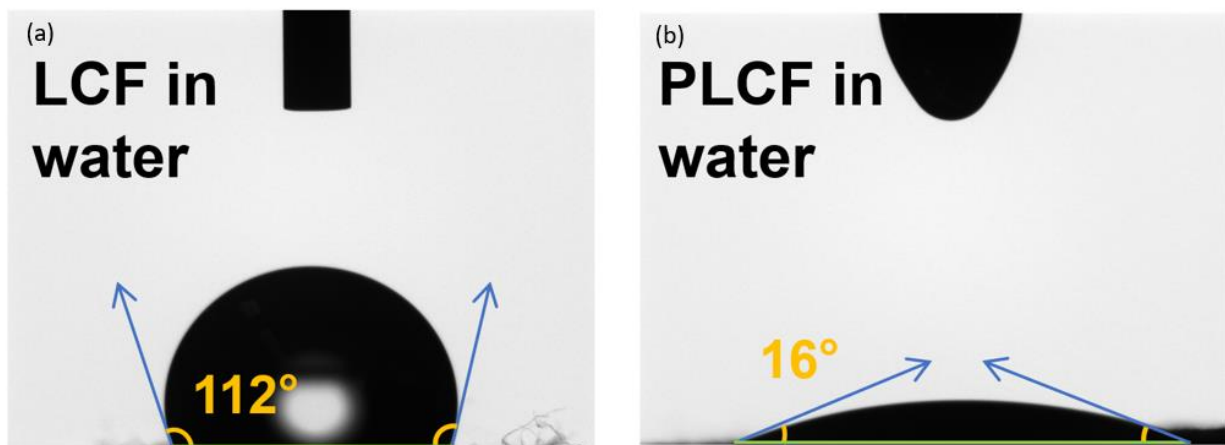


Figure 26. Wettability test indicating (a) hydrophobic nature of LCF mat samples before and (b) hydrophilic nature after plasma treatment for 60 seconds at 25W power.

The use of plasma treatment, even for short durations, has proven effective in eliminating hydrophobicity (Figure 26), thereby enhancing access to the internal surface area of the carbon fiber material that would otherwise remain underutilized.

4.2.2. Metal Oxide Decoration to Enhance Performance in Lignin-Based Carbon Fiber Electrodes

To enhance the capacitance of lignin-based electrodes, MOs can be decorated on carbon materials. This hybrid approach leverages the conductivity of carbon fibers and the redox properties of MOs, resulting in improved performance for supercapacitors. The combination of MO electrodeposition on carbon fibers is seen as a promising strategy, with enhanced efficiencies and higher capacitive performance due to the increased available surface area for reactions.

(Du et al., 2023), decorated iron oxide (Fe_3O_4) on lignin carbon nanofibers prepared through electrospinning followed by stabilization and carbonization, resulting in a specific capacitance of 539 F/g. This kind of approach significantly increases the specific surface area and introduced pseudocapacitive behavior, contributing to improved overall performance and good cycling stability in similar studies (L. Wang et al., 2017). Similarly, manganese dioxide (MnO_2) nanowhiskers were hydrothermally grown on electrospun lignin nanofibers, yielding a high specific capacitance of 83 F/g. This method provided additional pseudocapacitance and increased

overall capacitance, demonstrating the benefits of MnO₂ in enhancing the performance and cycling stability of lignin-based electrodes (X. Ma et al., 2016a). In contrast, similar carbonized electrospun lignin carbon fibers without MOs showed a specific capacitance of 64 F/g (Lai et al., 2014). Comparing these methods, it appears that MO decoration can enhance the specific capacitance by introducing pseudocapacitive behavior. The choice of MO and decoration method significantly impacts on the electrochemical performance of lignin-based carbon fiber electrodes for supercapacitors (X. Ma et al., 2016b; L. Wang et al., 2017).

In our extended investigation of ELCFs as potential supercapacitor electrodes in [Paper I](#), we explored the use of LCF-MnO₂ coated electrode via hydrothermal treatment with MnO₂, known for its high theoretical capacitance, which is commonly used to enhance the electrochemical performance of carbon-based materials (Toupin et al., 2004). However, this approach presented challenges, as the MnO₂ coating separated during the post-synthesis washing process, indicating surface incompatibility and weak adhesion to the underlying LCFs.

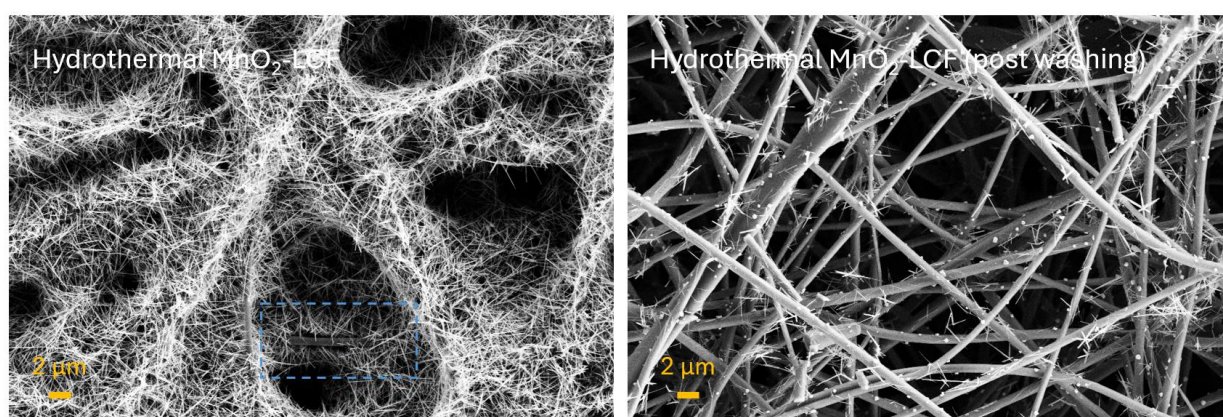


Figure 27. SEM images of manganese oxide-coated electrospun lignin carbon fibers obtained through hydrothermal treatment, shown before and after water washing. The blue dotted square in the SEM image highlights issues with the MnO₂ coating on the carbon fiber, indicating areas where it is poorly adhered or insufficiently bonded to the LCF.

The SEM images in Figure 27 depict the morphological changes before and after one water washing, clearly illustrating the issue of insufficient bonding of MnO₂ onto the carbon fiber associated with the coating. Initially, the MnO₂ forms a dense, non-uniform layer across the LCF surface. Following the washing process, the MnO₂ layer is almost entirely removed, revealing that the adhesion between the MnO₂ and LCF substrate is a challenge that requires processing method optimization.

The lack of adhesion can be attributed to the differences in surface characteristics between the lignin-based carbon fibers and the MnO₂. While lignin-based carbons are porous and exhibit high surface area, they may lack the necessary surface functional groups or micro-roughness to anchor the MnO₂ effectively. To address this, we attempted a plasma treatment on the LCFs prior to MnO₂ deposition, aiming to enhance surface adhesion. However, the plasma treatment did not yield any significant improvement in MnO₂ retention, suggesting that a more robust approach, such as functionalizing the LCF surface with adhesion-promoting agents, may be required for better integration.

Electrochemical performance of the electrodes tested in a 6M KOH aqueous electrolyte within a coin cell configuration, as reflected in the CV curves in Figure 28, further substantiates the need for improved coating stability. The uncoated LCF electrodes exhibit a rectangular CV profile,

indicative of ideal capacitive behavior with relatively consistent current density. In contrast, the MnO₂-coated LCF electrodes, prior to washing, show very similar profiles but with lower current densities. This distortion is likely due to a reduction in the active area of the electrode, where the impact of the MnO₂ in this configuration only seems to be to reduce access to the LCF electrode. After the washing process, the capacitance performance remains compromised, and it is now less similar to the original characteristics in its shape. It can be speculated that this can be related to a modification of the original surface features of the LCF after the MnO₂ washing procedure.

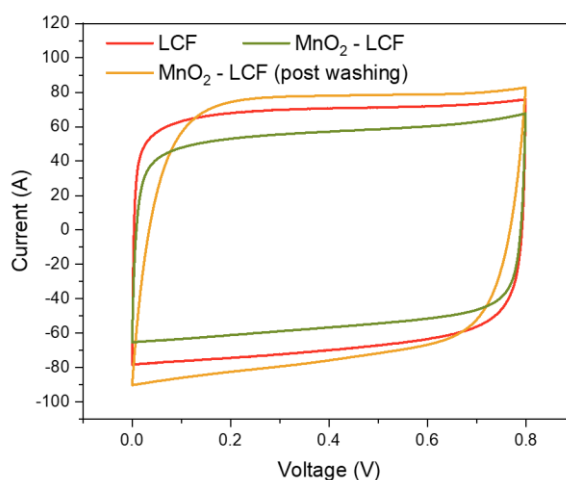


Figure 28. CV curves of manganese oxide-coated electrospun lignin carbon fibers obtained through hydrothermal treatment, compared with untreated LCF.

The challenges encountered with MnO₂ decoration on LCFs highlight the importance of optimizing both the material compatibility and the deposition technique for effective electrode development. Future work should consider alternative MO coatings or dual-modification strategies that incorporate both adhesion-promoting layers and active materials. By achieving a uniform, well-adhered MnO₂ layer, it may be possible to fully leverage the pseudocapacitive properties of MnO₂ while maintaining the structural integrity and high surface area of lignin-based carbon fibers.

4.2.3. Blending Lignin with Cellulose for Composite Electrode Materials

In the pursuit of sustainable carbon fiber alternatives, blending lignin with cellulose offers compelling advantages for composite electrode materials. Lignin, known for its carbon-rich phenolic structure, and cellulose, with its linear, high molecular weight, synergistically enhance dry-wet jet spinning fiber spinnability and carbonization efficiency. This combination can not only improve mechanical strength and electrical conductivity (Figure 29) but also facilitates the formation of microstructures conducive to higher energy storage capacities in supercapacitors and batteries.

Our investigation in [Paper III](#) highlights the significant influence of HKL/cellulose precursor composition on the electrical conductivity and tensile strength of resulting CFs. Increasing the lignin content in the blend with the highest lignin to the cellulose blend (65%) led to substantial enhancements in electrical conductivity, reaching approximately 42 S/cm compared to cellulose's 15 S/cm. Moreover, CFs with higher lignin content also exhibit superior tensile strength, achieving approximately 312 MPa, significantly surpassing pure cellulose fibers. The study further unveils a distinct skin-core morphology in HKL-cellulose fibers, with a higher degree of graphitization observed in the skin region compared to the core. This phenomenon enhances the mechanical properties of CFs, where the graphitized cellulose-lignin blend in the skin provides stiffness, while

the lignin-rich core enhances carbon content, electrical conductivity, and overall strength. Our findings underscore the potential of lignin-cellulose blends as a novel approach in carbon fiber precursor design, offering unique advantages in both mechanical robustness and electrical conductivity.

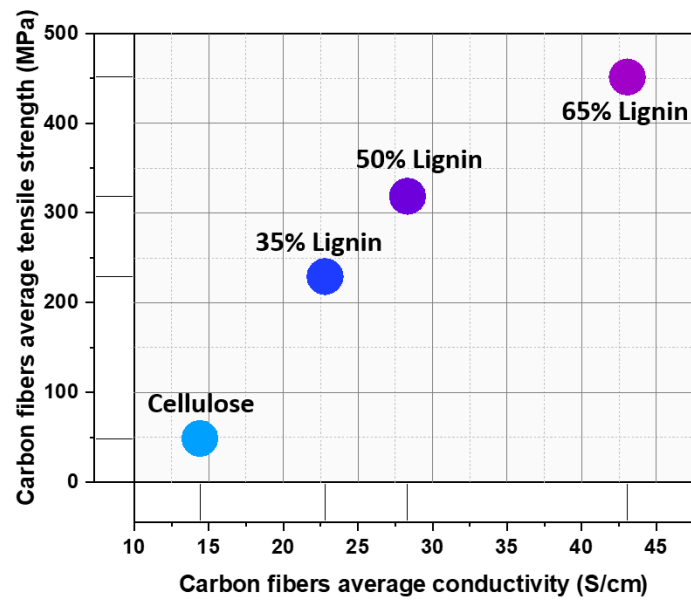


Figure 29. Average conductivity vs tensile strength of carbon fibers with increasing blends of lignin in cellulose.

Chapter 5

Electrochemical Performance Evaluation

5.1. Electrochemical Performance of Electrospun Lignin Carbon Fibers as Electrodes

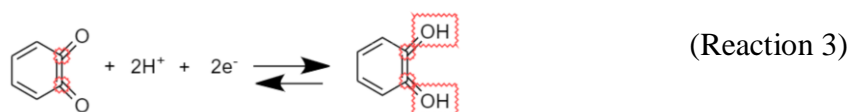
5.1.1. Effect of O-functional Groups on Electrochemical Behavior

The characteristics of an electrode's charge storage are significantly influenced by the surface functional groups present. The redox activity of these functional groups depends on the type of electrolyte used. In acidic media, functional groups involving CO (such as hydroxyl, carbonyl, and lactone groups) contribute positively to charge storage mechanisms. These groups, particularly quinones, undergo reversible redox reactions, storing and releasing both electrons and protons. Conversely, CO₂-containing groups (like carboxylic acids and anhydrides) are generally less active or inactive in acidic conditions. In basic media, different groups become active, with phenolic hydroxyl groups playing a primary role through deprotonation reactions (Z. J. Zhang & Sun, 2016). Therefore, selecting an appropriate electrolyte that activates the desired functional groups is crucial for optimizing the performance of lignin-based electrodes in applications such as supercapacitors.

Some oxygen functional groups on carbon-based electrode materials provide more advantageous properties for supercapacitor applications than others. The beneficial contributions include:

1. Enhanced hydrophilicity: C-OH (hydroxyl) and C=O (carbonyl) groups promote surface wettability, improving electrolyte accessibility.
2. Pseudocapacitive effects: Certain functional groups contribute additional charge storage through fast, reversible redox reactions. This pseudocapacitance is highly dependent on the electrolyte type.

In acidic electrolytes like H₂SO₄, carbonyl and quinone groups are particularly active, undergoing proton-induced redox reactions that manifest as distinct peaks in CV curves. This redox activity follows the general chemical reactions:



This pseudocapacitive contribution significantly enhances the overall capacitance of the electrode material beyond simple EDL capacitance. The electrochemical profile of the same electrode can vary considerably with different electrolytes, highlighting the importance of matching functional groups with appropriate electrolyte systems for optimal performance (Figure 30).

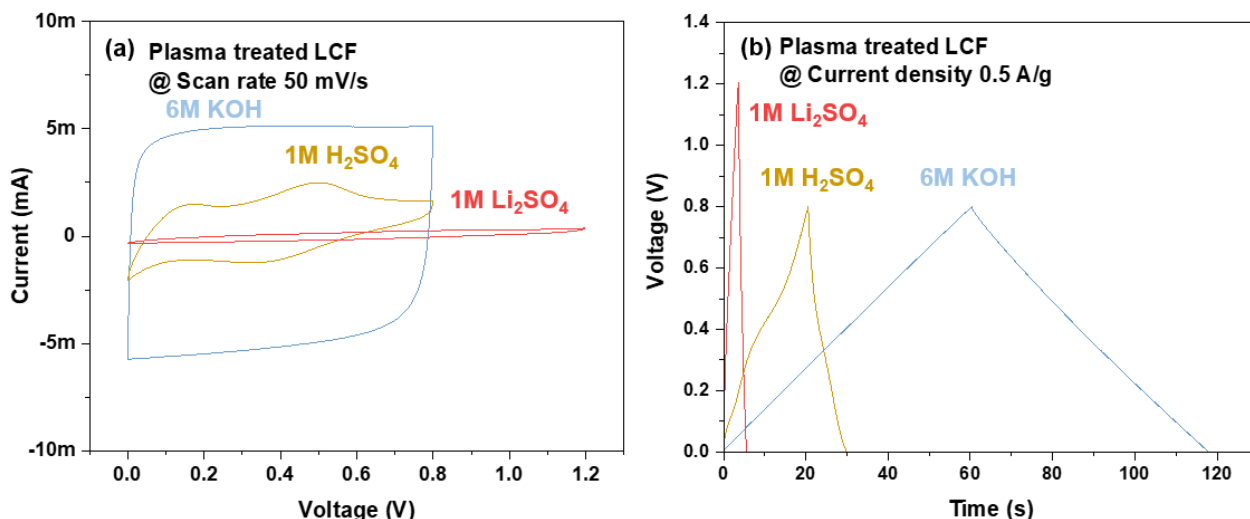
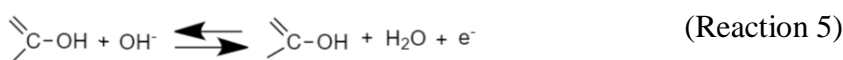
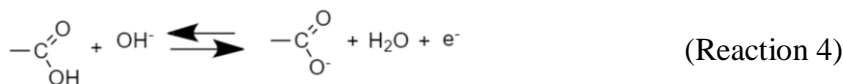


Figure 30. Electrochemical (a) CV and (b) GCD response curves of plasma treated LCF electrodes in KOH, Li₂SO₄, and H₂SO₄ electrolytes.

As from the XPS spectra data on the oxygen configurations for the materials on display in Figure 30, the contributions here are from carbonyl and quinone groups ([Paper I](#)). But on the other hand, it is mostly the carboxyl and hydroxyl groups that act as favorable sites for the KOH electrolyte to react as shown below:



While oxygen functionalization can enhance electrode performance, it also raises concerns about electrolyte decomposition. However, in our extended studies PLCF electrodes have demonstrated good performance without hydrogen evolution, even at increased voltages up to 1 V. It is important to note that excessive oxygen functional groups can be detrimental to electrode performance in two main ways:

1. Exacerbation of self-discharge behavior: High concentrations of oxygen functional groups can increase the rate of self-discharge in supercapacitors (K. Liu, Yu, et al., 2021).
2. Increased internal resistance: Oxygen functional groups, particularly bulky ones like -COOH, can disrupt the conductive network and increase the electrode's internal resistance (Jerigová et al., 2022; Qiu et al., 2023).

When these disadvantages become predominant, they can compromise the efficiency of tailored high surface area pores in the electrode material. Therefore, a careful balance must be struck between the beneficial effects of oxygen functionalization and its potential drawbacks to optimize electrode performance.

5.3. Electrochemical Performance of Lignin-Cellulose-based Carbon Fibers as Electrodes

As an extension to our material study in [Paper III](#), we have explored the electrochemical performance of lignin-cellulose carbon fiber electrodes prepared with varying lignin content, which were assembled in a rudimentary supercapacitor device. This device was constructed manually on a microscope slide and contained two electrode stacks infused with a PVA-KOH gel

electrolyte. It is essential to note that this setup was intended to provide a quick preliminary indication of the performance of the lignin-cellulose carbon fibers in a supercapacitor format. As such, the results serve as a benchmark for understanding trends rather than a definitive performance metric, due to potential variances arising from manual assembly. To ensure consistency and eliminate discrepancies between devices with different electrode materials, the electrode pairs in all four devices: cellulose, L35, L50, and L65 were carefully weighed to ensure they had the same weight. Additionally, the CV data were normalized with their masses to make the comparison between the devices more reliable.

The carbon fiber electrodes studied in this work were created with differing lignin-to-cellulose ratios, ranging from samples with minimal lignin content (L35) to those with high lignin concentration (L65). This variation in lignin percentage enables us to examine the impact of lignin inclusion on electrochemical properties when cellulose remains the predominant matrix component. For comparative purposes, electrodes composed entirely of cellulose-derived carbon fibers (L0) were utilized as a reference. This section discusses the findings with reference to [Paper III](#), which details the materials characterization of these lignin-cellulose composites.

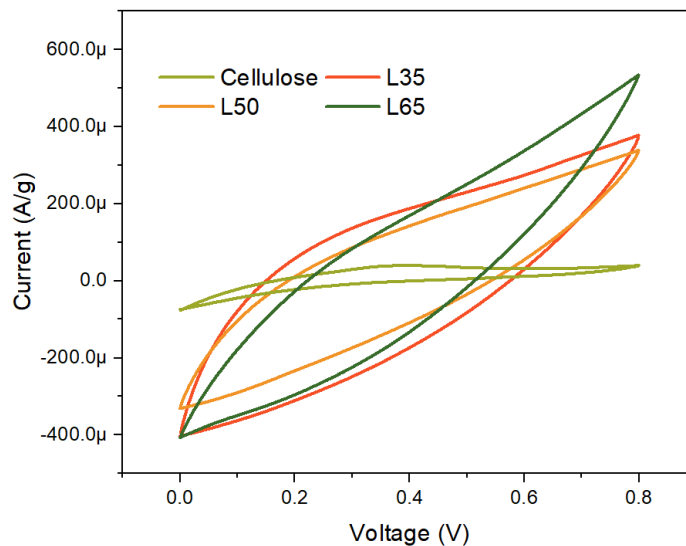


Figure 31. CV curves tested with lignin-cellulose carbon fiber electrodes with PVA- KOH electrolyte at scan rate 20 mV/s.

As seen from Figure 31, the CV curves (not quasi-rectangular), are far from ideal, which is likely due to limitations in the assembly and device structure. For example, the glass substrate could provide a leakage current path, contributing to the observed slope in the curves. Additionally, the distance between electrodes could play a significant role in influencing leakage currents, although the intention was to maintain the distances the same for all devices. Variations in the voltage ramp rate can also influence the shape of the CV curves, with higher ramp rates typically reducing the impact of leakage currents while potentially masking slower diffusion processes.

Regarding the lignin content, while there is a clear difference between the pure cellulose-derived reference and the lignin-cellulose composites, no definitive trend in capacitance improvement is evident between L35 and L65. These results serve as support in the conclusion from [Paper III](#) that the composites should have favorable features when used as electrodes compared to electrodes derived from pure cellulose.

5.4. Towards Thicker Electrodes

For any supercapacitor design, a thick electrode with high areal mass loading is preferred due to its benefits in increasing the supercapacitor device's energy density. Optimizing packing density of the electroactive electrode materials, lowers the excessive inactive material by avoiding or somehow utilizing them. During practical applications, a supercapacitor is made up of materials/components more than electrode materials such as a current collector, electrolyte, binders, additives, separator, and package. Commercial supercapacitors have an active electrode material coating of about 10 mg/cm^2 with $0.1\text{-}0.2 \text{ }\mu\text{m}$ thickness (Dong et al., 2020). Current collectors containing the active material are an expensive component that comprises a major weight proportion in a device. They are available in the form of graphite, aluminum, stainless steel, carbon foils and even foams made of nickel that allows easier percolation. Secondly, the electrolyte is an essential component that is needed in a high dose for highly porous and thick electrodes.

Electrode materials with lower mass loading and electrode thickness store a lower amount of energy per unit device weight due to fewer active sites. Increasing the mass seems to be a simple way to increase the capacitance and energy density of electrodes and/or devices. However, increased mass loading or electrode thickness has a detrimental effect on specific capacitance rate performance, cycling and structural stability of the electrode materials due to decreased accessible surface area (active sites), increased charge-transfer resistance (Wan et al., 2014), sluggish ion transport channels, and even electrolyte wettability issues (Figure 32).

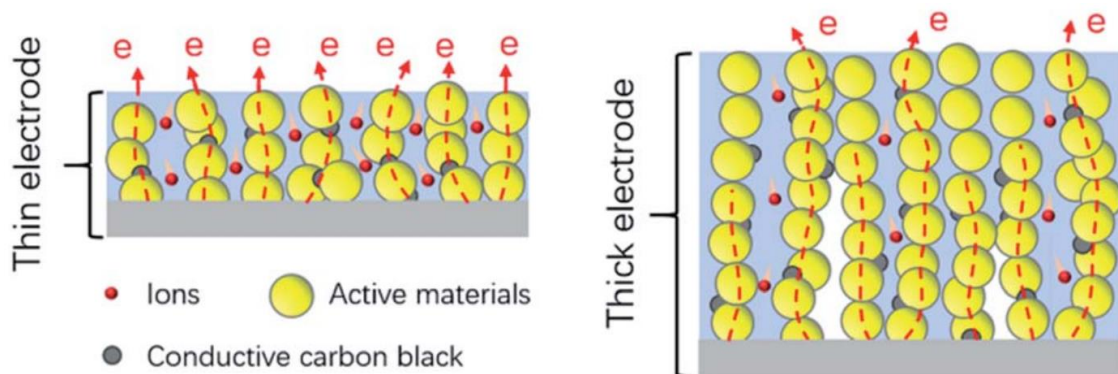


Figure 32. Electron and ion transport and electrolyte wetting in thin and thick electrodes are depicted schematically. The electron and ion transport channels are severely blocked and are inaccessible to the electrolyte in the thick electrode. Reproduced with permission from Dong et al., 2020.

Highly porous materials are at risk of lacking interconnectivity due to broken electrical conductivity networks. The addition of conductive carbon materials is a way to re-build conductive pathways. Materials such as graphene quantum dots (GQDs), graphene sheets (Figure 33), and carbon fibers (Paper II) have been introduced into an activated carbon matrix and increase the capacitances and rate capability with improved charge transfer kinetics and efficient ion migration (Qing et al., 2019). Incorporation of conductive additives enhances the electrical connectivity within the electrode, which mitigates resistances associated with poor binding and mechanical stability at the interface with the current collector (Yücel et al., 2024).

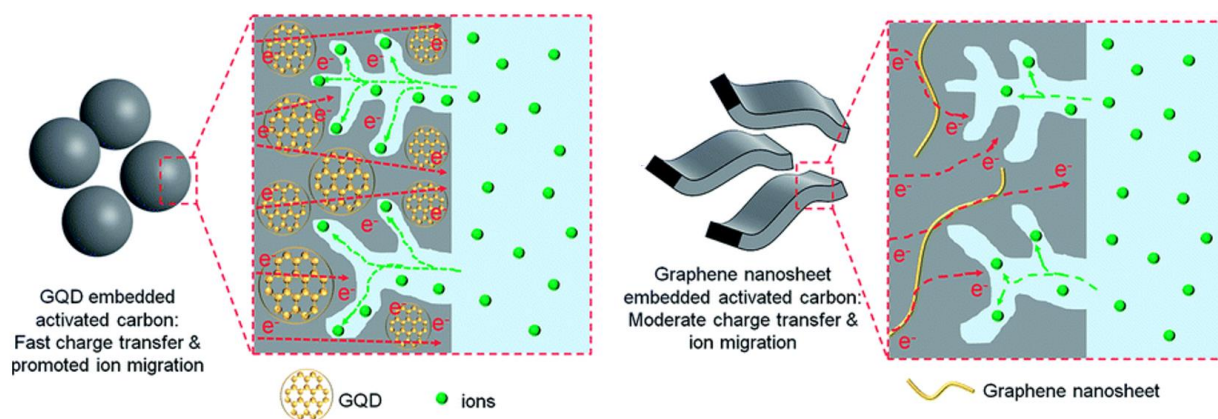


Figure 33. a) Graphene quantum dots (GQD) and b) graphene nanosheets act as electron transfer highways in an activated carbon matrix by significantly promoting electron transport through the particles, thereby improving the utilization of the large surface area. Reproduced with permission from Qing et al., 2019.

GQDs particularly enhance ion migration in carbon electrodes for supercapacitors due to their high surface area and functional groups that facilitate interactions with electrolytes, leading to improved charge transfer kinetics. In contrast, graphene nanosheets, being larger, provide excellent electrical conductivity but do not exhibit the same effects as GQDs. The incorporation of GQDs into activated carbon not only boosts electrochemical performance by enhancing charge-transfer and ion migration kinetics but also helps reduce resistances associated with poor binding and mechanical stability at the electrode-current collector interface (Qing et al., 2019).

An aim towards thicker electrodes, fracturing of electrodes due to heavy mass loading of active material is an issue. Employing robust electron conducting interconnected structures such as carbon nanofibers is a way to achieve mechanical strength, which is critical for long-term cycling and flexibility of the electrodes.

5.4.1. Electrochemical performance of AC/LCF Composite and Cellulose Binder Electrodes

We have evaluated AC electrodes with cellulose binder and LCF inclusions for supercapacitor performance using a coin cell configuration with 6M KOH aqueous electrolyte in [Paper II](#). The design of these electrodes incorporates LCF as a conductive additive alongside CB, with the dual purpose of enhancing both conductivity and structural integrity. By leveraging the reinforcing properties of lignin-based fibers, we aimed to improve electrode stability, particularly at higher mass loadings, while maximizing electrochemical performance. Although conductive materials like CB create electronic pathways in between particles, they are broken as their frequency of contact with these particles is reduced at several points in thicker electrodes. Introducing 2 wt% of longitudinal 1-D conductive carbon fibers alongside 3 wt% CB increases the surface contact creating multiple electron transport channels. The capacitances of AC improved from 85 F/g to 97 F/g under a mass loading of 5 mg/cm² ([Paper II](#)). With higher mass loadings the charge transfer resistance of the electrodes considerably reduces. In thicker electrodes, these fibers act as reinforcements that could keep larger masses of material together without falling apart. To some extent flexibility can also be induced on these electrodes on choosing stronger binders.

The CV curves shown in Figure 34 demonstrate the electrochemical behavior of AC-only electrodes compared to AC/LCF composite electrodes at three different mass loadings: 5, 7, and 10 mg/cm². The CV profiles for each loading exhibit typical EDLC characteristics, with nearly rectangular shapes, suggesting efficient ion adsorption-desorption at the electrode-electrolyte interface. However, at the highest loading of 10 mg/cm², some distortion and slanting are observed, which can be attributed to limitations in ionic transport within the thicker electrodes. Despite these deviations, the AC/LCF composite electrodes maintained capacitances similar to the AC-only electrodes across all mass loadings, highlighting that the incorporation of LCF in place of CB enhances electrochemical performance. These differences are more pronounced in the EIS curves from this study, which reveal lower diffusion and interfacial resistance, particularly for electrodes with mass loadings of 5 and 7 mg/cm².

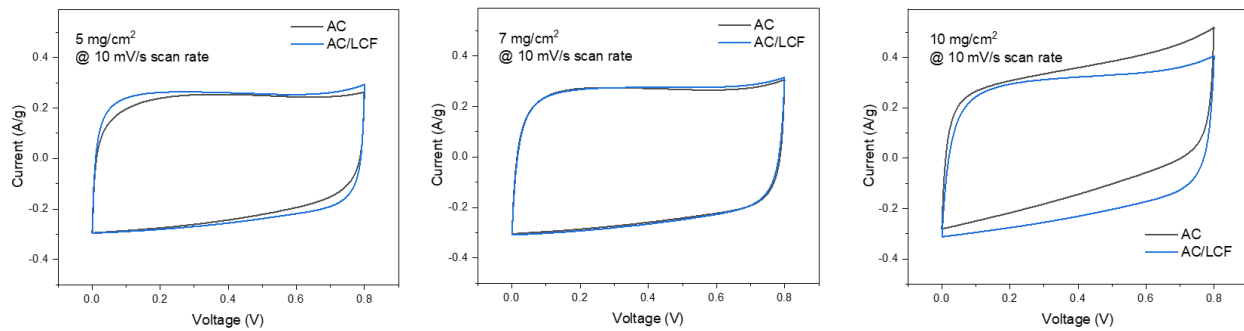


Figure 34. CV curves of AC and AC with lignin carbon fiber inclusions-included electrodes, fabricated using a cellulose binder and tested in a 6M KOH electrolyte assembled device with varying mass loadings.

From a structural standpoint, the lignin fibers serve as a framework within the composite, holding the activated carbon particles together, which may prevent material degradation and maintain mechanical integrity even at high mass loadings. The fibrous structure of LCF likely enhances the electrode's porosity, providing pathways for electrolyte diffusion and improving ion transport. These properties explain why the AC/LCF electrodes performed consistently better than AC alone (Figure 34), especially at mass loadings that usually present challenges for ion accessibility.

Chapter 6

Analysis and Future Perspectives

This section provides a comprehensive overview of my research contributions to the supercapacitor field, specifically examining the performance of lignin-based carbon electrodes developed in this thesis in comparison with other carbon-based materials. Additionally, I offer insights into the future potential of this work, with a focus on pathways to further enhance the electrochemical performance of lignin-based electrodes. Key technical and processing challenges associated with lignin and cellulose-based electrodes, as well as issues related to scalability and material uniformity, are discussed to address critical insights for their large-scale adoption in supercapacitor technology.

6.1. Comparison with State-of-the-Art Electrode Materials

As discussed in [Paper IV](#), comparing performance metrics across various supercapacitors poses challenges due to the lack of standardized testing protocols. In **Table 3-8**, the capacitance, ED, and PD values for different devices are tested at varying current densities, making direct comparison difficult. To provide some perspective, a relative comparison has been made here between selected materials developed in this thesis and existing device datasets to give a general performance overview. The device dataset for **Table 12** was selected based on the device data from **Tables 3 and 4**, which include carbon, and carbon/heteroatom-doped devices. These devices were chosen for their cycling stability of over 95% beyond 5000 cycles, with data defined at current densities of 0.5 A/g or 1 A/g. Only those utilizing 6M KOH as the electrolyte were deliberately selected for a fair and consistent comparison with our devices.

Table 12: Comparative performance metrics of supercapacitor devices in this thesis and other high-performing lab-scale devices.

Electrode materials	Specific capacitance (F/g)	Energy density (Wh/kg)	Power density (W/kg)	Cycling stability
Electrospun lignin carbon fibers (ELCFs) Paper I	95 (0.5 A/g)	8	800	100% after 10000 cycles
Plasma treated lignin carbon fibers (PLCFs) Paper I	120 (0.5 A/g)	11	800	110% after 10000 cycles
AC electrodes Paper II	85 (1 A/g)	31	-	-
AC/LCF Electrodes Paper II	97 (1 A/g)	34	7100	98% after 5000 cycles
Traditional AC	160 (20 mV/s)	-	-	-
Corn stalk lignin/DMF*/PAN CF	429 (1 A/g)	37	400	97% after 10000 cycles

Alkali lignin/DMF*/plant protein CF	410 (1 A/g)	–	–	95% after 10000 cycles
Kraft lignin/H₂O/PEO CF	344 (1 A/g)	8	–	96% after 5000 cycles
N/S co-doped graphene modified lignin/PAN CNFs	267 (1 A/g)	~9	493	97% after 5000 cycles
Lignin sulfonate-derived porous carbon	340 (0.5 A/g)	~10	250	95% after 5000 cycles
Enzymatic hydrolysis lignin-derived 3D hierarchical porous carbon	324 (0.5 A/g)	18	458	100% after 5000 cycles
Corn stalk lignin-derived cage-like mesoporous carbon	217 (0.5 A/g)	–	–	95% after 5000 cycles
O/N/S codoped enzymatic hydrolysis lignin hierarchical porous carbon	318 (0.5 A/g)	~17	249	100% after 10000 cycles
N/S codoped lignin sulfonate porous carbon	269 (0.5 A/g)	~37	62	98% after 10000 cycles

The data presented in **Table 12** reveals several key trends in the performance of various carbon-based electrodes, particularly those derived from lignin, including ELCFs, PLCFs, and composites with other materials such as activated carbon or graphene. Lignin-based electrodes generally show moderate specific capacitance, with values ranging from 95 F/g for LCFs to 120 F/g for PLCFs, demonstrating the positive effect of plasma treatment on capacitance. Additionally, when combined with conductive materials or secondary polymer, such as in Lignin/PAN/graphene CF or Corn stalk lignin/DMF/PAN CF and alkali lignin derived porous carbon, the capacitance increases significantly, reaching values as high as 429 F/g. This trend suggests that compositing with fossil-based polymers and the modification of lignin fibers play a crucial role in enhancing electrochemical performance.

In terms of energy density, lignin-based carbon materials also demonstrate strong performance, with EDs ranging from 4 to 78 Wh/kg, depending on the composition and treatment of the fibers. The porous carbon with hierarchical morphology has higher EDs as expected with Kraft lignin-derived porous carbon having decently good PD as well. Cycling stability, a critical factor for the practical application of supercapacitors, with values exceeding 95% in these devices, is comparable to that of conventional carbon-based electrodes. When compared to nitrogen- and sulfur-co-doped electrodes, PLCF electrodes in **Table 10** exhibit higher capacitance values, despite being tested at higher scan rates. However, research (Schlee et al., 2020) has demonstrated

that HKL-LCF electrodes could achieve a capacitance of 164 F/g at 0.1 A/g and 120 F/g at 250 A/g, with over 90% capacitance retention after 10000 cycles. Notably, the enhanced surface affinity of PLCFs, owing to their modified surface chemistry, suggests that they could serve as promising candidates for future studies involving coatings with MO or conductive polymers such as PEDOT or PEDOT/PSS to further enhance electrochemical performance.

Overall, lignin-based carbon materials, particularly when modified or combined with other materials, show significant promise in enhancing the performance of supercapacitors. While their energy density and cycling stability are already competitive, further optimization, particularly in improving conductivity and power density, could help make these materials more viable sustainable alternatives to conventional carbon electrodes.

Studies on lignin in supercapacitors are still emerging, as shown by bibliometric analysis using the Web of Science database (Zhong et al., 2024) (Figure 35).

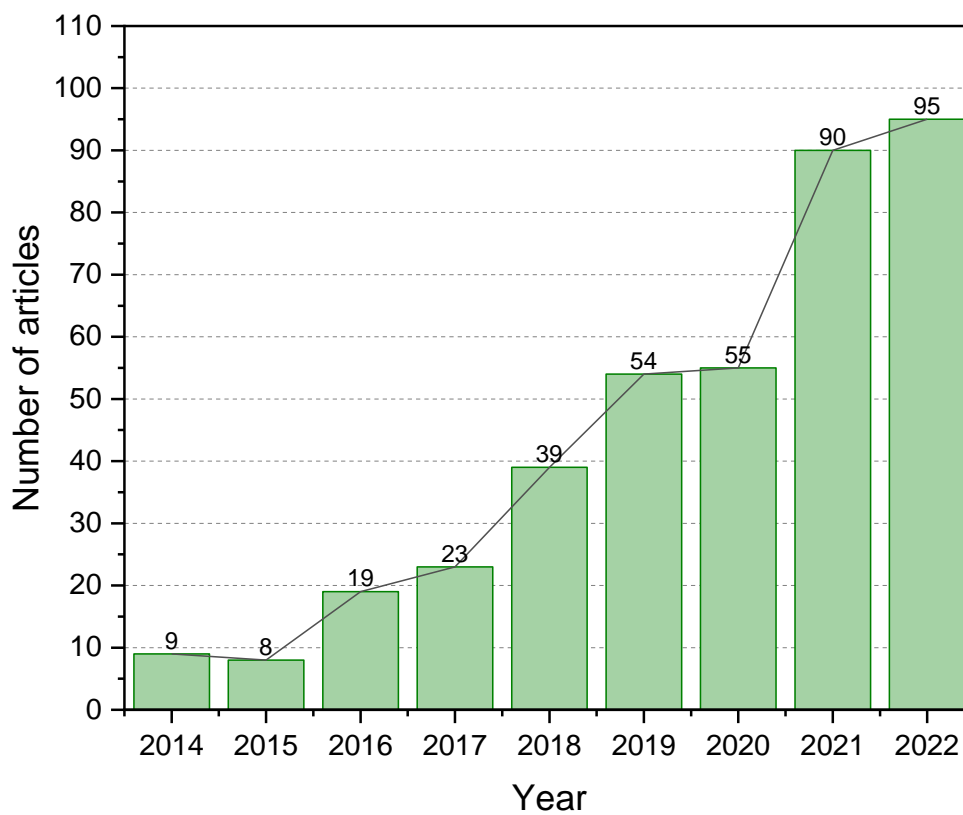


Figure 35. Trend of the number of articles on supercapacitors with lignin-based materials over the years. Reproduced with permission from Zhong et al., 2024.

The studies on lignin-based supercapacitors primarily focus on synthesizing porous carbon structures, with prominent keywords like “carbon fiber,” “aerogel,” and “hierarchical porous carbon.” Highly cited papers emphasize lignin’s role in forming porous carbon materials, carbon fibers, and graphene, each contributing to enhanced electrochemical properties (Beaucamp et al., 2022; Madhu et al., 2023; Q. Cao et al., 2024; Jyothibasud et al., 2022; H. Liu, Xu, et al., 2021; Tong et al., 2023; Zhong et al., 2024). This growing interest suggests significant interest in engineering lignin for producing supercapacitor materials with improved energy storage capabilities. Therefore, comprehensive comparisons of these energy storage devices must also consider factors like self-discharge rates, leakage current, and voltage stability to ensure optimal performance of the electrodes in diverse applications.

The future scope of work in this field can lead to several pathways to enhance the electrochemical performance of lignin-based electrodes without compromising their sustainability. Future efforts could focus on surface modifications to improve conductivity, energy storage capacity, and durability, such as through targeted doping, coatings, or hybrid systems. Structural optimization, including tailoring interconnected pore architecture for improved ion transport, is another promising direction. Integrating lignin-based materials into advanced composite systems could further bridge the gap between performance and eco-friendliness. Ensuring green synthesis methods and conducting lifecycle assessments is crucial for maintaining the sustainability advantage of bio-derived materials. The research studies in this thesis work contribute to these goals by demonstrating strategies to replace fossil-based polymers, such as PAN and PET, with bio-derived alternatives. For instance, lignin of higher molecular weight, extracted through fractionation and modification, was utilized as a primary feedstock for spinning carbon fibers. This approach minimizes reliance on fossil-based precursors, aligning with the principles of green chemistry and sustainability. Additionally, selecting the appropriate type of lignin and compositing it with cellulose, another renewable resource proved effective in developing sustainable carbon materials. Cellulose was used as a binder, offering a safer and eco-friendly alternative to toxic binders such as PVDF and PTFE. The thesis also explored the use of efficient morphologies of green conductive agents for electrodes and electrolytes, such as lignin-derived carbon fibers, which enhanced highly mass-loaded AC electrodes performance. Furthermore, sustainable separators were tested using materials like thermostabilized lignin fibers, in place of conventional glass fibers and polymer-based separators such as PPy and polyethylene. These findings pave the way for high-performance, sustainable energy storage solutions by addressing key challenges in material synthesis and design, all while adhering to eco-friendly principles.

Chapter 7

Conclusion

This thesis explores the potential of wood-derived lignin- and cellulose-based materials as sustainable alternatives for building supercapacitor electrodes, contributing to the growing need of sustainable energy storage solutions. Through material engineering and advanced characterization techniques, we have shown how these wood-based materials can offer viable options compared to traditional electrode materials while aligning with sustainability goals.

Key findings from the thesis include:

- **Plasma exposure enhances capacitance:** Low-power plasma exposure improves the capacitance of electrospun LCF electrodes by 20% in alkaline electrolytes (6M KOH). This enhancement is attributed to the increased presence of CO-type oxygen functional groups on the fiber surface.
- **Composite electrodes with high mass loading are a significant improvement to traditional contacts:** Electrodes with 7 mg/cm² of AC and LCF (2 wt%), using MFC binders, exhibit reduced resistance compared to pure AC electrodes. The LCF enhances binding, provides conductive pathways, and facilitates electronic conductivity in deeper layers, resulting in improved capacitance.
- **Improved electrical conductivity and tensile strength with higher lignin content:** In a study on HKL and cellulose blends, fibers with the highest lignin content (65%) exhibited an electrical conductivity of approximately 42 S/cm, surpassing that of pure cellulose (approximately 15 S/cm). These high-lignin content fibers also demonstrated significantly improved tensile strength (~312 MPa), showcasing a 5-fold increase compared to pure cellulose while maintaining lower stiffness. The observed skin-core morphology of these fibers, with ordered skin regions, contributes significantly to these improvements.
- **Supercapacitors can surpass the classical battery based technologies:** Current trends suggest that supercapacitors may match the energy density of commercial batteries within two decades, although battery technology is expected to remain ahead. Future advancements in supercapacitor systems will likely require careful engineering of technological hybridization with materials and novel designs, such as composites and asymmetric/hybrid systems.

These findings collectively demonstrate that wood-based carbon materials can indeed compete with traditional materials in supercapacitor applications. Our work contributes to the growing body of research aimed at creating more efficient and environmentally friendly energy storage solutions.

Other emerging research relevant to the thesis: Manuscript in preparation

[1] “Comprehensive electrochemical investigation of IrO₂-based microsupercapacitor with different electrolytes,” Mazharul Haque, Qi Li, Lukas Matter, **R.K. Azega**, Hanna, Per Lundgren.

[2] “Supercapacitors unleashed: pushing the boundaries in space, transport, and beyond,” **R.K. Azega**, Mohammad Hassan, Jinhua Sun, Yue Sun, Per Lundgren, Peter Enoksson.

[3] “Investigation of Electrospun Lignin Fiber Separators for Supercapacitor Applications,” **R.K. Azega**, Mohammad Hassan, Peter Enoksson, Per Lundgren.

References

- Abik, F., Palasingh, C., Bhattarai, M., Leivers, S., Ström, A., Westereng, B., Mikkonen, K. S., & Nypelö, T. (2023). Potential of Wood Hemicelluloses and Their Derivates as Food Ingredients. *Journal of Agricultural and Food Chemistry*, *71*(6), 2667–2683. <https://doi.org/10.1021/acs.jafc.2c06449>
- Adam, A. A., Ojur Dennis, J., Al-Hadeethi, Y., Mkawi, E. M., Abubakar Abdulkadir, B., Usman, F., Mudassir Hassan, Y., Wadi, I. A., & Sani, M. (2020). State of the Art and New Directions on Electrospun Lignin/Cellulose Nanofibers for Supercapacitor Application: A Systematic Literature Review. *Polymers*, *12*(12), 2884. <https://doi.org/10.3390/polym12122884>
- Agarwal, U. P. (2019). Analysis of Cellulose and Lignocellulose Materials by Raman Spectroscopy: A Review of the Current Status. *Molecules*, *24*(9), 1659. <https://doi.org/10.3390/molecules24091659>
- Agrawal, M., Prasad, V., Nijhawan, G., Jalal, S. S., Rajalakshmi, B., & Dwivedi, S. P. (2024). A Comprehensive Review of Electron Microscopy in Materials Science: Technological Advances and Applications. *E3S Web of Conferences*, *505*, 01029. <https://doi.org/10.1051/e3sconf/202450501029>
- Ahmad, E., & Pant, K. K. (2018). Lignin Conversion: A Key to the Concept of Lignocellulosic Biomass-Based Integrated Biorefinery. In *Waste Biorefinery* (pp. 409–444). Elsevier. <https://doi.org/10.1016/B978-0-444-63992-9.00014-8>
- Ajjan, F. N., Vagin, M., Rębiś, T., Aguirre, L. E., Ouyang, L., & Inganäs, O. (2017). Scalable Asymmetric Supercapacitors Based on Hybrid Organic/Biopolymer Electrodes. *Advanced Sustainable Systems*, *1*(8), 1700054. <https://doi.org/10.1002/adsu.201700054>
- An, C., Zhang, Y., Guo, H., & Wang, Y. (2019). Metal oxide-based supercapacitors: Progress and perspectives. *Nanoscale Advances*, *1*, 4644–4658.
- Ardizzone, S., Fregonara, G., & Trasatti, S. (1990). “Inner” and “outer” active surface of RuO₂ electrodes. *Electrochimica Acta*, *35*(1), 263–267. [https://doi.org/10.1016/0013-4686\(90\)85068-X](https://doi.org/10.1016/0013-4686(90)85068-X)
- Baer, D. R., Artyushkova, K., Cohen, H., Easton, C. D., Engelhard, M., Gengenbach, T. R., Greczynski, G., Mack, P., Morgan, D. J., & Roberts, A. (2020). XPS guide: Charge neutralization and binding energy referencing for insulating samples. *Journal of Vacuum Science & Technology A*, *38*(3), 031204. <https://doi.org/10.1116/6.0000057>
- Bai, Y., Zhao, W., Bi, S., Liu, S., Huang, W., & Zhao, Q. (2021). Preparation and application of cellulose gel in flexible supercapacitors. *Journal of Energy Storage*, *42*, 103058. <https://doi.org/10.1016/j.est.2021.103058>
- Balakshin, M. Yu., Capanema, E. A., Sulaeva, I., Schlee, P., Huang, Z., Feng, M., Borghei, M., Rojas, O. J., Potthast, A., & Rosenau, T. (2021). New Opportunities in the Valorization of Technical Lignins. *ChemSusChem*, *14*(4), 1016–1036. <https://doi.org/10.1002/cssc.202002553>
- Barzegar, F., Dangbegnon, J. K., Bello, A., Momodu, D. Y., Johnson, A. T. C., & Manyala, N. (2015). Effect of conductive additives to gel electrolytes on activated carbon-based supercapacitors. *AIP Advances*, *5*(9), 097171. <https://doi.org/10.1063/1.4931956>
- Beaucamp, A., Muddasar, M., Amiinu, I. S., Moraes Leite, M., Culebras, M., Latha, K., Gutiérrez, M. C., Rodríguez-Padron, D., Del Monte, F., Kennedy, T., Ryan, K. M., Luque, R., Titirici, M.-M., & Collins, M. N. (2022). Lignin for energy applications – state of the art, life cycle, techno-economic analysis and future trends. *Green Chemistry*, *24*(21), 8193–8226. <https://doi.org/10.1039/D2GC02724K>
- Becker, J., & Wittmann, C. (2019). A field of dreams: Lignin valorization into chemicals, materials, fuels, and health-care products. *Biotechnology Advances*, *37*(6). <https://doi.org/10.1016/j.biotechadv.2019.02.016>
- Bengtsson, A. (2022). *Biobased carbon fibers from solution spun lignocellulosic precursors*. <https://kth.diva-portal.org/smash/record.jsf?dswid=2733&pid=diva2%3A1708591>
- Bengtsson, A., Bengtsson, J., Sedin, M., & Sjöholm, E. (2019). Carbon Fibers from Lignin-Cellulose Precursors: Effect of Stabilization Conditions. *ACS Sustainable Chemistry & Engineering*, *7*(9), 8440–8448. <https://doi.org/10.1021/acssuschemeng.9b00108>
- Bengtsson, A., Hecht, P., Sommertune, J., Ek, M., Sedin, M., & Sjöholm, E. (2020). Carbon Fibers from Lignin–Cellulose Precursors: Effect of Carbonization Conditions. *ACS Sustainable Chemistry & Engineering*, *8*(17), 6826–6833. <https://doi.org/10.1021/acssuschemeng.0c01734>
- Bengtsson, J. (2021). *Air-gap spinning of lignin-cellulose fibers* [Doctoral thesis]. CHALMERS UNIVERSITY OF TECHNOLOGY.
- Böhm, R., Thieme, M., Wohlfahrt, D., Wolz, D. S., Richter, B., & Jäger, H. (2018). Reinforcement Systems for Carbon Concrete Composites Based on Low-Cost Carbon Fibers. *Fibers*, *6*(3), 56. <https://doi.org/10.3390/fib6030056>
- Bonhivers, J.-C., & Stuart, Paul. R. (2013). Applications of Process Integration Methodologies in the Pulp and Paper Industry. In *Handbook of Process Integration (PI)* (pp. 765–798). Elsevier. <https://doi.org/10.1533/9780857097255.5.765>

- Braun, J. L., Holtman, K. M., & Kadla, J. F. (2005). Lignin-based carbon fibers: Oxidative thermostabilization of kraft lignin. *Carbon*, *43*(2), 385–394. <https://doi.org/10.1016/j.carbon.2004.09.027>
- Brousse, T., Bélanger, D., & Long, J. W. (2015). To Be or Not To Be Pseudocapacitive? *Journal of The Electrochemical Society*, *162*(5), A5185–A5189. <https://doi.org/10.1149/2.0201505jes>
- Bryan, A. M., Santino, L. M., Lu, Y., Acharya, S., & D'Arcy, J. M. (2016). Conducting Polymers for Pseudocapacitive Energy Storage. *Chemistry of Materials*, *28*(17), 5989–5998. <https://doi.org/10.1021/acs.chemmater.6b01762>
- Bu, F., Zhou, W., Xu, Y., Du, Y., Guan, C., & Huang, W. (2020). Recent developments of advanced micro-supercapacitors: Design, fabrication and applications. *Npj Flexible Electronics*, *4*(1), 31. <https://doi.org/10.1038/s41528-020-00093-6>
- Butnoi, P., Pagon, A., Berger, R., Butt, H.-J., & Intasanta, V. (2021). Electrospun nanocomposite fibers from lignin and iron oxide as supercapacitor material. *Journal of Materials Research and Technology*, *12*, 2153–2167. <https://doi.org/10.1016/j.jmrt.2021.04.017>
- Cao, M., Cheng, W., Ni, X., Hu, Y., & Han, G. (2020). Lignin-based multi-channels carbon nanofibers @ SnO₂ nanocomposites for high-performance supercapacitors. *Electrochimica Acta*, *345*, 136172. <https://doi.org/10.1016/j.electacta.2020.136172>
- Cao, Q., Zhu, H., Xu, J., Zhang, M., Xiao, T., Xu, S., & Du, B. (2024). Research progress in the preparation of lignin-based carbon nanofibers for supercapacitors using electrospinning technology: A review. *International Journal of Biological Macromolecules*, *273*, 133037. <https://doi.org/10.1016/j.ijbiomac.2024.133037>
- Chatterjee, D. P., & Nandi, A. K. (2021). A review on the recent advances in hybrid supercapacitors. *Journal of Materials Chemistry A*, *9*(29), 15880–15918. <https://doi.org/10.1039/D1TA02505H>
- Chatterjee, S., Clingenpeel, A., McKenna, A., Rios, O., & Johs, A. (2014). Synthesis and characterization of lignin-based carbon materials with tunable microstructure. *RSC Adv.*, *4*(9), 4743–4753. <https://doi.org/10.1039/C3RA46928J>
- Chatterjee, S., Saito, T., Rios, O., & Johs, A. (2014). Lignin Based Carbon Materials for Energy Storage Applications. In S. O. Obare & R. Luque (Eds.), *ACS Symposium Series* (Vol. 1186, pp. 203–218). American Chemical Society. <https://doi.org/10.1021/bk-2014-1186.ch011>
- Choi, W., Shin, H.-C., Kim, J. M., Choi, J.-Y., & Yoon, W.-S. (2020). Modeling and Applications of Electrochemical Impedance Spectroscopy (EIS) for Lithium-ion Batteries. *Journal of Electrochemical Science and Technology*, *11*(1), 1–13. <https://doi.org/10.33961/jecst.2019.00528>
- Conway, B. E., & Kannangara, D. C. W. (1987). Zinc Oxidation and Redeposition Processes in Aqueous Alkali and Carbonate Solutions: II. Distinction Between Dissolution and Oxide Film Formation Processes. *Journal of The Electrochemical Society*, *134*(4), 906–918. <https://doi.org/10.1149/1.2100594>
- Dai, Z., Ren, P.-G., Jin, Y.-L., Zhang, H., Ren, F., & Zhang, Q. (2019). Nitrogen-sulphur Co-doped graphenes modified electrospun lignin/polyacrylonitrile-based carbon nanofiber as high performance supercapacitor. *Journal of Power Sources*, *437*, 226937. <https://doi.org/10.1016/j.jpowsour.2019.226937>
- Di Francesco, D., Dahlstrand, C., Löfstedt, J., Orebom, A., Verendel, J., Carrick, C., Håkansson, Å., Eriksson, S., Rådberg, H., Wallmo, H., Wimby, M., Huber, F., Federsel, C., Backmark, M., & Samec, J. S. M. (2021). Debottlenecking a Pulp Mill by Producing Biofuels from Black Liquor in Three Steps. *ChemSusChem*, *14*(11), 2414–2425. <https://doi.org/10.1002/cssc.202100496>
- Ding, J., Yang, Y., Poisson, J., He, Y., Zhang, H., Zhang, Y., Bao, Y., Chen, S., Chen, Y. M., & Zhang, K. (2024). Recent Advances in Biopolymer-Based Hydrogel Electrolytes for Flexible Supercapacitors. *ACS Energy Letters*, *9*(4), 1803–1825. <https://doi.org/10.1021/acsenergylett.3c02567>
- Dinh, K. H., Roussel, P., & Lethien, C. (2023). Advances on Microsupercapacitors: Real Fast Miniaturized Devices toward Technological Dreams for Powering Embedded Electronics? *ACS Omega*, *8*(10), 8977–8990. <https://doi.org/10.1021/acsomega.2c07549>
- Dong, Y., Zhu, J., Li, Q., Zhang, S., Song, H., & Jia, D. (2020). Carbon materials for high mass-loading supercapacitors: Filling the gap between new materials and practical applications. *Journal of Materials Chemistry A*, *8*(42), 21930–21946. <https://doi.org/10.1039/D0TA08265A>
- Drabek, J., & Zatloukal, M. (2019). Meltblown technology for production of polymeric microfibers/nanofibers: A review. *Physics of Fluids*, *31*(9), 091301. <https://doi.org/10.1063/1.5116336>
- Dresselhaus, M. S., & Dresselhaus, G. (2002). Intercalation compounds of graphite. *Advances in Physics*, *51*(1), 1–186. <https://doi.org/10.1080/00018730110113644>
- Driese, S. G., Mora, C. I., & Elick, J. M. (1997). Morphology and Taphonomy of Root and Stump Casts of the Earliest Trees (Middle to Late Devonian), Pennsylvania and New York, U.S.A. *PALAIOS*, *12*(6), 524. <https://doi.org/10.2307/3515409>
- Du, B., Shi, X., Zhu, H., Xu, J., Bai, Y., Wang, Q., Wang, X., & Zhou, J. (2023). Preparation and characterization of bifunctional wolfsbane-like magnetic Fe₃O₄ nanoparticles-decorated lignin-based carbon nanofibers composites for electromagnetic wave absorption and electrochemical energy storage. *International Journal of Biological Macromolecules*, *246*, 125574. <https://doi.org/10.1016/j.ijbiomac.2023.125574>

- Du, B., Zhu, H., Chai, L., Cheng, J., Wang, X., Chen, X., Zhou, J., & Sun, R.-C. (2021). Effect of lignin structure in different biomass resources on the performance of lignin-based carbon nanofibers as supercapacitor electrode. *Industrial Crops and Products*, *170*, 113745. <https://doi.org/10.1016/j.indcrop.2021.113745>
- Farid, M. A. A., Zheng, A. L. T., Tsubota, T., & Andou, Y. (2023). Catalytic graphitization of biomass-derived ethanosolv lignin using Fe, Co, Ni, and Zn: Microstructural and chemical characterization. *Journal of Analytical and Applied Pyrolysis*, *173*, 106064. <https://doi.org/10.1016/j.jaap.2023.106064>
- Feng, X., Bai, Y., Liu, M., Li, Y., Yang, H., Wang, X., & Wu, C. (2021). Untangling the respective effects of heteroatom-doped carbon materials in batteries, supercapacitors and the ORR to design high performance materials. *Energy & Environmental Science*, *14*(4), 2036–2089. <https://doi.org/10.1039/D1EE00166C>
- Fiber Analysis – Using SEM for the Quality Analysis of Fibers. (2024, July 18). *Thermo Fisher Scientific Phenom-World BV*. <https://www.azom.com/article.aspx?ArticleID=14308>.
- Fu, F., Jiao, X., Yang, Y., Yin, X., & Zheng, Z.-J. (2025). Wood-based materials for high-energy-density lithium metal batteries. *Nano Energy*, *133*, 110464. <https://doi.org/10.1016/j.nanoen.2024.110464>
- Gao, C., An, Q., Zhang, F., Zhou, J., Wang, H., & Zhai, S. (2022). Double Crosslinked Lignin/Hydrogel Electrolyte with High Ion Conductivity and Super Ductility for High Voltage Window Supercapacitor. *SSRN Electronic Journal*. <https://doi.org/10.2139/ssrn.4074326>
- Gao, D., Luo, Z., Liu, C., & Fan, S. (2023). A survey of hybrid energy devices based on supercapacitors. *Green Energy & Environment*, *8*(4), 972–988. <https://doi.org/10.1016/j.gee.2022.02.002>
- García-Mateos, F. J., Rosas, J. M., Ruiz-Rosas, R., Rodríguez-Mirasol, J., & Cordero, T. (2022). Highly porous and conductive functional carbon fibers from electrospun phosphorus-containing lignin fibers. *Carbon*, *200*, 134–148. <https://doi.org/10.1016/j.carbon.2022.08.050>
- García-Mateos, F. J., Ruiz-Rosas, R., María Rosas, J., Morallón, E., Cazorla-Amorós, D., Rodríguez-Mirasol, J., & Cordero, T. (2020). Activation of electrospun lignin-based carbon fibers and their performance as self-standing supercapacitor electrodes. *Separation and Purification Technology*, *241*, 116724. <https://doi.org/10.1016/j.seppur.2020.116724>
- Ge, L., Zhao, C., Zuo, M., Tang, J., Ye, W., Wang, X., Zhang, Y., & Xu, C. (2022). Review on the preparation of high value-added carbon materials from biomass. *Journal of Analytical and Applied Pyrolysis*, *168*, 105747. <https://doi.org/10.1016/j.jaap.2022.105747>
- Gogotsi, Y., & Penner, R. M. (2018). Energy Storage in Nanomaterials – Capacitive, Pseudocapacitive, or Battery-like? *ACS Nano*, *12*(3), 2081–2083. <https://doi.org/10.1021/acsnano.8b01914>
- González-Gil, R. M., Borràs, M., Chbani, A., Abitbol, T., Fall, A., Aulin, C., Aucher, C., & Martínez-Crespiera, S. (2022). Sustainable and Printable Nanocellulose-Based Ionogels as Gel Polymer Electrolytes for Supercapacitors. *Nanomaterials*, *12*(2), 273. <https://doi.org/10.3390/nano12020273>
- Götz, A., Senz, V., Illner, S., & Grabow, N. (2020). Computed fiber evaluation of SEM images using DiameterJ. *Current Directions in Biomedical Engineering*, *6*(3), 438–441. <https://doi.org/10.1515/cdbme-2020-3113>
- Gratz, E., Sa, Q., Apelian, D., & Wang, Y. (2014). A closed loop process for recycling spent lithium ion batteries. *Journal of Power Sources*, *262*, 255–262. <https://doi.org/10.1016/j.jpowsour.2014.03.126>
- Greene, J., & Denny, J. (2022, August 17). *How wood-based batteries could alleviate energy pressures*. <https://www.orbichem.com/blog/how-wood-based-batteries-could-alleviate-energy-pressures>
- Guo, C., Ma, H., Zhang, Q., Li, M., Jiang, H., Chen, C., Wang, S., & Min, D. (2020). Nano MnO₂ Radially Grown on Lignin-Based Carbon Fiber by One-Step Solution Reaction for Supercapacitors with High Performance. *Nanomaterials*, *10*(3), 594. <https://doi.org/10.3390/nano10030594>
- He, N., Song, J., Liao, J., Zhao, F., & Gao, W. (2022). Separator threads in yarn-shaped supercapacitors to avoid short-circuiting upon length. *Npj Flexible Electronics*, *6*(1), 19. <https://doi.org/10.1038/s41528-022-00150-2>
- Hosseinaei, O., Harper, D., Bozell, J., & Rials, T. (2017). Improving Processing and Performance of Pure Lignin Carbon Fibers through Hardwood and Herbaceous Lignin Blends. *International Journal of Molecular Sciences*, *18*(7), 1410. <https://doi.org/10.3390/ijms18071410>
- How Does Coating Thickness Affect SEM Imaging? (n.d.). [Instruments website]. *How Does Coating Thickness Affect SEM Imaging?* <https://www.nanoscience.com/blogs/how-does-coating-thickness-affect-sem-imaging/>
- Hsieh, Y.-C., Lee, K.-T., Lin, Y.-P., Wu, N.-L., & Donne, S. W. (2008). Investigation on capacity fading of aqueous MnO₂·nH₂O electrochemical capacitor. *Journal of Power Sources*, *177*(2), 660–664. <https://doi.org/10.1016/j.jpowsour.2007.11.026>
- Hu, S., & Hsieh, Y.-L. (2013). Ultrafine microporous and mesoporous activated carbon fibers from alkali lignin. *Journal of Materials Chemistry A*, *1*(37), 11279. <https://doi.org/10.1039/c3ta12538f>
- Hubbe, M., Alén, R., Paleologou, M., Kannangara, M., & Kihlman, J. (2019). Lignin recovery from spent alkaline pulping liquors using acidification, membrane separation, and related processing steps: A review. *BioResources*, *14*(1), 2300–2351. <https://doi.org/10.15376/biores.14.1.2300-2351>
- I. Becker, H. (1957). *Low voltage electrolytic capacitor* (Patent 423,042).
- Jerigová, M., Odziomek, M., & López-Salas, N. (2022). “We Are Here!” Oxygen Functional Groups in Carbons for Electrochemical Applications. *ACS Omega*, *7*(14), 11544–11554. <https://doi.org/10.1021/acsomega.2c00639>

- Jha, S., Mehta, S., Chen, Y., Likhari, R., Stewart, W., Parkinson, D., & Liang, H. (2020). Design and synthesis of high performance flexible and green supercapacitors made of manganese-dioxide-decorated alkali lignin. *Energy Storage*, 2(5), e184. <https://doi.org/10.1002/est2.184>
- Jha, S., Mehta, S., Chen, Y., Ma, L., Renner, P., Parkinson, D. Y., & Liang, H. (2020). Design and Synthesis of Lignin-Based Flexible Supercapacitors. *ACS Sustainable Chemistry & Engineering*, 8(1), 498–511. <https://doi.org/10.1021/acssuschemeng.9b05880>
- Jiang, X., Ouyang, Q., Liu, D., Huang, J., Ma, H., Chen, Y., Wang, X., & Sun, W. (2018). Preparation of low-cost carbon fiber precursors from blends of wheat straw lignin and commercial textile-grade polyacrylonitrile (PAN). *Holzforchung*, 72(9), 727–734. <https://doi.org/10.1515/hf-2017-0191>
- Jyothibasu, J. P., Wang, R.-H., Tien, Y.-C., Kuo, C.-C., & Lee, R.-H. (2022). Lignin-Derived Quinone Redox Moieties for Bio-Based Supercapacitors. *Polymers*, 14(15), 3106. <https://doi.org/10.3390/polym14153106>
- Kadla, J. F., Kubo, S., Venditti, R. A., Gilbert, R. D., Compere, A. L., & Griffith, W. (2002). Lignin-based carbon fibers for composite fiber applications. *Carbon*, 40(15), 2913–2920. [https://doi.org/10.1016/S0008-6223\(02\)00248-8](https://doi.org/10.1016/S0008-6223(02)00248-8)
- Kang, D. H. P., Chen, M., & Ogunseitan, O. A. (2013). Potential Environmental and Human Health Impacts of Rechargeable Lithium Batteries in Electronic Waste. *Environmental Science & Technology*, 47(10), 5495–5503. <https://doi.org/10.1021/es400614y>
- Karume, I., Bbumba, S., Tewolde, S., Mukasa, I. Z. T., & Ntale, M. (2023). Impact of carbonization conditions and adsorbate nature on the performance of activated carbon in water treatment. *BMC Chemistry*, 17(1), 162. <https://doi.org/10.1186/s13065-023-01091-1>
- Kasprzak, D., Stępnik, I., & Galiński, M. (2018). Electrodes and hydrogel electrolytes based on cellulose: Fabrication and characterization as EDLC components. *Journal of Solid State Electrochemistry*, 22(10), 3035–3047. <https://doi.org/10.1007/s10008-018-4015-y>
- Kienberger, M., Maitz, S., Pichler, T., & Demmelmayer, P. (2021). Systematic Review on Isolation Processes for Technical Lignin. *Processes*, 9(5), 804. <https://doi.org/10.3390/pr9050804>
- Kim, D.-Y., Ma, C.-H., Jang, Y., Radhakrishnan, S., Ko, T. H., & Kim, B.-S. (2022). A simple and green approach to develop porous carbons from biomass lignin for advanced asymmetric supercapacitors. *Colloids and Surfaces A: Physicochemical and Engineering Aspects*, 652, 129785. <https://doi.org/10.1016/j.colsurfa.2022.129785>
- Lai, C., Zhou, Z., Zhang, L., Wang, X., Zhou, Q., Zhao, Y., Wang, Y., Wu, X.-F., Zhu, Z., & Fong, H. (2014). Free-standing and mechanically flexible mats consisting of electrospun carbon nanofibers made from a natural product of alkali lignin as binder-free electrodes for high-performance supercapacitors. *Journal of Power Sources*, 247, 134–141. <https://doi.org/10.1016/j.jpowsour.2013.08.082>
- Lallave, M., Bedia, J., Ruiz-Rosas, R., Rodríguez-Mirasol, J., Cordero, T., Otero, J. C., Marquez, M., Barrero, A., & Loscertales, I. G. (2007). Filled and Hollow Carbon Nanofibers by Coaxial Electrospinning of Alcell Lignin without Binder Polymers. *Advanced Materials*, 19(23), 4292–4296. <https://doi.org/10.1002/adma.200700963>
- Landi, G., La Notte, L., Palma, A. L., Sorrentino, A., Maglione, M. G., & Puglisi, G. (2021). A Comparative Evaluation of Sustainable Binders for Environmentally Friendly Carbon-Based Supercapacitors. *Nanomaterials*, 12(1), 46. <https://doi.org/10.3390/nano12010046>
- Le, N.-D., Trogen, M., Ma, Y., Varley, R. J., Hummel, M., & Byrne, N. (2020). Cellulose-lignin composite fibers as precursors for carbon fibers: Part 2 – The impact of precursor properties on carbon fibers. *Carbohydrate Polymers*, 250, 116918. <https://doi.org/10.1016/j.carbpol.2020.116918>
- Lee, H. Y., & Goodenough, J. B. (1999). Supercapacitor Behavior with KCl Electrolyte. *Journal of Solid State Chemistry*, 144(1), 220–223. <https://doi.org/10.1006/jssc.1998.8128>
- Lee, J. J., Chae, S.-H., Lee, J. J., Lee, M. S., Yoon, W., Kwac, L. K., Kim, H. G., & Shin, H. K. (2023). Waste-Wood-Isolated Cellulose-Based Activated Carbon Paper Electrodes with Graphene Nanoplatelets for Flexible Supercapacitors. *Molecules*, 28(23), 7822. <https://doi.org/10.3390/molecules28237822>
- Lei, D., Li, X.-D., Seo, M.-K., Khil, M.-S., Kim, H.-Y., & Kim, B.-S. (2017). NiCo₂O₄ nanostructure-decorated PAN/lignin based carbon nanofiber electrodes with excellent cyclability for flexible hybrid supercapacitors. *Polymer*, 132, 31–40. <https://doi.org/10.1016/j.polymer.2017.10.051>
- Li, J., Tang, J., Yuan, J., Zhang, K., Sun, Y., Zhang, H., & Qin, L.-C. (2017). Enlarging energy density of supercapacitors using unequal graphene electrodes and ionic liquid electrolyte. *Electrochimica Acta*, 258, 1053–1058. <https://doi.org/10.1016/j.electacta.2017.11.157>
- Li, L., Lu, F., Wang, C., Zhang, F., Liang, W., Kuga, S., Dong, Z., Zhao, Y., Huang, Y., & Wu, M. (2018). Flexible double-cross-linked cellulose-based hydrogel and aerogel membrane for supercapacitor separator. *Journal of Materials Chemistry A*, 6(47), 24468–24478. <https://doi.org/10.1039/C8TA07751G>
- Li, P., Wu, S., & Ding, Y. (2024). Research progress on lignin-based carbon electrode materials in rechargeable batteries. *BioResources*, 19(2). <https://doi.org/10.15376/biores.19.2.Li>

- Li, Q., Hu, C., Li, M., Truong, P., Li, J., Lin, H.-S., Naik, M. T., Xiang, S., Jackson, B. E., Kuo, W., Wu, W., Pu, Y., Ragauskas, A. J., & Yuan, J. S. (2021). Enhancing the multi-functional properties of renewable lignin carbon fibers *via* defining the structure–property relationship using different biomass feedstocks. *Green Chemistry*, 23(10), 3725–3739. <https://doi.org/10.1039/D0GC03828H>
- Liang, D., Xie, Q., Liu, J., Xie, F., Liu, D., & Wan, C. (2020). Mechanism of the evolution of pore structure during the preparation of activated carbon from Zhundong high-alkali coal based on gas–solid diffusion and activation reactions. *RSC Advances*, 10(55), 33566–33575. <https://doi.org/10.1039/D0RA06105K>
- Lignin Market Size, Share & Trends Analysis Report By Product (Ligno-Sulphonates, Kraft, Organosolv), By Application (Macromolecule, Aromatic), By Region, And Segment Forecasts, 2020–2027. (2020). <https://www.grandviewresearch.com/industry-analysis/lignin-market#:~:text=The%20global%20lignin%20market%20size,revenue%2C%20from%202020%20to%202027.&text=In%20addition%2C%20the%20well%2Destablished,likely%20to%20support%20the%20market.>
- LignoBoost®—The process. (n.d.). *High-Quality Lignin from a Unique Two-Step Process*. Retrieved June 19, 2024, from <https://www.valmet.com/pulp/other-value-adding-processes/lignin-extraction/lignoboost-process/>
- Lin, J., Kubo, S., Yamada, T., Koda, K., & Uraki, Y. (2012). Chemical thermostabilization for the preparation of carbon fibers from softwood lignin. *BioResources*, 7(4), 5634–5646. <https://doi.org/10.15376/biores.7.4.5634-5646>
- Lin, X., Wang, M., Zhao, J., Wu, X., Xie, J., & Yang, J. (2023). Super-tough and self-healable all-cellulose-based electrolyte for fast degradable quasi-solid-state supercapacitor. *Carbohydrate Polymers*, 304, 120502. <https://doi.org/10.1016/j.carbpol.2022.120502>
- Liu, A., Jiang, Z., Li, S., Du, J., Tao, Y., Lu, J., Cheng, Y., & Wang, H. (2022). A degradable membrane based on lignin-containing cellulose for high-energy lithium-ion batteries. *International Journal of Biological Macromolecules*, 213, 690–698. <https://doi.org/10.1016/j.ijbiomac.2022.06.004>
- Liu, C., Lei, T., Seidi, F., Ahmad, M., Cao, D., Yu, Z., Li, Y., Wang, H., Lu, H., Bian, H., Han, G., & Xiao, H. (2024). Multiscale wood-derived materials for advanced supercapacitors: From macro to micro and nano. *Energy Storage Materials*, 72, 103774. <https://doi.org/10.1016/j.ensm.2024.103774>
- Liu, F., Wang, Q., Zhai, G., Xiang, H., Zhou, J., Jia, C., Zhu, L., Wu, Q., & Zhu, M. (2022). Continuously processing waste lignin into high-value carbon nanotube fibers. *Nature Communications*, 13(1), 5755. <https://doi.org/10.1038/s41467-022-33496-2>
- Liu, H., Mulderrig, L., Hallinan, D., & Chung, H. (2021). Lignin-Based Solid Polymer Electrolytes: Lignin-Graft-Poly(ethylene glycol). *Macromolecular Rapid Communications*, 42(3), 2000428. <https://doi.org/10.1002/marc.202000428>
- Liu, H., Xu, T., Liu, K., Zhang, M., Liu, W., Li, H., Du, H., & Si, C. (2021). Lignin-based electrodes for energy storage application. *Industrial Crops and Products*, 165, 113425. <https://doi.org/10.1016/j.indcrop.2021.113425>
- Liu, J., Bengtsson, J., Yu, S., Burghammer, M., & Jedvert, K. (2023). Variation in the hierarchical structure of lignin-blended cellulose precursor fibers. *International Journal of Biological Macromolecules*, 225, 1555–1561. <https://doi.org/10.1016/j.ijbiomac.2022.11.211>
- Liu, K., Yu, C., Guo, W., Ni, L., Yu, J., Xie, Y., Wang, Z., Ren, Y., & Qiu, J. (2021). Recent research advances of self-discharge in supercapacitors: Mechanisms and suppressing strategies. *Journal of Energy Chemistry*, 58, 94–109. <https://doi.org/10.1016/j.jechem.2020.09.041>
- Liu, T. -C., Pell, W. G., Conway, B. E., & Roberson, S. L. (1998). Behavior of Molybdenum Nitrides as Materials for Electrochemical Capacitors: Comparison with Ruthenium Oxide. *Journal of The Electrochemical Society*, 145(6), 1882–1888. <https://doi.org/10.1149/1.1838571>
- Liu, T., Ren, X., Zhang, J., Liu, J., Ou, R., Guo, C., Yu, X., Wang, Q., & Liu, Z. (2020). Highly compressible lignin hydrogel electrolytes via double-crosslinked strategy for superior foldable supercapacitors. *Journal of Power Sources*, 449, 227532. <https://doi.org/10.1016/j.jpowsour.2019.227532>
- Lota, G., & Milczarek, G. (2011). The effect of lignosulfonates as electrolyte additives on the electrochemical performance of supercapacitors. *Electrochemistry Communications*, 13(5), 470–473. <https://doi.org/10.1016/j.elecom.2011.02.023>
- Lu Huiran. (2017). *Wood-based Materials for Lithium-ion Batteries* [Doctoral thesis]. KTH Royal Institute of Technology.
- Ma, C., Li, Z., Li, J., Fan, Q., Wu, L., Shi, J., & Song, Y. (2018). Lignin-based hierarchical porous carbon nanofiber films with superior performance in supercapacitors. *Applied Surface Science*, 456, 568–576. <https://doi.org/10.1016/j.apsusc.2018.06.189>
- Ma, X., Kolla, P., Zhao, Y., Smirnova, A. L., & Fong, H. (2016a). Electrospun lignin-derived carbon nanofiber mats surface-decorated with MnO₂ nanowhiskers as binder-free supercapacitor electrodes with high performance. *Journal of Power Sources*, 325, 541–548. <https://doi.org/10.1016/j.jpowsour.2016.06.073>

- Ma, X., Kolla, P., Zhao, Y., Smirnova, A. L., & Fong, H. (2016b). Electrospun lignin-derived carbon nanofiber mats surface-decorated with MnO₂ nanowhiskers as binder-free supercapacitor electrodes with high performance. *Journal of Power Sources*, 325, 541–548. <https://doi.org/10.1016/j.jpowsour.2016.06.073>
- Madhu, R., Periasamy, A. P., Schlee, P., Hérou, S., & Titirici, M.-M. (2023). Lignin: A sustainable precursor for nanostructured carbon materials for supercapacitors. *Carbon*, 207, 172–197. <https://doi.org/10.1016/j.carbon.2023.03.001>
- Mäntyranta, H. (2023, 01). *Wood-based battery can triple charging speed of car batteries*. <https://forest.fi/article/wood-based-battery-can-triple-charging-speed-of-car-batteries/#6ee05d60>
- Mehta, S., Jha, S., & Liang, H. (2020). Lignocellulose materials for supercapacitor and battery electrodes: A review. *Renewable and Sustainable Energy Reviews*, 134, 110345. <https://doi.org/10.1016/j.rser.2020.110345>
- Mei, B.-A., Munteshari, O., Lau, J., Dunn, B., & Pilon, L. (2018). Physical Interpretations of Nyquist Plots for EDLC Electrodes and Devices. *The Journal of Physical Chemistry C*, 122(1), 194–206. <https://doi.org/10.1021/acs.jpcc.7b10582>
- Mishra, S., Srivastava, R., Muhammad, A., Amit, A., Chiavazzo, E., Fasano, M., & Asinari, P. (2023). The impact of physicochemical features of carbon electrodes on the capacitive performance of supercapacitors: A machine learning approach. *Scientific Reports*, 13(1), 6494. <https://doi.org/10.1038/s41598-023-33524-1>
- Momodu, D., Bello, A., Oyedotun, K., Ochai-Ejeh, F., Dangbegnon, J., Madito, M., & Manyala, N. (2017). Enhanced electrochemical response of activated carbon nanostructures from tree-bark biomass waste in polymer-gel active electrolytes. *RSC Advances*, 7(59), 37286–37295. <https://doi.org/10.1039/C7RA05810A>
- Moulder, J. F., Stickle, W. F., Sobol, P. E., Bomben, K. D., Chastain, J., King Jr., R. C., & Physical Electronics, Incorporation (Eds.). (1995). *Handbook of X-ray photoelectron spectroscopy: A reference book of standard spectra for identification and interpretation of XPS data*. Physical Electronics.
- Muddasar, M., Beaucamp, A., Culebras, M., & Collins, M. N. (2024). High performance all lignin derived supercapacitors for energy storage applications. *Materials Today Sustainability*, 26, 100767. <https://doi.org/10.1016/j.mtsust.2024.100767>
- Nasouri, K., Haji, A., Mousavi Shoushtari, A., & Kaflu, A. (n.d.). A Novel Study of Electrospun Nanofibers Morphology as a Function of Polymer Solution Properties. *Proceedings of the international conference nanomaterials: applications and properties*.
- Nasri, K., Loranger, É., & Toubal, L. (2023). Effect of cellulose and lignin content on the mechanical properties and drop-weight impact damage of injection-molded polypropylene-flax and -pine fiber composites. *Journal of Composite Materials*, 57(21), 3347–3364. <https://doi.org/10.1177/00219983231186208>
- Nitta, N., Wu, F., Lee, J. T., & Yushin, G. (2015). Li-ion battery materials: Present and future. *Materials Today*, 18(5), 252–264.
- Norberg, I., Nordström, Y., Drougge, R., Gellerstedt, G., & Sjöholm, E. (2013). A new method for stabilizing softwood kraft lignin fibers for carbon fiber production. *Journal of Applied Polymer Science*, 128(6), 3824–3830. <https://doi.org/10.1002/app.38588>
- Nowak, A. P., Hagberg, J., Leijonmarck, S., Schweinebarth, H., Baker, D., Uhlin, A., Tomani, P., & Lindbergh, G. (2018). Lignin-based carbon fibers for renewable and multifunctional lithium-ion battery electrodes. *Holzforschung*, 72(2), 81–90. <https://doi.org/10.1515/hf-2017-0044>
- O. Hosseinaei, & D. A. Baker. (n.d.). *High Glass Transition Lignins and Lignin Derivatives for the Manufacture of Carbon and Graphite Fibers*.
- Pang, T., Wang, G., Sun, H., Sui, W., & Si, C. (2021). Lignin fractionation: Effective strategy to reduce molecule weight dependent heterogeneity for upgraded lignin valorization. *Industrial Crops and Products*, 165, 113442. <https://doi.org/10.1016/j.indcrop.2021.113442>
- Park, J. H., Rana, H. H., Lee, J. Y., & Park, H. S. (2019). Renewable flexible supercapacitors based on all-lignin-based hydrogel electrolytes and nanofiber electrodes. *Journal of Materials Chemistry A*, 7(28), 16962–16968. <https://doi.org/10.1039/C9TA03519B>
- Pasangulapati, V., Ramachandriya, K. D., Kumar, A., Wilkins, M. R., Jones, C. L., & Huhnke, R. L. (2012). Effects of cellulose, hemicellulose and lignin on thermochemical conversion characteristics of the selected biomass. *Bioresource Technology*, 114, 663–669. <https://doi.org/10.1016/j.biortech.2012.03.036>
- Perdana, M. Y., Johan, B. A., Abdallah, M., Hossain, Md. E., Aziz, Md. A., Baroud, T. N., & Drmoh, Q. A. (2024). Understanding the Behavior of Supercapacitor Materials via Electrochemical Impedance Spectroscopy: A Review. *The Chemical Record*, 24(5), e202400007. <https://doi.org/10.1002/tcr.202400007>
- Pérez-Madrigal, M. M., Edo, M. G., & Alemán, C. (2016). Powering the future: Application of cellulose-based materials for supercapacitors. *Green Chemistry*, 18(22), 5930–5956. <https://doi.org/10.1039/C6GC02086K>
- Poursorkhabi, V., A. Abdelwahab, M., Misra, M., Khalil, H., Gharabaghi, B., & K. Mohanty, A. (2020). Processing, Carbonization, and Characterization of Lignin Based Electrospun Carbon Fibers: A Review. *Frontiers in Energy Research*, 8(208). <https://doi.org/10.3389/fenrg.2020.00208>

- Prauchner, M. J., Sapag, K., & Rodríguez-Reinoso, F. (2016). Tailoring biomass-based activated carbon for CH₄ storage by combining chemical activation with H₃PO₄ or ZnCl₂ and physical activation with CO₂. *Carbon*, *110*, 138–147. <https://doi.org/10.1016/j.carbon.2016.08.092>
- Qin, X., Lu, Y., Xiao, H., Wen, Y., & Yu, T. (2012). A comparison of the effect of graphitization on microstructures and properties of polyacrylonitrile and mesophase pitch-based carbon fibers. *Carbon*, *50*(12), 4459–4469. <https://doi.org/10.1016/j.carbon.2012.05.024>
- Qing, Y., Jiang, Y., Lin, H., Wang, L., Liu, A., Cao, Y., Sheng, R., Guo, Y., Fan, C., Zhang, S., Jia, D., & Fan, Z. (2019). Boosting the supercapacitor performance of activated carbon by constructing overall conductive networks using graphene quantum dots. *Journal of Materials Chemistry A*, *7*(11), 6021–6027. <https://doi.org/10.1039/C8TA11620B>
- Qiu, C., Jiang, L., Gao, Y., & Sheng, L. (2023). Effects of oxygen-containing functional groups on carbon materials in supercapacitors: A review. *Materials & Design*, *230*, 111952. <https://doi.org/10.1016/j.matdes.2023.111952>
- Ramachandran, T., Sana, S. S., Kumar, K. D., Kumar, Y. A., Hegazy, H. H., & Kim, S. C. (2023). Asymmetric supercapacitors: Unlocking the energy storage revolution. *Journal of Energy Storage*, *73*, 109096. <https://doi.org/10.1016/j.est.2023.109096>
- Randles, J. E. B. (1947). Kinetics of rapid electrode reactions. *Discussions of the Faraday Society*, *1*, 11. <https://doi.org/10.1039/df9470100011>
- Ranjith, K. S., Raju, G. S. R., Chodankar, N. R., Ghoreishian, S. M., Cha, Y. L., Huh, Y. S., & Han, Y. (2021). Lignin-derived carbon nanofibers-laminated redox-active-mixed metal sulfides for high-energy rechargeable hybrid supercapacitors. *International Journal of Energy Research*, *45*(5), 8018–8029. <https://doi.org/10.1002/er.6312>
- Rashid Khan, H., & Latif Ahmad, A. (2024). Supercapacitors: Overcoming current limitations and charting the course for next-generation energy storage. *Journal of Industrial and Engineering Chemistry*, S1226086X24004593. <https://doi.org/10.1016/j.jiec.2024.07.014>
- Ray, P. K., Mohanty, R., & Parida, K. (2023). Recent advancements of NiCo LDH and graphene based nanohybrids for supercapacitor application. *Journal of Energy Storage*, *72*, 108335. <https://doi.org/10.1016/j.est.2023.108335>
- Rebouillat, S., & Lyons, M. E. G. (2011). Measuring the Electrical Conductivity of Single Fibres. *International Journal of Electrochemical Science*, *6*(11), 5731–5740. [https://doi.org/10.1016/S1452-3981\(23\)18440-9](https://doi.org/10.1016/S1452-3981(23)18440-9)
- Remesh, S., Loganathan, N. N., Perumal, V., Ovinis, M., Karuppanan, S., Edison, T. N. J. I., Raja, P. B., Ibrahim, M. N. M., Arumugam, N., & Kumar, R. S. (2024). A high performance selectively grown nano-octahedral Mn₃O₄ on lignin derived laser scribed graphene for microsupercapacitor applications. *Journal of Energy Storage*, *77*, 109920. <https://doi.org/10.1016/j.est.2023.109920>
- Remesh, S., Vasudevan, M., Perumal, V., Edison, T. N. J. I., Raja, P. B., Ibrahim, M. N. M., Karuppanan, S., Ovinis, M., Arumugam, N., & Kumar, R. S. (2024). Study on current collector and electrolyte design/electrochemical behaviour of an in-plane lignin derived laser scribed graphene for microsupercapacitor application. *Ain Shams Engineering Journal*, *15*(9), 102889. <https://doi.org/10.1016/j.asej.2024.102889>
- Remesh, S., Vasudevan, M., Perumal, V., Ovinis, M., Karuppanan, S., Edison, T. N. J. I., Raja, P. B., Ibrahim, M. N. M., Voon, C. H., Arumugam, N., & Kumar, R. S. (2023). Oil palm lignin-derived laser scribed graphene in neutral electrolyte for high-performance microsupercapacitor application. *Journal of Environmental Chemical Engineering*, *11*(5), 110600. <https://doi.org/10.1016/j.jece.2023.110600>
- Remesh, S., Vasudevan, M., Sivakumar, M., Perumal, V., Ovinis, M., Karuppanan, S., Edison, T. N. J. I., Raja, P. B., Ibrahim, M. N. M., Latip, A. F. B. A., Arumugam, N., & Kumar, R. S. (2023). In-situ Mg-Al LDH infused lignin-derived laser scribed graphene for facilitated ion transport in flexible supercapacitor application. *Journal of the Taiwan Institute of Chemical Engineers*, *153*, 105247. <https://doi.org/10.1016/j.jtice.2023.105247>
- Rennhofer, H., Köhnke, J., Keckes, J., Tintner, J., Unterweger, C., Zinn, T., Deix, K., Lichtenegger, H., & Gindl-Altmutter, W. (2021). Pore Development during the Carbonization Process of Lignin Microparticles Investigated by Small Angle X-ray Scattering. *Molecules*, *26*(7), 2087. <https://doi.org/10.3390/molecules26072087>
- Report on other components and polymers present in the Black Liquors.* (n.d.). EUCalyptus Lignin Valorisation for Advanced Materials and Carbon Fibres. [https://ec.europa.eu/research/participants/documents/downloadPublic?documentIds=080166e5d082a2ad&appId=PPGMS#:~:text=After%20the%20recovery%20of%20the,40%25%20inorganics%20\(i.e.%20the%20residual](https://ec.europa.eu/research/participants/documents/downloadPublic?documentIds=080166e5d082a2ad&appId=PPGMS#:~:text=After%20the%20recovery%20of%20the,40%25%20inorganics%20(i.e.%20the%20residual)
- Sagues, W. J., Yang, J., Monroe, N., Han, S.-D., Vinzant, T., Yung, M., Jameel, H., Nimlos, M., & Park, S. (2020). A simple method for producing bio-based anode materials for lithium-ion batteries. *Green Chemistry*, *22*(20), 7093–7108. <https://doi.org/10.1039/D0GC02286A>

- Salinas-Torres, D., Ruiz-Rosas, R., Valero-Romero, M. J., Rodríguez- Mirasol, J., Cordero, T., Morallón, E., & Cazorla-Amorós, D. (2016). Asymmetric capacitors using lignin-based hierarchical porous carbons. *Journal of Power Sources*, 326, 641–651. <https://doi.org/10.1016/j.jpowsour.2016.03.096>
- Schlee, P., Hosseinaei, O., Baker, D., Landmér, A., Tomani, P., Mostazo-López, M. J., Cazorla-Amorós, D., Herou, S., & Titirici, M.-M. (2019). From Waste to Wealth: From Kraft Lignin to Free-standing Supercapacitors. *Carbon*, 145, 470–480. <https://doi.org/10.1016/j.carbon.2019.01.035>
- Schlee, P., Hosseinaei, O., O' Keefe, C. A., Mostazo-López, M. J., Cazorla-Amorós, D., Herou, S., Tomani, P., Grey, C. P., & Titirici, M.-M. (2020). Hardwood versus softwood Kraft lignin – precursor-product relationships in the manufacture of porous carbon nanofibers for supercapacitors. *Journal of Materials Chemistry A*, 8(44), 23543–23554. <https://doi.org/10.1039/D0TA09093J>
- Seddiqi, H., Olliaei, E., Honarkar, H., Jin, J., Geonzon, L. C., Bacabac, R. G., & Klein-Nulend, J. (2021). Cellulose and its derivatives: Towards biomedical applications. *Cellulose*, 28(4), 1893–1931. <https://doi.org/10.1007/s10570-020-03674-w>
- Shen, C., Xu, S., Xie, Y., Sanghadasa, M., Wang, X., & Lin, L. (2017). A Review of On-Chip Micro Supercapacitors for Integrated Self-Powering Systems. *Journal of Microelectromechanical Systems*, 26(5), 949–965. <https://doi.org/10.1109/JMEMS.2017.2723018>
- Shi, F., Li, J., Xiao, J., Zhao, X., Li, H., An, Q., Zhai, S., Wang, K., Wei, L., & Tong, Y. (2021). Three-dimensional hierarchical porous lignin-derived carbon/WO₃ for high-performance solid-state planar micro-supercapacitor. *International Journal of Biological Macromolecules*, 190, 11–18. <https://doi.org/10.1016/j.ijbiomac.2021.08.183>
- Singh, M., Gupta, A., Sundriyal, S., Jain, K., & Dhakate, S. R. (2021). Kraft lignin-derived free-standing carbon nanofibers mat for high-performance all-solid-state supercapacitor. *Materials Chemistry and Physics*, 264, 124454. <https://doi.org/10.1016/j.matchemphys.2021.124454>
- Smith, A., Li, Q., Vyas, A., Haque, M., Wang, K., Velasco, A., Zhang, X., Thurakkal, S., Quellmalz, A., Niklaus, F., Gylfason, K., Lundgren, P., & Enoksson, P. (2019). Carbon-Based Electrode Materials for Microsupercapacitors in Self-Powering Sensor Networks: Present and Future Development. *Sensors*, 19(19), 4231. <https://doi.org/10.3390/s19194231>
- Södra signs agreement to supply UPM with kraft lignin from world-leading new plant. (2024, September 20). [Industry News]. <https://www.sodra.com/en/gb/about-sodra/press/press-releases/sodra-signs-agreement-to-supply-upm-with-kraft-lignin-from-world-leading-new-plant/>
- Song, C., Gao, C., Peng, Q., Gibril, M. E., Wang, X., Wang, S., & Kong, F. (2023). A novel high-performance electrospun of polyimide/lignin nanofibers with unique electrochemical properties and its application as lithium-ion batteries separators. *International Journal of Biological Macromolecules*, 246, 125668. <https://doi.org/10.1016/j.ijbiomac.2023.125668>
- Song, M., Yu, L., Song, B., Meng, F., & Tang, X. (2019). Alkali promoted the adsorption of toluene by adjusting the surface properties of lignin-derived carbon fibers. *Environmental Science and Pollution Research*, 26(22), 22284–22294. <https://doi.org/10.1007/s11356-019-05456-9>
- Sreevani, P. (2018). *Wood as a renewable source of energy and future fuel*. 040007. <https://doi.org/10.1063/1.5047972>
- Stora Enso and Northvolt partner to develop wood-based batteries. (2022, July 22). *Stora Enso and Northvolt Partner to Develop Wood-Based Batteries*. <https://northvolt.com/articles/stora-enso-and-northvolt/>
- Sun, Z., Qu, K., You, Y., Huang, Z., Liu, S., Li, J., Hu, Q., & Guo, Z. (2021). Overview of cellulose-based flexible materials for supercapacitors. *Journal of Materials Chemistry A*, 9(12), 7278–7300. <https://doi.org/10.1039/D0TA10504J>
- Tenhaeff, W. E., Rios, O., More, K., & McGuire, M. A. (2014). Highly Robust Lithium Ion Battery Anodes from Lignin: An Abundant, Renewable, and Low-Cost Material. *Advanced Functional Materials*, 24(1), 86–94. <https://doi.org/10.1002/adfm.201301420>
- Thielke, M. W., Lopez Guzman, S., Victoria Tafoya, J. P., García Tamayo, E., Castro Herazo, C. I., Hosseinaei, O., & Sobrido, A. J. (2022). Full Lignin-Derived Electrospun Carbon Materials as Electrodes for Supercapacitors. *Frontiers in Materials*, 9, 859872. <https://doi.org/10.3389/fmats.2022.859872>
- Tong, Y., Yang, J., Li, J., Cong, Z., Wei, L., Liu, M., Zhai, S., Wang, K., & An, Q. (2023). Lignin-derived electrode materials for supercapacitor applications: Progress and perspectives. *Journal of Materials Chemistry A*, 11(3), 1061–1082. <https://doi.org/10.1039/D2TA07203C>
- Torres-Canas, F., Bentaleb, A., Föllmer, M., Roman, J., Neri, W., Ly, I., Derré, A., & Poulin, P. (2020). Improved structure and highly conductive lignin-carbon fibers through graphene oxide liquid crystal. *Carbon*, 163, 120–127. <https://doi.org/10.1016/j.carbon.2020.02.077>
- Toupin, M., Brousse, T., & Bélanger, D. (2004). Charge Storage Mechanism of MnO₂ Electrode Used in Aqueous Electrochemical Capacitor. *Chemistry of Materials*, 16(16), 3184–3190. <https://doi.org/10.1021/cm049649j>
- Trasatti, S., & Buzzanca, G. (1971). Ruthenium dioxide: A new interesting electrode material. Solid state structure and electrochemical behaviour. *Journal of Electroanalytical Chemistry and Interfacial Electrochemistry*, 29(2), A1–A5. [https://doi.org/10.1016/S0022-0728\(71\)80111-0](https://doi.org/10.1016/S0022-0728(71)80111-0)

- Trogen, M., Le, N.-D., Sawada, D., Guizani, C., Lourençon, T. V., Pitkänen, L., Sixta, H., Shah, R., O'Neill, H., Balakshin, M., Byrne, N., & Hummel, M. (2021). Cellulose-lignin composite fibres as precursors for carbon fibres. Part 1 – Manufacturing and properties of precursor fibres. *Carbohydrate Polymers*, 252, 117133. <https://doi.org/10.1016/j.carbpol.2020.117133>
- Uddin, M.-J., Alaboina, P. K., Zhang, L., & Cho, S.-J. (2017). A low-cost, environment-friendly lignin-polyvinyl alcohol nanofiber separator using a water-based method for safer and faster lithium-ion batteries. *Materials Science and Engineering: B*, 223, 84–90. <https://doi.org/10.1016/j.mseb.2017.05.004>
- US DOE. 2005. *Genomics:GTL Roadmap, DOE/SC-0090, U.S. Department of Energy Office of Science*. (P. 204). (n.d.). [Graphic]. <https://public.ornl.gov/site/gallery/detail.cfm?id=181>
- Volta, A. (1800). XVII. On the electricity excited by the mere contact of conducting substances of different kinds. In a letter from Mr. Alexander Volta, F. R. S. Professor of Natural Philosophy in the University of Pavia, to the Rt. Hon. Sir Joseph Banks, Bart. K.B. P. R. S. *Philosophical Transactions of the Royal Society of London*, 90, 403–431. <https://doi.org/10.1098/rstl.1800.0018>
- Wan, C., Yuan, L., & Shen, H. (2014). Effects of Electrode Mass-loading on the Electrochemical Properties of Porous MnO₂ for Electrochemical Supercapacitor. <https://www.researchgate.net/journal/International-Journal-of-Electrochemical-Science-1452-3981>, 9(7), 4024–4038.
- Wang, D., Yang, F., Cong, L., Feng, W., Wang, C., Chu, F., Nan, J., & Chen, R. (2022). Lignin-containing hydrogel matrices with enhanced adhesion and toughness for all-hydrogel supercapacitors. *Chemical Engineering Journal*, 450, 138025. <https://doi.org/10.1016/j.cej.2022.138025>
- Wang, D.-W., Li, F., Liu, M., Lu, G. Q., & Cheng, H.-M. (2008). Mesopore-Aspect-Ratio Dependence of Ion Transport in Rodtype Ordered Mesoporous Carbon. *The Journal of Physical Chemistry C*, 112(26), 9950–9955. <https://doi.org/10.1021/jp800173z>
- Wang, J., Polleux, J., Lim, J., & Dunn, B. (2007). Pseudocapacitive Contributions to Electrochemical Energy Storage in TiO₂ (Anatase) Nanoparticles. *The Journal of Physical Chemistry C*, 111(40), 14925–14931. <https://doi.org/10.1021/jp074464w>
- Wang, L., Aorigele, & Sun, Y. (2017). Preparation of Iron Oxide Particle-Decorated Lignin-Based Carbon Nanofibers as Electrode Material for Pseudocapacitor. *Journal of Wood Chemistry and Technology*, 37(6), 423–432. <https://doi.org/10.1080/02773813.2017.1310900>
- Wang, L., Jian, W., Jiang, Z., Wu, B., Zu, X., Yang, G., Zhang, W., & Qiu, X. (2024). Lignin hydrogel-derived hierarchical porous carbon materials using low dosage of alkaline activation agents for high-performance zinc-ion hybrid supercapacitors. *Journal of Energy Storage*, 92, 112191. <https://doi.org/10.1016/j.est.2024.112191>
- Wang, S., Bai, J., Innocent, M. T., Wang, Q., Xiang, H., Tang, J., & Zhu, M. (2022). Lignin-based carbon fibers: Formation, modification and potential applications. *Green Energy & Environment*, 7(4), 578–605. <https://doi.org/10.1016/j.gee.2021.04.006>
- Wang, S., Ma, J., Shi, X., Zhu, Y., & Wu, Z.-S. (2022). Recent status and future perspectives of ultracompact and customizable micro-supercapacitors. *Nano Research Energy*, 1, e9120018. <https://doi.org/10.26599/NRE.2022.9120018>
- Wang, S., Yu, Y., Luo, S., Cheng, X., Feng, G., Zhang, Y., Wu, Z., Compagnini, G., Pooran, J., & Hu, A. (2019). All-solid-state supercapacitors from natural lignin-based composite film by laser direct writing. *Applied Physics Letters*, 115(8), 083904. <https://doi.org/10.1063/1.5118340>
- Wang, W., Li, Z., Huang, H., Li, W., & Wang, J. (2022). Facile design of novel nanocellulose-based gel polymer electrolyte for lithium-ion batteries application. *Chemical Engineering Journal*, 445, 136568. <https://doi.org/10.1016/j.cej.2022.136568>
- Wang, X., Zhang, W., Chen, M., & Zhou, X. (2018). Electrospun Enzymatic Hydrolysis Lignin-Based Carbon Nanofibers as Binder-Free Supercapacitor Electrodes with High Performance. *Polymers*, 10(12), 1306. <https://doi.org/10.3390/polym10121306>
- Wang, Y., Lu, C., Cao, X., Wang, Q., Yang, G., & Chen, J. (2022). Porous Carbon Spheres Derived from Hemicelluloses for Supercapacitor Application. *International Journal of Molecular Sciences*, 23(13), 7101. <https://doi.org/10.3390/ijms23137101>
- Wang, Y., Song, Y., & Xia, Y. (2016). Electrochemical capacitors: Mechanism, materials, systems, characterization and applications. *Chemical Society Reviews*, 45(21), 5925–5950. <https://doi.org/10.1039/C5CS00580A>
- Wang, Z., Tammela, P., Huo, J., Zhang, P., Strømme, M., & Nyholm, L. (2016). Solution-processed poly(3,4-ethylenedioxythiophene) nanocomposite paper electrodes for high-capacitance flexible supercapacitors. *Journal of Materials Chemistry A*, 4(5), 1714–1722. <https://doi.org/10.1039/C5TA10122K>
- Wang, Z., Tammela, P., Strømme, M., & Nyholm, L. (2017). Cellulose-based Supercapacitors: Material and Performance Considerations. *Advanced Energy Materials*, 7(18), 1700130. <https://doi.org/10.1002/aenm.201700130>

- Wu, H., Liu, C., Jiang, Z., Yang, Z., Mao, X., Wei, L., & Sun, R. (2022). Electrospun flexible lignin/polyacrylonitrile-based carbon nanofiber and its application in electrode materials for supercapacitors. *Textile Research Journal*, 92(3–4), 456–466. <https://doi.org/10.1177/00405175211037191>
- Xu, Y., Yu, S., Johnson, H. M., Wu, Y., Liu, X., Fang, B., & Zhang, Y. (2024). Recent progress in electrode materials for micro-supercapacitors. *iScience*, 27(2), 108786. <https://doi.org/10.1016/j.isci.2024.108786>
- Yan, Q., Li, J., Zhang, J., & Cai, Z. (2018). Thermal Decomposition of Kraft Lignin under Gas Atmospheres of Argon, Hydrogen, and Carbon Dioxide. *Polymers*, 10(7), 729. <https://doi.org/10.3390/polym10070729>
- Yang, S. M., Shaffer, M. S. P., & Brandt-Talbot, A. (2023). High Lignin Content Carbon Fiber Precursors Wet-Spun from Low-Cost Ionic Liquid Water Mixtures. *ACS Sustainable Chemistry & Engineering*, 11(24), 8800–8811. <https://doi.org/10.1021/acssuschemeng.3c00234>
- Yang, X., Shi, K., Zhitomirsky, I., & Cranston, E. D. (2015). Cellulose Nanocrystal Aerogels as Universal 3D Lightweight Substrates for Supercapacitor Materials. *Advanced Materials*, 27(40), 6104–6109. <https://doi.org/10.1002/adma.201502284>
- Yao, M., Bi, X., Wang, Z., Yu, P., Dufresne, A., & Jiang, C. (2022). Recent advances in lignin-based carbon materials and their applications: A review. *International Journal of Biological Macromolecules*, 223, 980–1014. <https://doi.org/10.1016/j.ijbiomac.2022.11.070>
- Yerkinbekova, Y., Kalybekkyzy, S., Tolganbek, N., Kahraman, M. V., Bakenov, Z., & Mentbayeva, A. (2022). Photo-crosslinked lignin/PAN electrospun separator for safe lithium-ion batteries. *Scientific Reports*, 12(1), 18272. <https://doi.org/10.1038/s41598-022-23038-7>
- Youe, W.-J., Kim, S. J., Lee, S.-M., Chun, S.-J., Kang, J., & Kim, Y. S. (2018). MnO₂-deposited lignin-based carbon nanofiber mats for application as electrodes in symmetric pseudocapacitors. *International Journal of Biological Macromolecules*, 112, 943–950. <https://doi.org/10.1016/j.ijbiomac.2018.02.048>
- Youe, W.-J., Lee, S.-M., Lee, S.-S., Lee, S.-H., & Kim, Y. S. (2016). Characterization of carbon nanofiber mats produced from electrospun lignin-g-polyacrylonitrile copolymer. *International Journal of Biological Macromolecules*, 82, 497–504. <https://doi.org/10.1016/j.ijbiomac.2015.10.022>
- Yücel, Y. D., Adolfsson, E., Dykhoff, H., Pettersson, J., Trey, S., Wysocki, M., Widenkvist Zetterström, E., Zenkert, D., Wreland Lindström, R., & Lindbergh, G. (2024). Enhancing structural battery performance: Investigating the role of conductive carbon additives in LiFePO₄-Impregnated carbon fiber electrodes. *Composites Science and Technology*, 251, 110571. <https://doi.org/10.1016/j.compscitech.2024.110571>
- Zhang, J., Xiang, H., Cao, Z., Wang, S., & Zhu, M. (2024). Research progress of lignin-derived materials in lithium/sodium ion batteries. *Green Energy & Environment*, S2468025724001274. <https://doi.org/10.1016/j.gee.2024.05.001>
- Zhang, P., Li, M., Jing, Y., Zhang, X., Su, S., Zhu, J., & Yu, N. (2023). Highly flexible cellulose-based hydrogel electrolytes: Preparation and application in quasi solid-state supercapacitors with high specific capacitance. *Journal of Materials Science*, 58(4), 1694–1707. <https://doi.org/10.1007/s10853-022-08112-9>
- Zhang, W., Lei, Y., Ming, F., Jiang, Q., Costa, P. M. F. J., & Alshareef, H. N. (2018). Lignin Laser Lithography: A Direct-Write Method for Fabricating 3D Graphene Electrodes for Microsupercapacitors. *Advanced Energy Materials*, 8(27), 1801840. <https://doi.org/10.1002/aenm.201801840>
- Zhang, W., Qiu, X., Wang, C., Zhong, L., Fu, F., Zhu, J., Zhang, Z., Qin, Y., Yang, D., & Xu, C. C. (2022). Lignin derived carbon materials: Current status and future trends. *Carbon Research*, 1(1), 14. <https://doi.org/10.1007/s44246-022-00009-1>
- Zhang, Z. J., & Sun, S. S. (2016). Understanding the redox effects of amine and hydroxyl groups of p-aminophenol upon the capacitive performance in KOH and H₂SO₄ electrolyte. *Journal of Electroanalytical Chemistry*, 778, 80–86. <https://doi.org/10.1016/j.jelechem.2016.08.021>
- Zhang, Z., Li, F., Chen, J., Yang, G., Ji, X., Tian, Z., Wang, B., Zhang, L., & Lucia, L. (2022). High performance bio-supercapacitor electrodes composed of graphitized hemicellulose porous carbon spheres. *Frontiers in Bioengineering and Biotechnology*, 10, 1030944. <https://doi.org/10.3389/fbioe.2022.1030944>
- Zhao, C., & Zheng, W. (2015). A Review for Aqueous Electrochemical Supercapacitors. *Frontiers in Energy Research*, 3. <https://doi.org/10.3389/fenrg.2015.00023>
- Zhao, D., Chen, C., Zhang, Q., Chen, W., Liu, S., Wang, Q., Liu, Y., Li, J., & Yu, H. (2017). High Performance, Flexible, Solid-State Supercapacitors Based on a Renewable and Biodegradable Mesoporous Cellulose Membrane. *Advanced Energy Materials*, 7(18), 1700739. <https://doi.org/10.1002/aenm.201700739>
- Zhao, L., Jian, W., Zhang, X., Wen, F., Zhu, J., Huang, S., Yin, J., Lu, K., Zhou, M., Zhang, W., & Qiu, X. (2022). Multi-scale self-templating synthesis strategy of lignin-derived hierarchical porous carbons toward high-performance zinc ion hybrid supercapacitors. *Journal of Energy Storage*, 53, 105095. <https://doi.org/10.1016/j.est.2022.105095>
- Zhen, Q., Bashir, S., & Liu, J. L. (Eds.). (2019). *Nanostructured materials for next-generation energy storage and conversion: Advanced battery and supercapacitors*. Springer.

- Zheng, Y., Chen, K., Jiang, K., Zhang, F., Zhu, G., & Xu, H. (2022). Progress of synthetic strategies and properties of heteroatoms-doped (N, P, S, O) carbon materials for supercapacitors. *Journal of Energy Storage*, *56*, 105995. <https://doi.org/10.1016/j.est.2022.105995>
- Zhi, M., Xiang, C., Li, J., Li, M., & Wu, N. (2013). Nanostructured carbon–metal oxide composite electrodes for supercapacitors: A review. *Nanoscale*, *5*(1), 72–88. <https://doi.org/10.1039/C2NR32040A>
- Zhong, W., Su, W., Li, P., Li, K., Wu, W., & Jiang, B. (2024). Preparation and research progress of lignin-based supercapacitor electrode materials. *International Journal of Biological Macromolecules*, *259*, 128942. <https://doi.org/10.1016/j.ijbiomac.2023.128942>
- Zhou, B., Liu, W., Gong, Y., Dong, L., & Deng, Y. (2019). High-performance pseudocapacitors from kraft lignin modified active carbon. *Electrochimica Acta*, *320*, 134640. <https://doi.org/10.1016/j.electacta.2019.134640>
- Zhou, L., You, X., Wang, L., Qi, S., Wang, R., Uraki, Y., & Zhang, H. (2023). Fabrication of Graphitized Carbon Fibers from Fusible Lignin and Their Application in Supercapacitors. *Polymers*, *15*(8), 1947. <https://doi.org/10.3390/polym15081947>
- Zhou, M., Bahi, A., Zhao, Y., Lin, L., Ko, F., Servati, P., Soltanian, S., Wang, P., Yu, Y., Wang, Q., & Cai, Z. (2021). Enhancement of charge transport in interconnected lignin-derived carbon fibrous network for flexible battery-supercapacitor hybrid device. *Chemical Engineering Journal*, *409*, 128214. <https://doi.org/10.1016/j.cej.2020.128214>
- Zhu, M., Liu, H., Cao, Q., Zheng, H., Xu, D., Guo, H., Wang, S., Li, Y., & Zhou, J. (2020). Electrospun Lignin-Based Carbon Nanofibers as Supercapacitor Electrodes. *ACS Sustainable Chemistry & Engineering*, *8*(34), 12831–12841. <https://doi.org/10.1021/acssuschemeng.0c03062>
- Zhu, W. (2015). *Precipitation of Kraft Lignin* [THESIS FOR THE DEGREE OF DOCTOR OF PHILOSOPHY]. CHALMERS UNIVERSITY OF TECHNOLOGY.
- Zhu, Y., & Fontaine, O. (2022). Most Modern Supercapacitor Designs Advanced Electrolyte and Interface. In D. Tashima & A. Kumar Samantara (Eds.), *Supercapacitors for the Next Generation*. IntechOpen. <https://doi.org/10.5772/intechopen.98352>
- Zubi, G., Dufo-López, R., Cavalho, M., & Pasaoglu, G. (2018). The lithium-ion battery: State of the art and future perspectives. *Renewable and Sustainable Energy Reviews*, *89*, 292–308.